Chapter 7

OPTICAL VISUALIZATION OF PROTEIN CRYSTAL GROWTH PROCESS

The applications of the three refractive index based optical techniques namely, interferometry, schlieren and shadowgraph, as tools for visualization of diffusion process, on-line monitoring of protein drop contraction during the equilibration process as well as evaporation of water from the drop and the mixing of condensed water in the reservoir are discussed in the present chapter. Images of long time-evolution of the diffusive field in the crystal growth chamber have been recorded. When equilibration is achieved between the droplet and the reservoir solution, the drop is supersaturated due to evaporation of water and spontaneous nucleation of lysozyme takes place. Growth takes place from a fixed volume of the solution in the droplet. Convection patterns are set-up owing to concentration and hence density differences. In all the experiments, the light beam is focused in such a manner that clear droplet region, the air-space and the reservoir region are clearly visualized. Crystallization process is initiated due to the of concentration gradient and hence a vapour pressure gradient between the droplet and reservoir solution. The three measurement techniques have been compared in terms of image quality and the potential as a tool for extracting quantitative information from the recorded images. In all the experiments, the reservoir solution was composed of 30% (w/v) NaCl solution, 70% (v/v) ethylene glycol solution and sodium acetate buffer (0.1M and 4.8 pH).

7.1 INTERFEROMETRY

In the hanging drop configuration for crystallization of lysozyme protein, there is a small inverted protein drop which is separated from the reservoir solution through an air space. Hence there are clearly three regions: (1) small drop, hemispherical in shape, (2) air gap,

and (3) reservoir solution. Experiments were conducted when the M-Z interferometer was set in the infinite fringe and wedge fringe setting. At the top region the black patch is the stopper portion inside the cavity over which the protein drops are kept. As the drop is of hemispherical shape and small in size, it cannot be imaged by interferometry. Thus, the overall configuration reduces to two-fluid convection. In the two-layer problem, it is difficult to achieve infinite fringe setting simultaneously in both the fluid media. Hence, the interferometer is individually adjusted for infinite fringe setting in air and reservoir solution regions. It is to be noted that the reference chamber is present in all the interferometric experiments.

Two configurations have been used to achieve infinite fringe setting in air: (1) the reference cell is fully filled with air and (2) the reference cell is filled with same amount of reservoir solution as that of test cell. For attaining the infinite fringe setting in reservoir solution, the reference cell is either fully filled with the reservoir solution or filled with an equal amount of reservoir solution. These options are considered to visualize the interface clearly and to identify the boundaries of the regions.

7.1.1 Infinite Fringe Setting

Figure 7.1 shows the formation and time-evolution of fringes in the infinite fringe setting in air. The compensation chamber is filled with reservoir solution upto the same height as that of the test cell. Figure 7.1(a) shows the initial infinite fringe setting in air. This experiment was carried out with 3 hanging drops placed on the coverslip attached to the stopper. Each drop has a 10 μl volume and the protein and reservoir solution ratio is 7:3. Reservoir solution is taken as 25 ml. The three drops are arranged in such a manner that a single drop is seen through interferometry. Initially when the solution is poured into the cavity, there are disturbances (turbidity). This phase is not shown here. After pouring the solution the cavity is covered by the hanging drop stopper for few hours till the turbidity dies out. It takes around 2-3 hours and the solution becomes still. The drop is placed on the top in a vertically inverted mode. In Figure 7.1(a), the shape of the fringes inside the reservoir solution is hazy. While placing the drops over the reservoir solution, atmospheric air is traped inside the cavity and gives a fuzzy effect to fringes. It is to be noted that for the reservoir solution the M-Z interferometer is not in the infinite fringe mode but wedge fringes are present. The initial wedge fringes in the reservoir solution are kept as a vertical straight fringes. After placing the drop in the test cell, concentration gradient comes into the picture between the drop and reservoir from vapour pressure differences. This creates an unstable configuration. To achieve equilibrium, water evaporates from the drop. Because of water evaporation, the drop size changes. Evaporation takes place till the vapour pressure gradient becomes zero.

The fringe profile changes because of the diffusion of condensed water into the reservoir. Figure 7.1(b) shows the interferogram taken one hour later after placing the drops. A reduction in drop size is clearly visible. The air region is fringe free which shows that the change in refractive index is very small to be observed. In the reservoir the fringe profile is altered. The straight vertical fringes become curved. Figure 7.1(c - d) show again a reduction in drop size and a fringe free zone in air after 2 and 3 hrs respectively. Very small effect is seen at the air-solution interface. But in 7.1(d) the curvature of fringes in the reservoir solution changes and become vertically straight as compared to the fringes in 7.1(c). After 5.5 h, the drop size is very small as shown in Figure 7.1(e) and no further reduction in drop size is seen. The fringe profile is somewhat slanted. Figure 7.1(f) is recorded after 24 h. This is similar to the base image Figure 7.1(a). The only difference in these two images is the size of drop. The reservoir is composed once again of straight vertical fringes. This is because the volume of evaporated vapour condensing over the air-reservoir interface is small as compared the reservoir solution. This is why there is no measurable difference in concentration between the reservoir region of the base image and the interferogram recorded after 24 hours. After attaining equilibration, the drop solution becomes supersaturated. In the presence of NaCl (precipitant), nucleation of lysozyme crystals in the drop is facilitated and growth of crystals take place.

Figure 7.2 shows three consecutive images for two different times recorded within 1 min to observe the movement of the single fringe present in the air region. Figure 7.2(a - c) shows three consecutive images taken within one minute after 45 min and Figure 7.2(d - f) after 4 hours. These consecutive images were taken for two different times to check whether any fringe had appeared in air during the experiment. These images show the movement of one fringe in air which is not due to concentration but present originally in the infinite fringe setting. It was confirmed, after completing the experiment, when the infinite fringe setting was recorded.

Figure 7.3 shows shadowgraphs recorded in the crystal growth experiment. Here, three protein drops of volume 10 μl each are placed on top of the cavity in the hanging position. All the three drops are in one line, due to which only one drop is observed. The shadowgrams are taken at t=0 (Figure 7.3(a)) and after t=3 hrs (Figure 7.3(b)). Drop size and shape are clearly visible in these two images. It is seen from the shadowgraphs that the drop radius is reduced and it is somewhat flat at the base. In air, no intensity variations are observed. While placing the drops in the crystal growth chamber atmospheric air is trapped in the cavity and disturbs the reservoir solution. The interface is clear in Figure 7.3(b) as compared to Figure 7.3(a).

Figures 7.4(a and b) show the comparison between the base images taken through interferometry and shadowgraph respectively. Both the images clearly show intensity

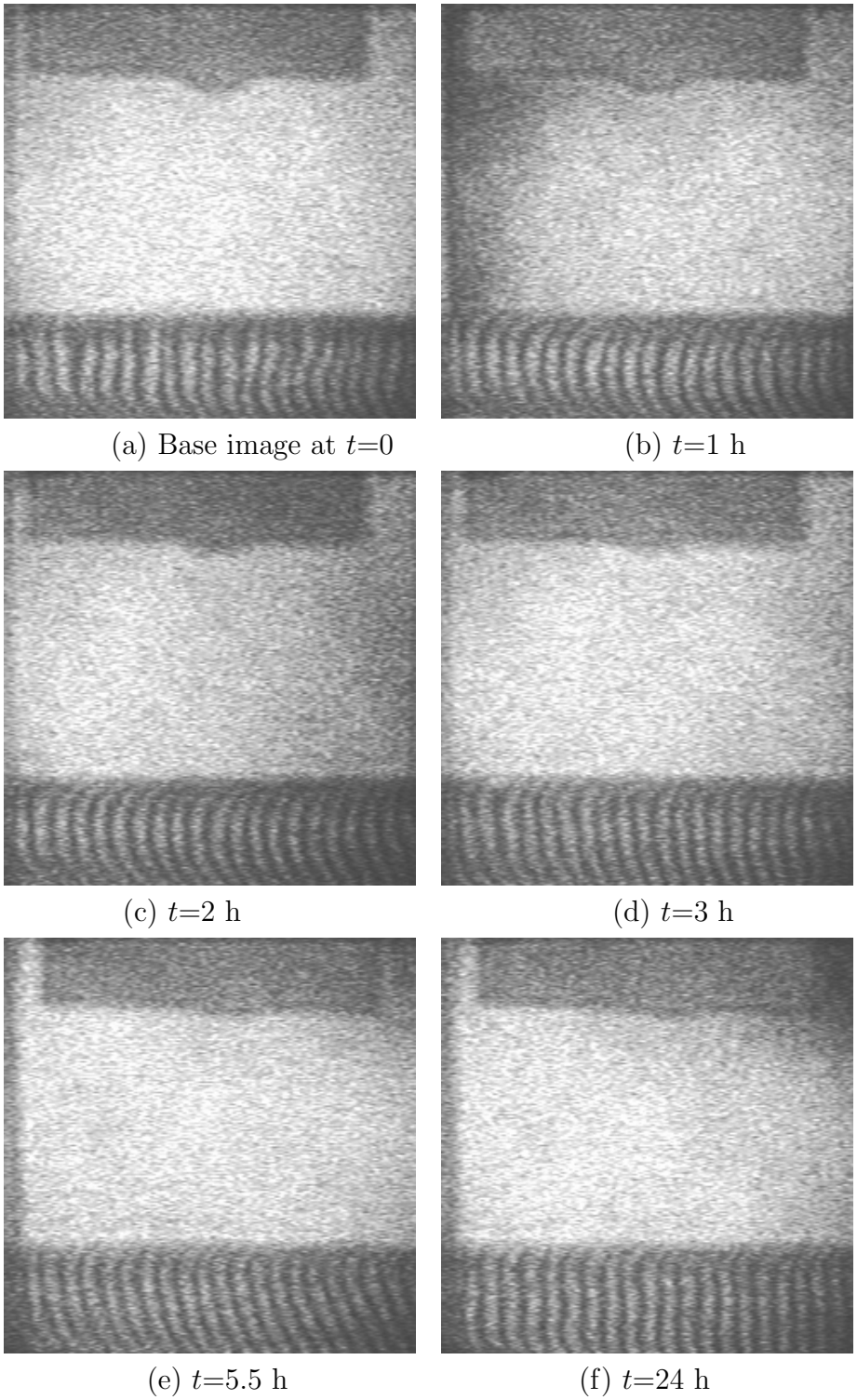

(a) Base image at t=0 (b) t=1 h

(c) t=2 h (d) t=3 h

(e) t=5.5 h (f) t=24 h

Figure 7.1: Mach-Zehnder interferograms of transient evolution of diffusive field in reservoir solution during equilibration process in lysozyme protein crystallization chamber. Three protein drops with drop concentration of 7:3, size 10 μl with 25 ml reservoir solution are used in infinite fringe setting in air.

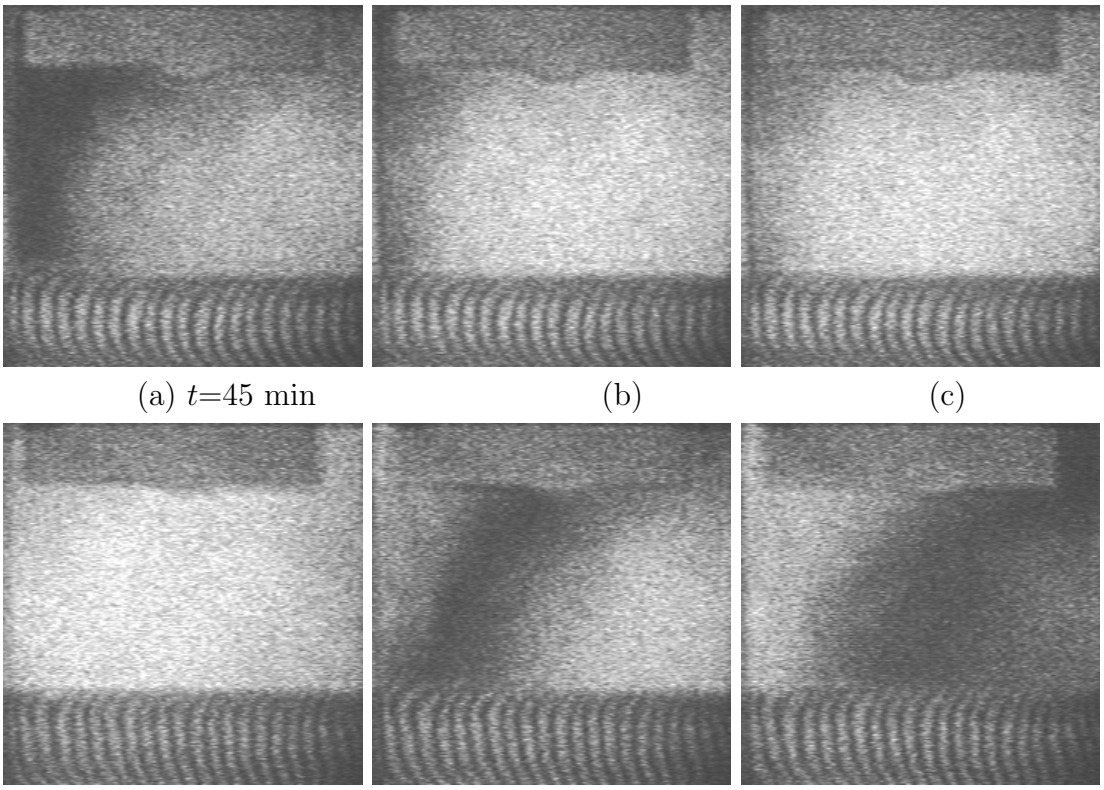

(a) t=45 min (b) (c)

(c) t=4 h (d) (e)

Figure 7.2: Three consecutive images recorded within 1 min to see the movement of a single fringe in the cavity.

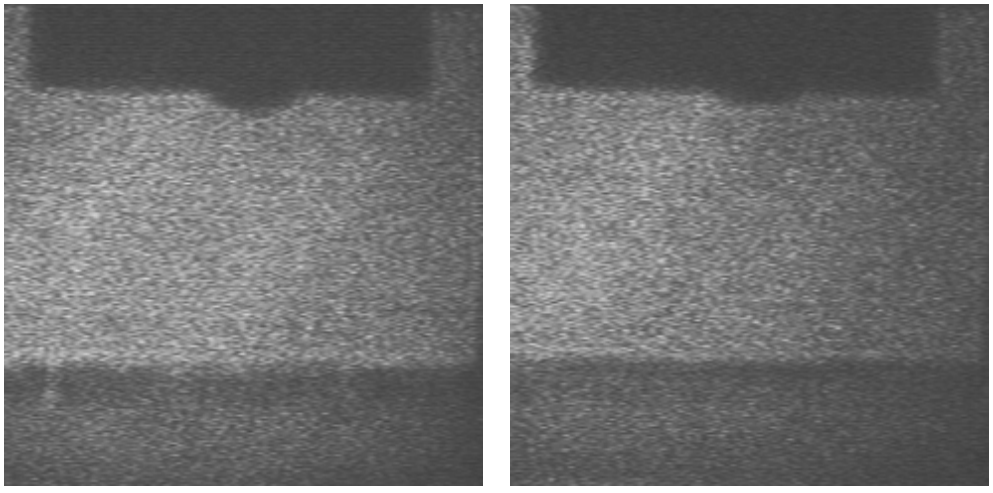

(a) (b)

Figure 7.3: Shadowgraphs at t=0 and t=3 hr when the lysozyme protein crystallization chamber has three protein drops in one line with drop concentration of 7:3, size 10 μl with 25 ml reservoir solution.

variations at the interface and in the solution region. In a shadowgraph, a dark patch is present at the interface. In interferogram straight fringes can be seen. It is because the solution is poured into the cavity resulting in fluid motion. The solution is left to stand for a few hours to dampen the resulting turbidity. While placing the drops in the apparatus, air is trapped inside the chamber and produces disturbances, although small. The shaky fringes in interferogram in the reservoir solution are due to this factor whereas in shadowgraph the interface is not smooth and hazyness is visualized. The two experiments have been conducted simultaneously since by blocking the reference beam of the M-Z interferometer, shadowgraphs are recorded.

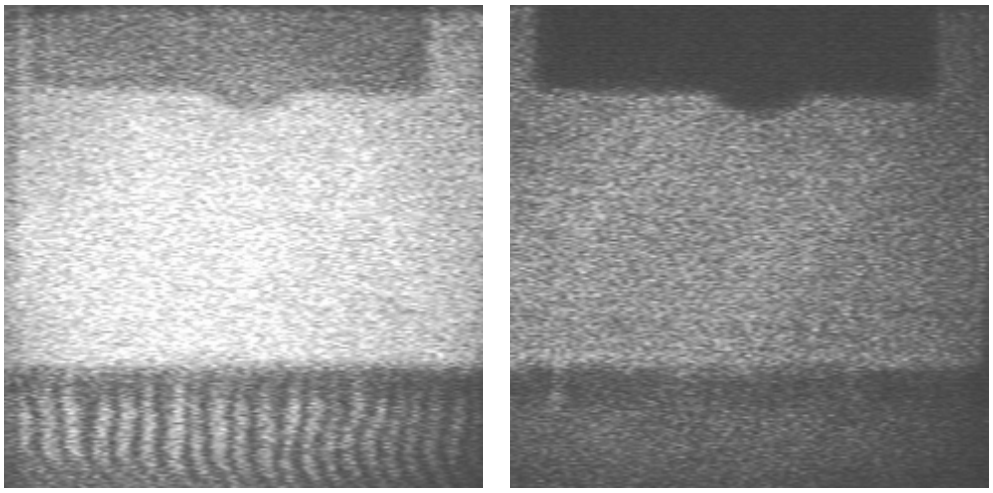

(a) (b)

Figure 7.4: Base images of (a) Mach-Zehnder interferogram and (b) shadowgram for the experiment in hanging drop configuration for a single protein drop with drop concentration of 7:3 and of size 10 μl with 25 ml reservoir solution.

The previous experiment was for 3 protein drops in the hanging mode. Since the images showed a fringe free region, it was decided to increase the gradient and the number of drops are increased. Thus seven drops in the hanging in the arrangement are shown in Figure 8.1(c). These drops are visualized in such a manner so that only three drops are seen in a single view.

The transient evolution of the diffusive field in the reservoir solution is shown in Figure 7.5. The experiment is conducted for 7 drops with concentration of 7:3 and each having size 10 μl with 75 ml reservoir solution. The compensation chamber is also filled with 75 ml reservoir solution and infinite fringe setting is achieved in air. In this experiment, the air gap is reduced, the reservoir height is increased accordingly and number of drops is higher. Figure 7.5(a) shows the base image. Here, the focus is at the interface and the reservoir. In this experiment, deformation of the interface and fringe profiles are clearly visible. In Figure 7.5(d), the central region of the interface and the

shape of fringes are changed. On right side the fringes are very clear and in continuation with the original fringes. In Figure 7.5(e), a constant thickness region at the interface is clearly visible which distinctly separates air region with reservoir. Also the fringe profile in reservoir region changes with time. After 24 hours, the interferogram, Figure 7.5(f), is quite similar to the initial interferogram, Figure 7.5(a). The interface region shows the change in shape with respect to the index of refraction of the reservoir solution, due to which the fringes are deformed. This change is only due to the presence of condensed water over the surface of the reservoir. Slight change is seen in the fringe profile in the reservoir due to the diffusion of water into the reservoir. The diffusion process causes the solution to move vertically downwards. Hence, the fringe displacement is also in the downward direction. The absence of fringes in air indicates the presence of very low concentration gradients in the growth chamber and transport of water vapour is solely due to the process of diffusion to the interface.

After only one hour considerable variation is seen at the interface (Figure 7.5(b)). The condensed water floats over the interface. A lower concentration fluid floats over the higher concentrated fluid. In this configuration of two fluids, convection process will not occur. Low density water diffuses into the high density reservoir solution. The interface gets deformed due to condensed water, which gradually changes its shape, Figure 7.5(c-e). Owing to a smaller air gap and high gradients, the condensation of water vapour is earlier as compared to the previous experiment. In this condition, equilibrium is attained earlier and the crystal nucleation is also early. Since the process is fast, the number of crystals is high and the crystal size is small.

In the next experiment, conditions of the previous experiment are retained. An air filled compensation chamber is used. Figure 7.6(a) shows the initial infinite fringe setting of the M-Z interferometer in air. Figure 7.6(b) shows the interferogram after placing and adjusting the test cell without drops and compensation chamber. In Figure 7.6(c), seven drops are mounted and the cavity is sealed. A very clear air-reservoir interface is seen as compared to the previous experiment, where the reference chamber is filled with air as well as solution. In Figure 7.6(d-e) the drop size is reduced as well as at the interface the fringes are deformed. In Figure 7.6(d), the deformed fringe region is greater as compared to Figure 7.6(e). It also shows a bright line in between the curved and straight fringes. Figure 7.6(f) shows interferograms after 24 hours, in which the drop size is reduced but the air and reservoir regions are similar to the initial interferogram. In summary, a clear interface as well as fringe deformation is seen in the experiment with seven drops and an air filled compensation chamber.

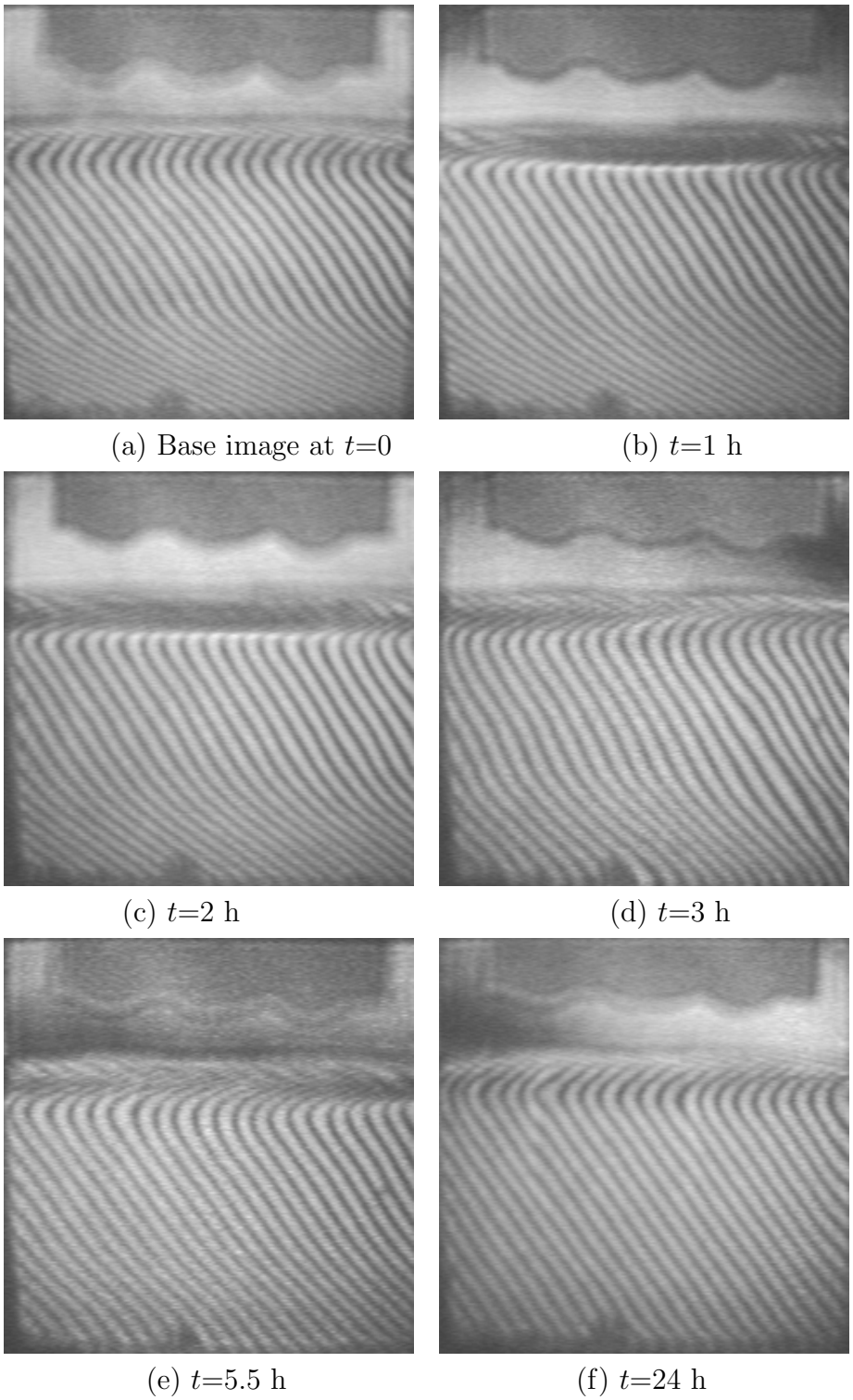

(a) Base image at t=0 (b) t=1 h

(c) t=2 h (d) t=3 h

(e) t=5.5 h (f) t=24 h

Figure 7.5: Mach-Zehnder interferograms of transient evolution of diffusive field in reservoir solution during equilibration process in lysozyme protein crystallization chamber. Seven protein drops with drop concentration of 7:3 and of size 10 μl with 75 ml reservoir solution are used. The compensation chamber is filled with 75 ml reservoir solution.

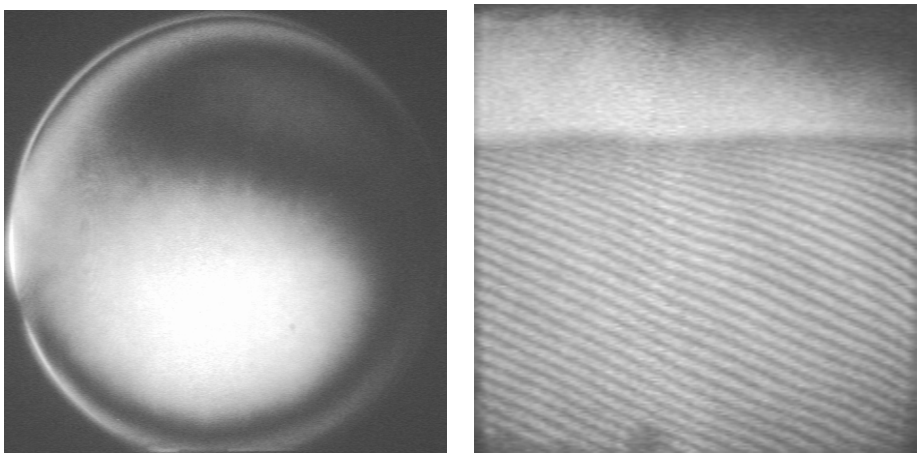

(a) Infinite fringe setting of M-Z (b) Both the cavities in place

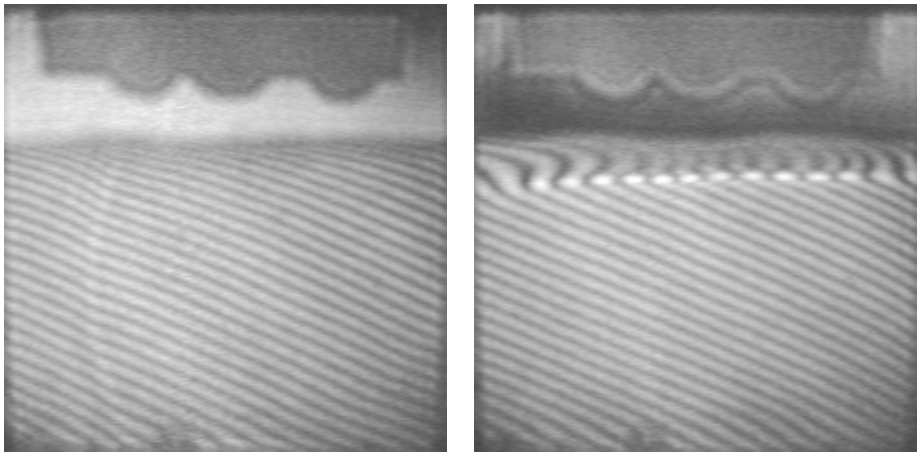

(c) 7 protein drops are placed at t=0 (d) t=1 h

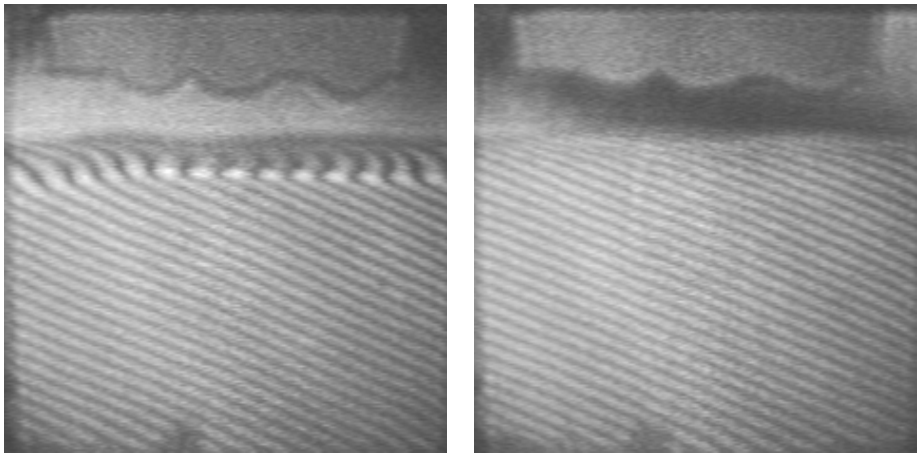

(e) t=2 h (f) t=24 h

Figure 7.6: Mach-Zehnder interferograms of transient evolution of diffusive field in reservoir solution during equilibration process in lysozyme protein crystallization chamber. Seven protein drops with drop concentration of 7:3 and of size 10 μl with 75 ml reservoir solution are used along with air filled compensation chamber.

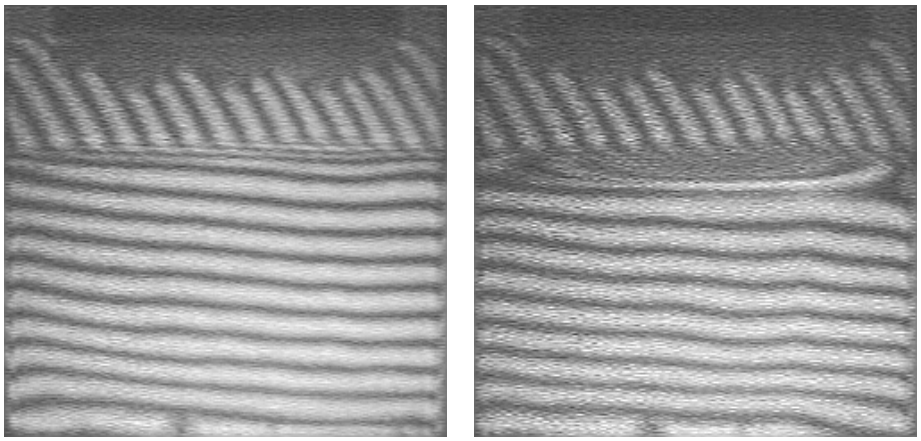

(a) t=0 (b) t=1 h

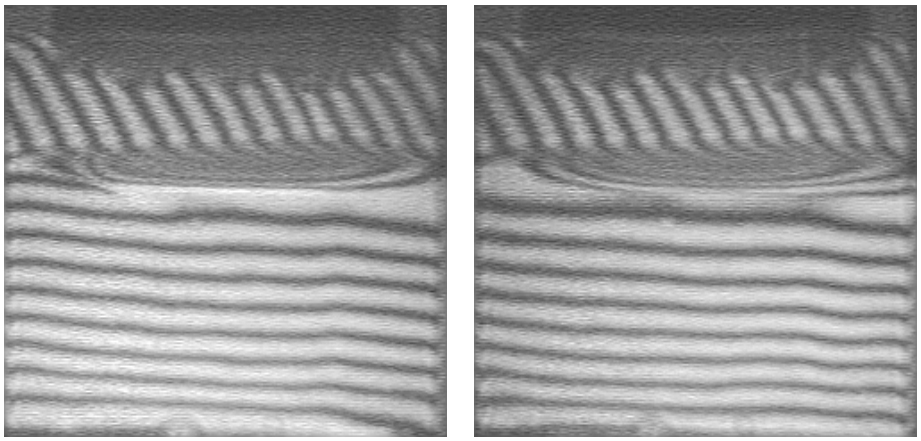

(c) t=2 h (d) t=3 h

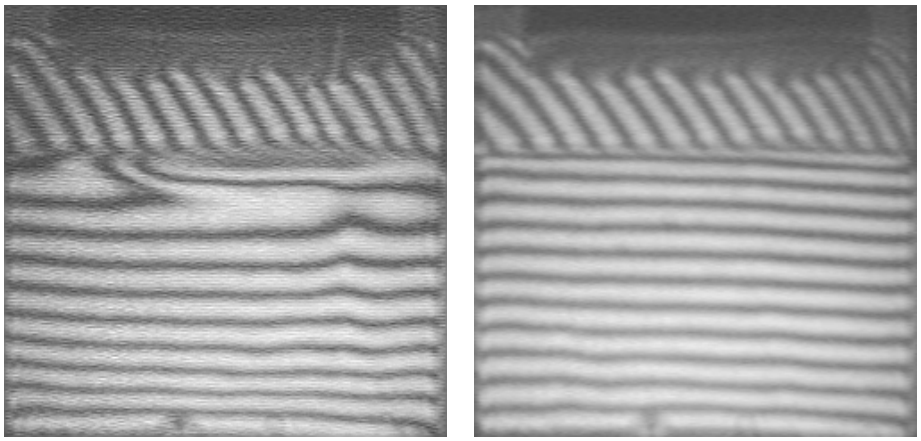

(e) t=7 h (f) t=24 h

Figure 7.7: Mach-Zehnder interferograms of transient evolution of diffusive field in reservoir solution during equilibration process in lysozyme protein crystallization chamber. Seven protein drops with drop concentration 7:3, size 10 μl and 75 ml reservoir solution are used in wedge fringe setting. The compensation chamber is fully filled with reservoir soluion.

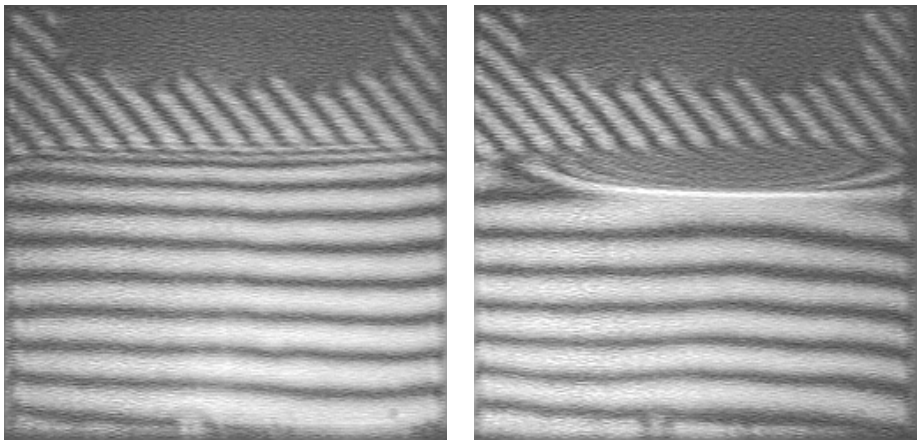

(a) t=0 (b) t=1 h

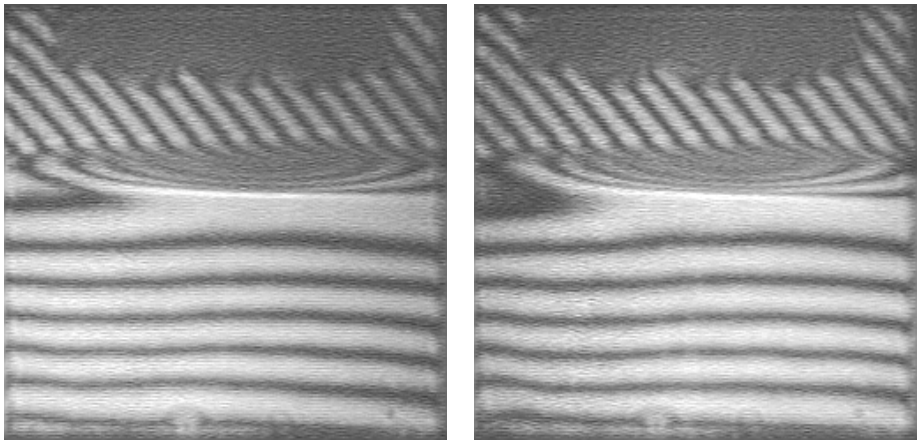

(c) t=2 h (d) t=3 h

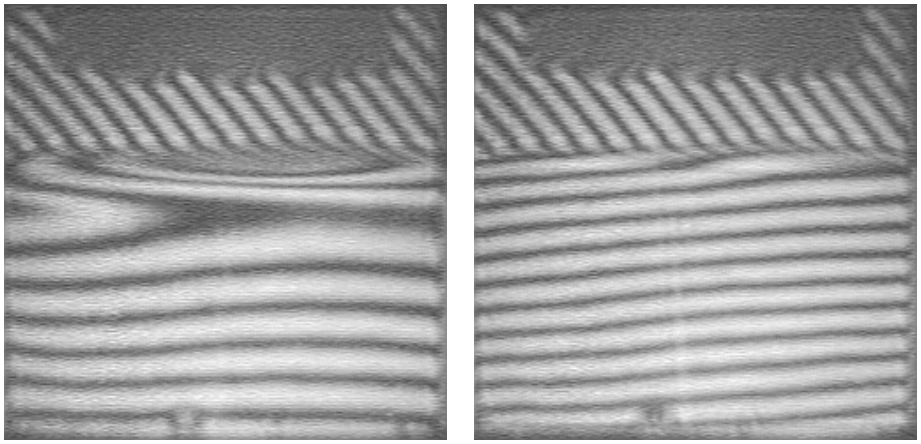

(e) t=7 h (f) t=24 h

Figure 7.8: Mach-Zehnder interferograms of transient evolution of diffusive field in reservoir solution during equilibration process in lysozyme protein crystallization chamber. Seven protein drops with drop concentration 7:3, size 10 μl and 75 ml reservoir solution are used in wedge fringe setting. The compensation chamber is filled with air.

7.1.2 Wedge Fringe Setting

In this section, experiments have been conducted in the wedge fringe setting mode of the Mach-Zehnder Interferometer. The experiments were conducted with the test cavity filled with 75 ml solution. The reference cell was either fully filled with reservoir solution or with air. The experiments were carried out with 7 drops. The drops were placed on top of the reservoir solution in hanging mode. The focus was on visualizing the transport process at the air-solution interface and in the reservoir.

Figure 7.7 shows the formation and time-evolution of fringes in the wedge fringe setting. In this experiment, the compensation chamber is fully filled with reservoir solution. The interferometer is aligned in such a way that in air slanted fringes and in reservoir region horizontal straight fringes are present. Again, the variation is shown at the interface region. Clear deformed fringe patterns are observed in air near the interface. Deformation is also seen in the reservoir specially close to the interface.

Figure 7.8 shows the formation and time-evolution of fringes in the wedge fringe setting. The compensation chamber is filled with air. Figure 7.8(a) shows the base image of the cavity. Two zones are clearly visible in interferograms. Water vapour leaving from the drop condenses at the interface. The deformation of fringes near the interface is visible.

Experiments in the wedge fringe setting of the interferometer reveal trends that are identical to the infinite fringe setting. The horizontal fringes deform vertically downwards due to an abrupt change in solute concentration. The wedge fringes get displaced in regions of a large change in concentration with respect to the bulk of the concentrated reservoir solution solution. This leads to concentration gradients adjacent to the interface, and a continuation of diffusion process into the reservoir solution. The infinite and the wedge fringes show considerable symmetry as well as stability in time, ensuring the presence of uniform concentration gradients near the interface. The downward movement of water is driven by molecular diffusion into the reservoir solution.

7.2 SCHLIEREN AND SHADOGRAPH TECHNIQUES

The evolution pattern of diffusion using schlieren (colour and monochrome) and shadowgraph techniques is shown in Figures 7.9, 7.10 and 7.11 during the protein crystal growth process respectively. These figures confirm the nature of transport phenomena recorded by the interferometer. The black region at the interface between air and the reservoir solution can be attributed to the surface tension at the contact surface between the reservoir solution and the glass window in the viewing direction. First image in schlieren (colour and monochrome) and shadowgraph are the base images just after

placing the drops in the growth chamber. After placing the drop, water evaporation process is initiated. Water vapour condenses over the solution creating a region free of NaCl. The gradients of salt concentration are small and localized in the vicinity of the interface. Figure 7.9(b), 7.10(b) and 7.11(b) show a greater amount of fresh water at the interface in the central portion after 0.5 h. This is due to the evaporation of water from the drop followed by the condensation of water vapour on the surface of the reservoir. Subsequently, condensation continues while the fresh water diffuses into the reservoir. Mass diffusion of the moisture in the reservoir generates its own spread of colours in the interface region (Figure 7.9(c-e)) whereas in monochrome schlieren and shadowgraph it is shown in terms of intensity change in the solution (Figure 7.10(c-e)) and 7.11(c-e). The diffusion process causes fresh water to propagate vertically downwards. Hence, gradual change of colour in colour schlieren images whereas gradual intensity change in monochrome schlieren and shadowgraph are seen in the downward direction. In the monochrome schlieren images, the region of brightness shifts away from the interface. The intensity contrast in monochrome schlieren and colour change in colour schlieren are related to an abrupt change at the air reservoir interface due to the change in concentration of reservoir solution and deposited water. It creates a jump in the refractive index, and deflects the light beam into the region of relatively large concentration gradients. In shadowgraph images, the intensity variation is large near the interface which gradually decreases in the downward direction, Figures 7.11(b-e). The absence of large colour changes in colour images and intensity variation in air indicates low concentration gradients in the growth chamber and transport of water vapour is solely due to the process of diffusion to the interface. After 24 h, the colour and monochrome schlieren images look similar to their respective base images. The hanging drops have almost disappeared at this time indicating the completion of the evaporation process. The volume of the condensed water being negligible compared to that of the reservoir solution, there is no significant change in colour or intensity between the final image and the base image. The schlieren images also reveal a continuous reduction in the drop size arising from evaporation.

Of the two techniques, the colour schlieren arrangement is more sensitive to the change in concentration, producing a greater variety of colours, when compared to monochrome schlieren. This result is brought out in the colour schlieren images as an increase in the number of colours inside the reservoir solution as well as in air region. As defined by the colours, the resulting transport indicates a diffusive pattern. The images also reveal the extent of symmetry of the solutal distribution and the underlying flow field in the reservoir. As in interferograms, shadowgraph, monochrome and colour schlieren reveal the following sequence of events: (a) Reduction in drop size; (b) negligible concentration gradient in air; (c) condensation of water on interface; (d) diffusion

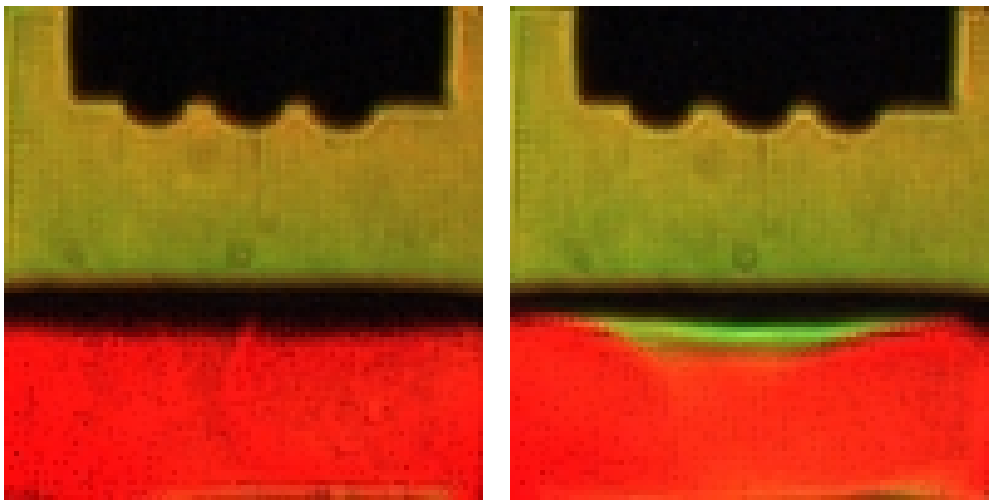

(a) t=0 (b) t=0.5 h

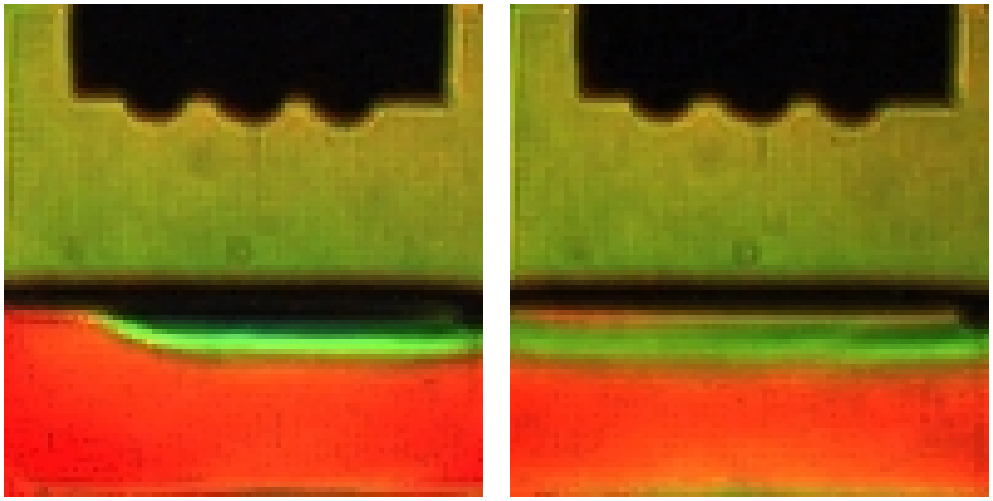

(c) t=1 h (d) t=3 h

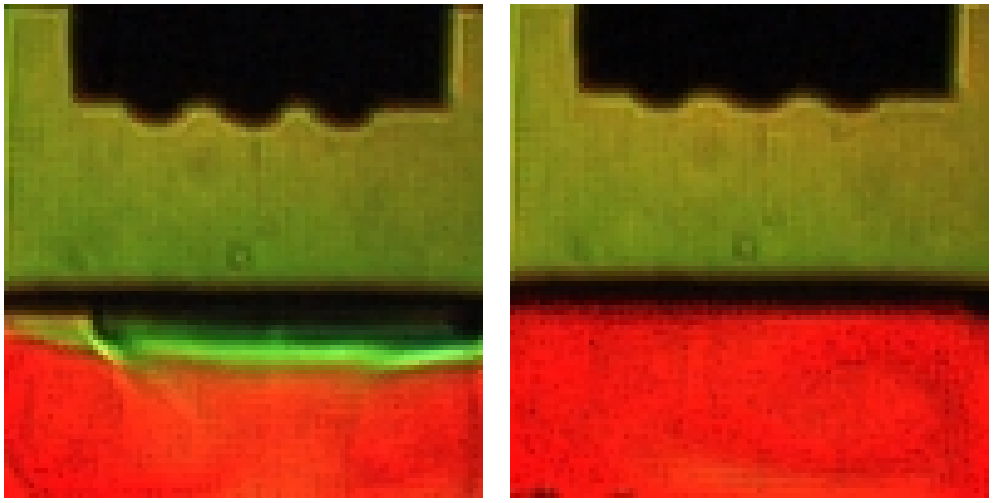

(e) t=5 h (f) t=24 h

Figure 7.9: Colour schlieren images of transient evolution of diffusion process in reservoir during lysozyme protein crystal growth. Seven protein drops with 7:3 drop concentration and 50 ml reservoir solution are used.

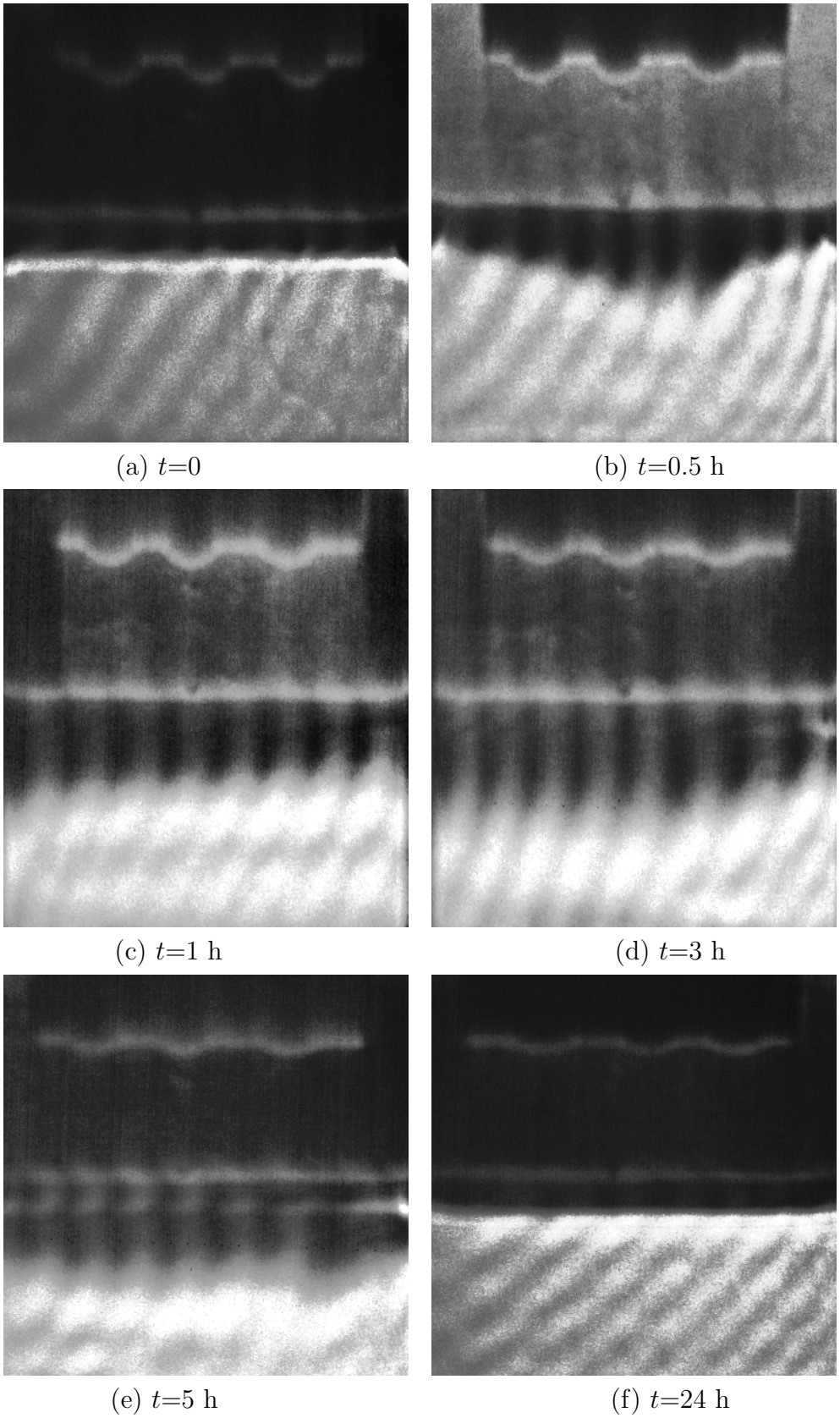

(a) t=0 (b) t=0.5 h

(c) t=1 h (d) t=3 h

(e) t=5 h (f) t=24 h

Figure 7.10: Monochrome schlieren images of transient evolution of diffusive field in reservoir solution during the equilibration process. Seven protein drops with drop concentration of 7:3, size 10 μl and 50 ml reservoir solution are considered.

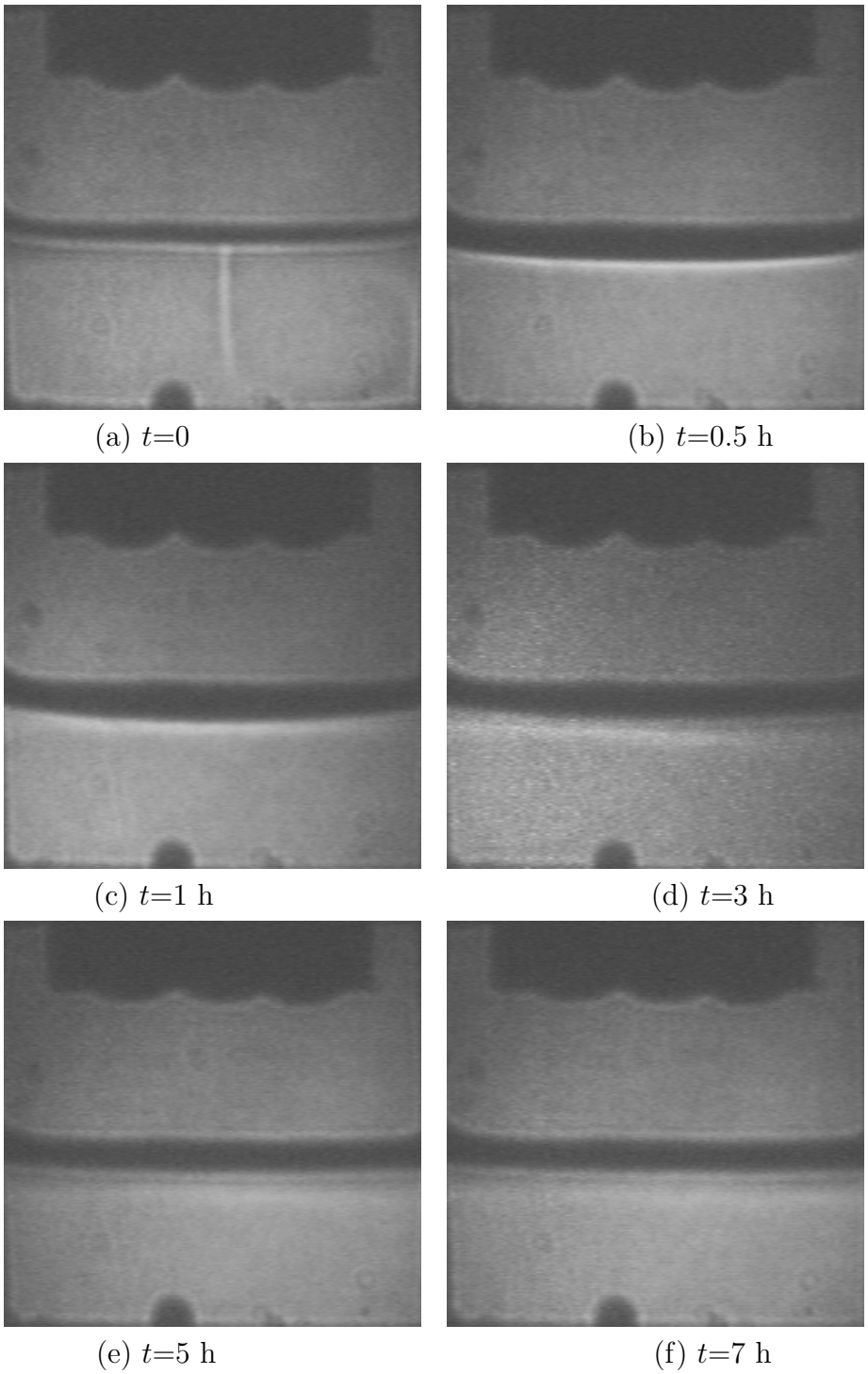

(a) t=0 (b) t=0.5 h

(c) t=1 h (d) t=3 h

(e) t=5 h (f) t=7 h

Figure 7.11: Shadowgraph images of transient evolution of diffusive field in reservoir solution during the equilibration process. Seven protein drops with drop concentration of 7:3, size 10 μl and 50 ml reservoir solution are considered.

of water into reservoir solution; and (e) finally stable undisturbed and uniform reservoir solution.

As opposed to interferometry, schlieren, and shadowgraph images do not show sufficient contrast in the recorded images. It gets localized in the vicinity of the interface. This is indicated by horizontal bands of relatively higher intensity. The limitation is understandable as the shadowgraph technique is most suitable for large gradients applications. It is to be differentiated from interferometry where the fringes are most sensitive to the changes in solution density, but suffer from refraction errors at very high gradients. In monochrome schlieren, it is possible to control the contrast of the images by adjusting the position of the knife-edge. In colour schlieren, the use of appropriate colour filter can control the colours of the images to highlight the points of interest under study. On the other hand, shadowgraph has its own advantages in terms of monitoring the symmetry and reduction of drop size since fringes in interferometry hinder the true location of the drop-air and air-solution interface. Monochrome schlieren images also present an ambiguous picture due to the presence of non-uniform high intensity zone adjacent to the drop boundary. But colour schliern can also give good information of high as well as low gradients by using a correctly designed colour filter. It is to be expected that shadowgraph images would show greater contrast when the gradients are very high. In the present work the effect on drop shape and size can be best understood with the help of shadowgraph as well as by colour schlieren images.

7.3 COMPARISON OF OPTICAL TECHNIQUES : CLOSURE

Refractive index-based optical techniques can be used to examine the diffusion phenomena as a function of time and hence the rate of diffusion. A comparison of the images of the three techniques shows interferograms to be the most vivid, since fringes deform and get displaced in relationship to the local concentration field. Thus, they offer the most direct information about concentration distribution as well as the underlying diffusion flow field in the solution. Monochrome schlieren and shadowgraph images reveal regions of high concentration gradients in the form of heightened brightness. Colour schlieren gives low as well as high concentration field information in terms of various colours with greater sensitivity. A review of Equations 5.4, 5.5 and 5.6 (Chapter 5) shows that interferograms are easy to analyze, monochrome schlieren requires integration of the intensity field and colour schlieren requires integration of colour field in terms of hue, while shadowgraph requires the solution of a Poisson equation to recover the local concentration.

The three optical techniques under discussion yield images that are integrated values of the concentration field in the direction of propagation of the light beam. Thus, if the spatial extent of the disturbed zone in the solution is small, the information contained in the image is small. In the context of interferometry, the consequence could be the appearance of too few fringes or no fringe in the infinite fringe setting and small fringe deformation in the wedge fringe setting. Hence one can measure concentration values only at those points where fringes appear, causing a limitation on the quantity of information that can be extracted directly from a given interferogram. On the other hand, schlieren (monochrome and colour) and shadowgraph generate information about the refractive index field at every pixel of the image in the form of intensities or hue in terms of various colours. This data avoids interpolation errors which are inherently associated with interferometry. In monochrome schlieren and shadowgraph, weak disturbances show up as small changes in intensity and hence contrast whereas in colour schlieren these disturbances show up in various colours and hence various hue values with the use of an appropriate colour filter. The difficulty can be alleviated in monochrome schlieren by using large focal length optics so that small deflections are amplified. In colour schlieren, use of appropriate size of colour filter alliviates the difficulty of weak contrast produced by monochrome schlieren. Instead of getting weak contrast, a good hue variation is obtained for each pixel. In shadowgraph, image quality for visualization purpose can be improved by moving the screen away from the test cell. Additional difficulties with interferometry are the need for maintaining identical experimental conditions during the crystal growth and compensation chambers, careful balancing of the test and the reference beams, and limitations arising from fact that quantitative information is localized at the fringes. This discussion shows that configuring the interferometer as the instrument for on-line process control poses the greatest challenge, schlieren and shadowgraph being relatively simpler. Based on the above discussion, colour schlieren may be considered as an optimum choice while comparing the ease of analysis with the difficulty of instrumentation and image quality.

Chapter 8

PARAMETRIC STUDY OF PROTEIN CRYSTAL GROWTH PROCESS USING COLOUR SCHLIEREN TECHNIQUE

8.1 INTRODUCTION

Colour schlieren technique is used for the parametric study of protein crystal growth process in the present chapter. Images of the 24 hours long time-evolution of the diffusive field in the growth chamber have been recorded. Experiments have been conducted in the free-diffusive regime with an air-reservoir interface. Mass transfer takes place during the equilibration process and diffusive patterns are set-up owing to concentration and hence density differences. In all the experiments the protein drops are adujusted in such a way that they are normal to the direction of the light beam. Crystals are grown after attaining equilibrium and the hanging protein solution becomes supersaturated.

When a drop of protein solution is placed on the coverslip and inverted on the reservoir, the initial vapour pressure difference between the drop and the reservoir solution leads to the evaporation of water from the drop and diffuses into the air gap between the drop and reservoir solution. The local concentration of the protein in the drop increases and reaches the supersaturation level after some time. On attaining supersaturation the protein crystals nucleate out and start growth. With the passage of time, equilibrium takes place and further evaporation stops. On the other hand, the water vapour evaporated out from the drop and diffused into the air, condenses over the air-reservoir interface. Diffusion of condensed water into the reservoir solution takes place. Lower density water condenses over the dense reservoir solution and a concentration gradient develops. Thus, diffusion of water in the reservoir solution takes place and fresh water

descends downwards. The diffusion is visible in the three visualization techniques: as fringe displacement in interferometry, and the spread of light colour in schlieren and spread of intensity in shadowgraph.

In this chapter the effect of various process parameters is studied. The parameters used here are variation of (a) reservoir height, (b) drop concentration, (c) drop radius,

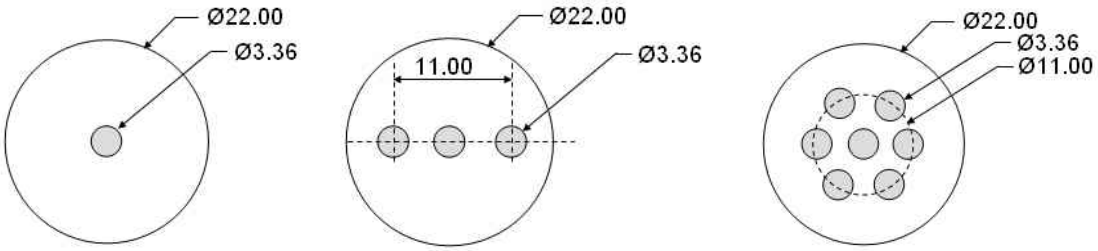

(a) (b) (c)

Figure 8.1: Drop arrangements on the stopper (a) single drop, (b) 3 drops and (c) 7 drops.

(d) number of drops and (e) three drops visualization from two angles. The various drop arrangements placed over the coverslip are shown in Figure 8.1. The three drops have been visualized from two views. In one view a single drop can be seen and in the other view three drops are to be seen.

The rectangular cavity shown in Figure 3.4 is filled with the reservoir solution. The drop of lysozyme solution is held underneath a horizontal surface above the reservoir solution. Vacuum grease is used at the joints to make the entire test cell a closed system. The reservoir solution contains sodium chloride, ethylene glycol and sodium acetate filled up to a certain height of the reservoir. A drop of lysozyme solution prepared in DI water mixed with the reservoir solution is placed on the stopper in an inverted position over the reservoir solution resulting in the hanging drop configuration. The system is sealed by vacuum grease. The concentration level in the drop is such that it is initially unsaturated compared to the reservoir conditions. Hence, the vapour pressure near the reservoir solution is less than that near the drop region. The vapour pressure difference thus created causes the evaporation of water from the drop. Water continues to evaporate from the drop till the vapour pressure difference becomes zero and a state of equilibrium is attained. After attaining equilibrium, the drop becomes supersaturated and lysozyme (a protein) nucleates out in a crystallization process.

8.2 EXPERIMENTS WITH VARIOUS RESERVOIR VOLUMES

Experiments have been conducted to study the effect of reservoir solution volume/height on the size of the drop and diffusion of water into the reservoir solution. In the hanging drop arrangement, seven drops each having 10 μl volume with concentration ratio of 7:3 (p:r) are placed on the cover slide with the help of micropipettes. The drops are arranged in a circular manner so that three drops are visible in the visualization images. In this set of experiments, the effect of reservoir heights on diffusion process as well as reduction in drop radius is studied. The experiments are conducted for various heights obtained from the cavity filled with 25, 50 and 75 ml reservoir solution. Rest of the conditions are kept identical.

Figures 8.2, 8.4 and 8.6 show the transient colour schlieren images recorded during the protein crystal growth process. The reservoir cavity is filled with 25, 50 and 75 ml reservoir solution corresponding to the reservoir heights of 6.35, 12.70 and 19.05 mm respectively. The corresponding Sherwood numbers (Sh), defined as $Sh = kL/D$, Equation 3.2 for air region are 6.59×10^{-4}, 4.88×10^{-4} and 3.19×10^{-4} respectively. For reservoir region Sherwood numbers (Sh) are 338.7, 677.3 and 1016.0 respectively. Table 8.1 gives the Sherwood numbers for reservoir solution and air medium for corresponding reservoir and air heights.

The first image, at time t=0 contains the drops, the reservoir solution, the air above and the air-reservoir interface. The black region at the interface between air and the reservoir solution can be attributed to surface tension at the contact surface between the reservoir solution and the glass window in the viewing direction. Figure 8.2(b) shows the deformation of the interface in the central portion after 7 min with reservoir volume of 25 ml, 10 min in 50 ml reservoir volume Figure 8.4(b), whereas in 10 min in 75 ml reservoir volume as shown in Figure 8.6(b). This is due to the evaporation of water from the drop followed by the condensation of water vapour on the surface of the reservoir. Subsequently, condensation continues while fresh water diffuses into the reservoir. Mass diffusion of the moisture in the reservoir generates its own spread of colours in the interface region (Figure 8.2(c-e), 8.4(c-e) and 8.6(c-e)). In the smallest reservoir volume experiment, the colour spreading and diffusion of water into the reservoir solution is very clear. In this experiment, various vibrant colours can be seen in the whole reservoir (Figure 8.2(e)) as compared to the other heights. This is because the reservoir solution is small and water has to diffuse in smaller reservoir height. Hence the refractive index variation is quite high as compared to the other heights. After 24 hr, the colour schlieren image looks similar to the base image as shown in Figure 8.4(e) and 8.6(e). In the smallest

height experiment this 24 hr colour schlieren image has not been shown. The hanging drops have almost disappeared at this time indicating the completion of the evaporation process. Thus, the evaporation of water has occurred from the protein drop followed by condensation and diffusion into the reservoir solution. The volume of the condensed water being negligible compared to that of the reservoir solution, there is no significant change of colour between the final image and the base image. The colour schlieren images also reveal a continuous reduction in the drop size arising from evaporation.

Figure 4.14 shows the calibration curve between the refractive index and the concentration of NaCl in the reservoir solution obtained from refractometer data. This relationship is used to determine the evolution of the concentration distribution within the reservoir solution and is shown in Figures 8.3, 8.5 and 8.7. The concentration of NaCl is normalized with its maximum value at saturation. The transient evolution of salt concentration in the reservoir arises from the diffusion of the condensed water at the air-solution interface. Figures 8.3, 8.5 and 8.7 correspond to the vertical mid-plane covering the distance from the interface to the base of the cavity. The plot shows a constant initial concentration of NaCl in the reservoir solution (Figures 8.3, 8.5 and 8.7). With condensation of the water at the interface, upto a certain time the concentration of NaCl reduces in the reservoir. The reduction in NaCl concentration is higher in the interface region compared to that away from it. Later, the average NaCl concentration increases with time (Figures 8.3, 8.5 and 8.7). This trend is attributed to both the reduction in the evaporation rate of the drop and also the diffusion of the fresh water into the reservoir solution. At t=24 h, the drop has completely evaporated and NaCl concentration attains a distribution similar to the initial (t=0) value. The negligible difference between the initial and final NaCl concentration is because of a very small water content in the evaporating drops.

Table 8.1: Sherwood number (Sh) for reservoir solution and air.

Res sol vol (ml)	Res height (mm)	Air region height (mm)	Sh_{res}	Sh_{air}
25	6.35	24.65	338.7	6.59×10^{-4}
50	12.70	18.30	677.3	4.88×10^{-4}
75	19.05	11.95	1016.0	3.19×10^{-4}

The comparison of the concentration profiles of NaCl in reservoir solution for the varying reservoir volumes (25, 50, and 75 ml) at time instants (a) 0.5, (b) 1, (c) 2, (d) 4 and (e) 5 h are shown in Figure 8.8. From these profiles panetration depth is clearly seen which is nearly equal to the corresponding reservoir heights. A very steep slop is seen in smallest reservoir height. In 50 and 75 ml reservoir volume solution the NaCl

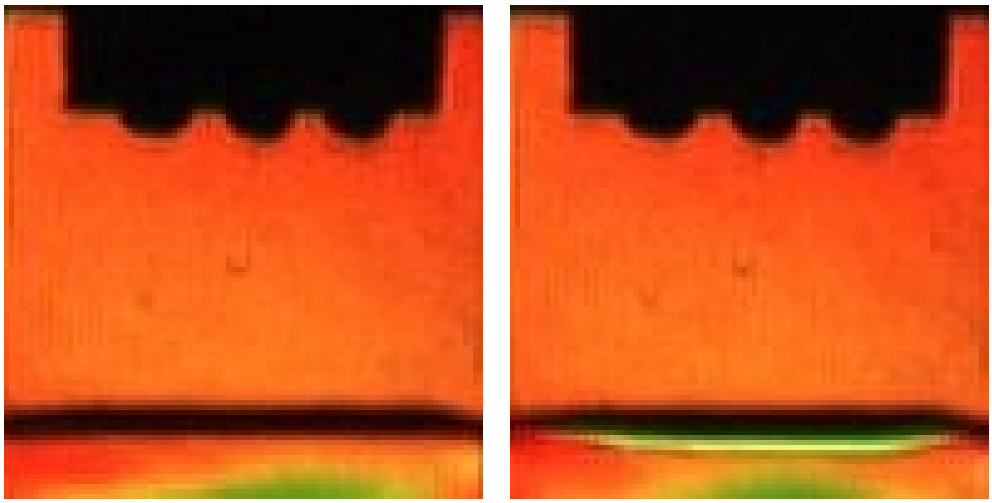

(a) t=0 (b) t=7 min

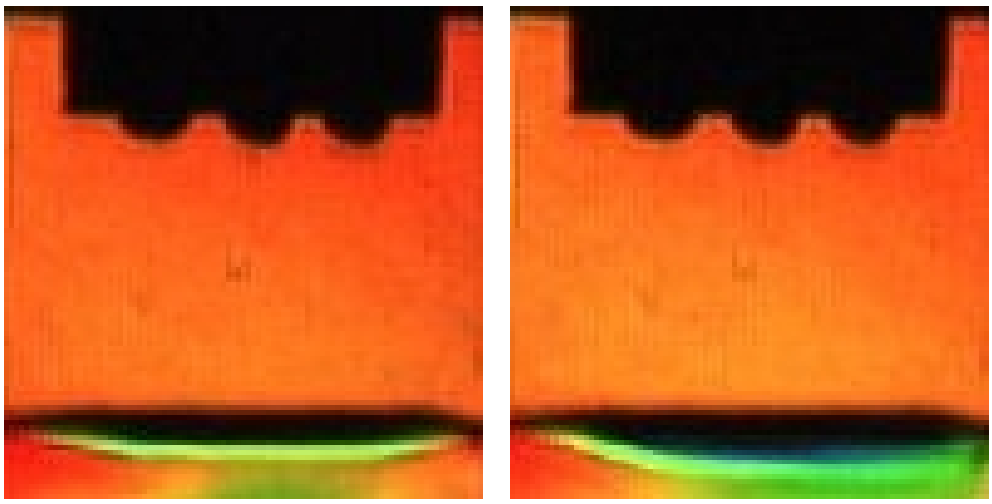

(c) t=15 min (d) t=0.5 h

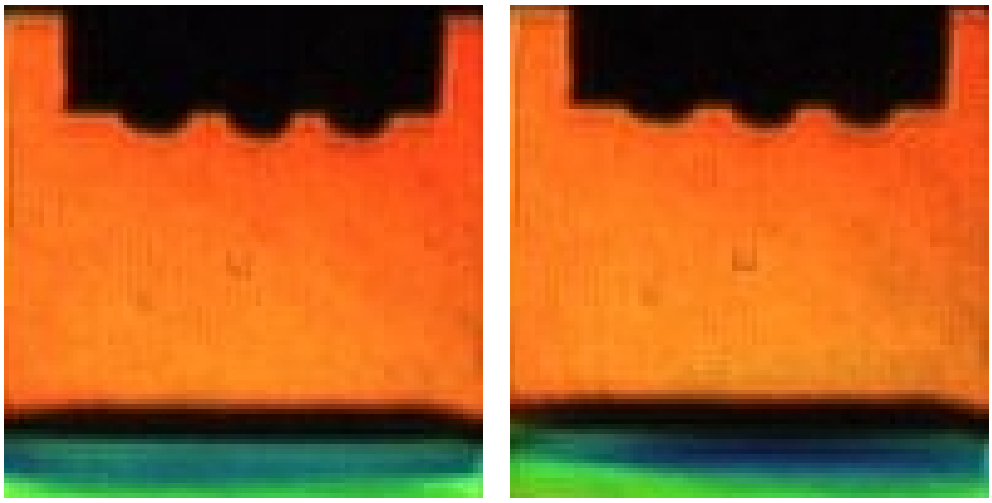

(e) t=4 h (f) t=6 h

Figure 8.2: Colour schlieren images of transient evolution of the diffusive field in the reservoir solution during lysozyme protein crystallization. Drop concentration = 7:3 and size = 10 μl, 7 drops, 25 ml reservoir solution.

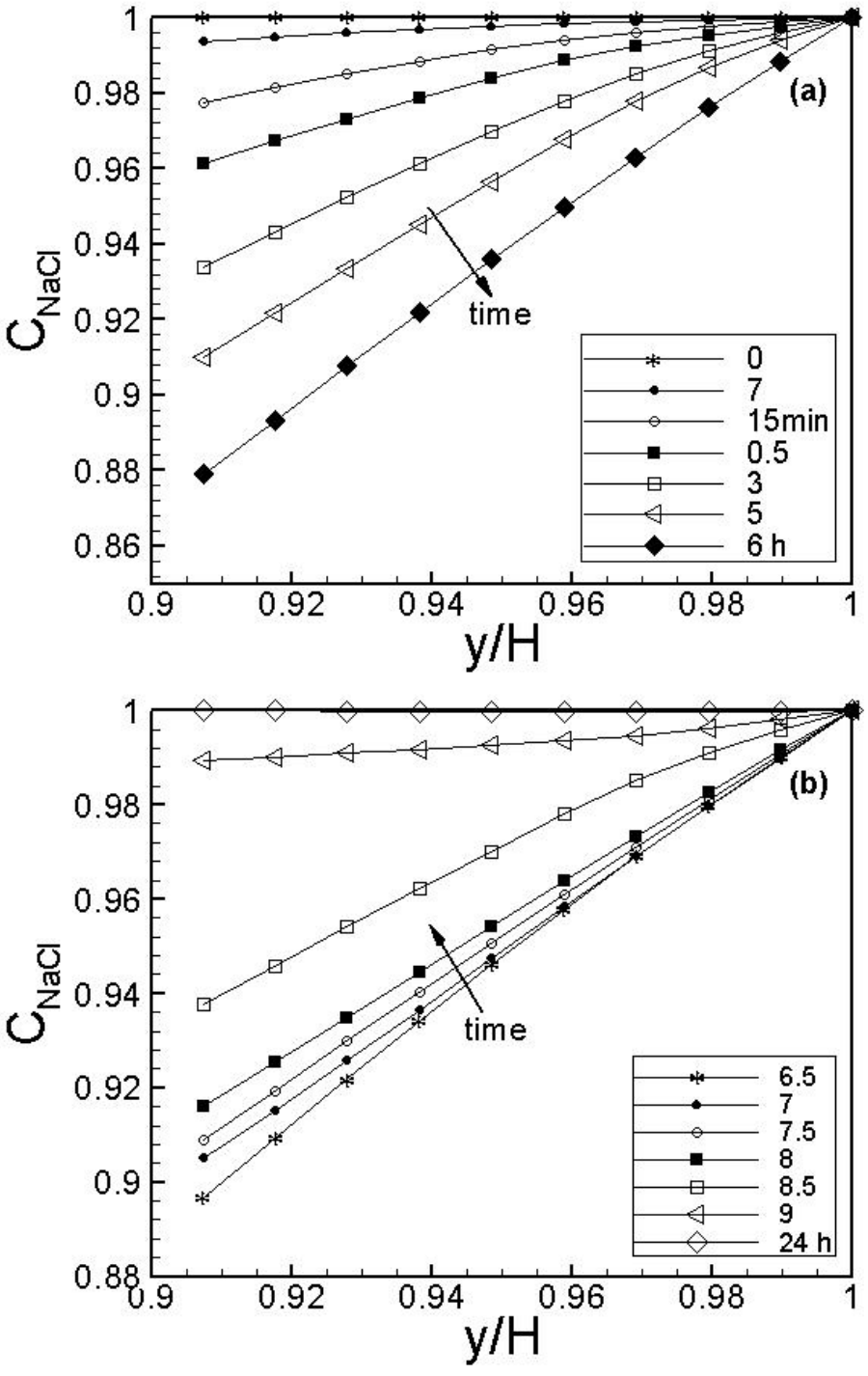

Figure 8.3: Transient evolution of NaCl concentration in the reservoir solution for 7:3 drop concentration. 7 drops of 10 μl volume each with 25 ml reservoir solution is considered. (a) Decreasing concentration of NaCl in reservoir solution. (b) Incresing concentration of NaCl in reservoir solution.

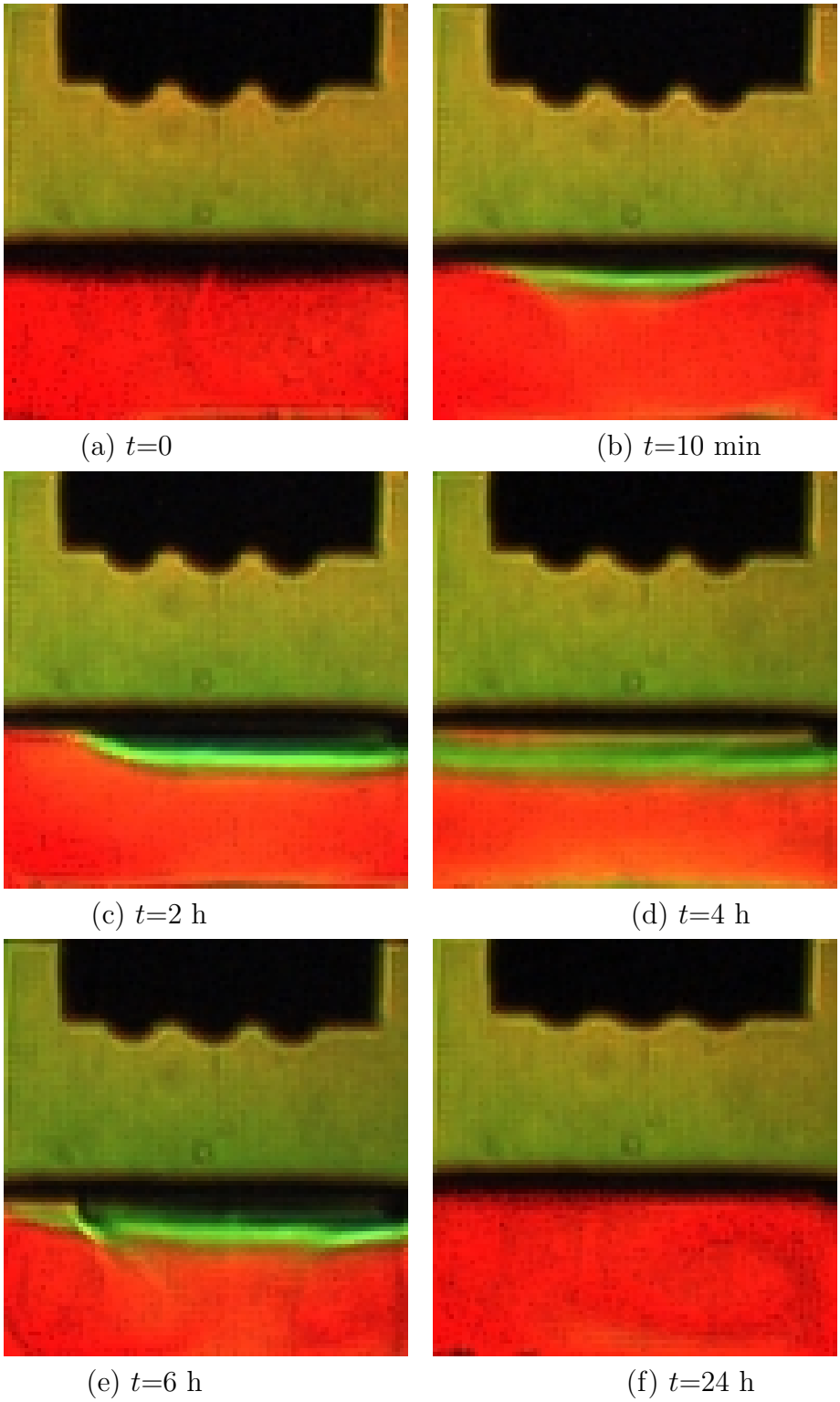

(a) t=0 (b) t=10 min

(c) t=2 h (d) t=4 h

(e) t=6 h (f) t=24 h

Figure 8.4: Colour schlieren images of transient evolution of the diffusive field in the reservoir solution during lysozyme protein crystallization. Drop concentration = 7:3 and size = 10 μl, 7 drops, 50 ml reservoir solution.

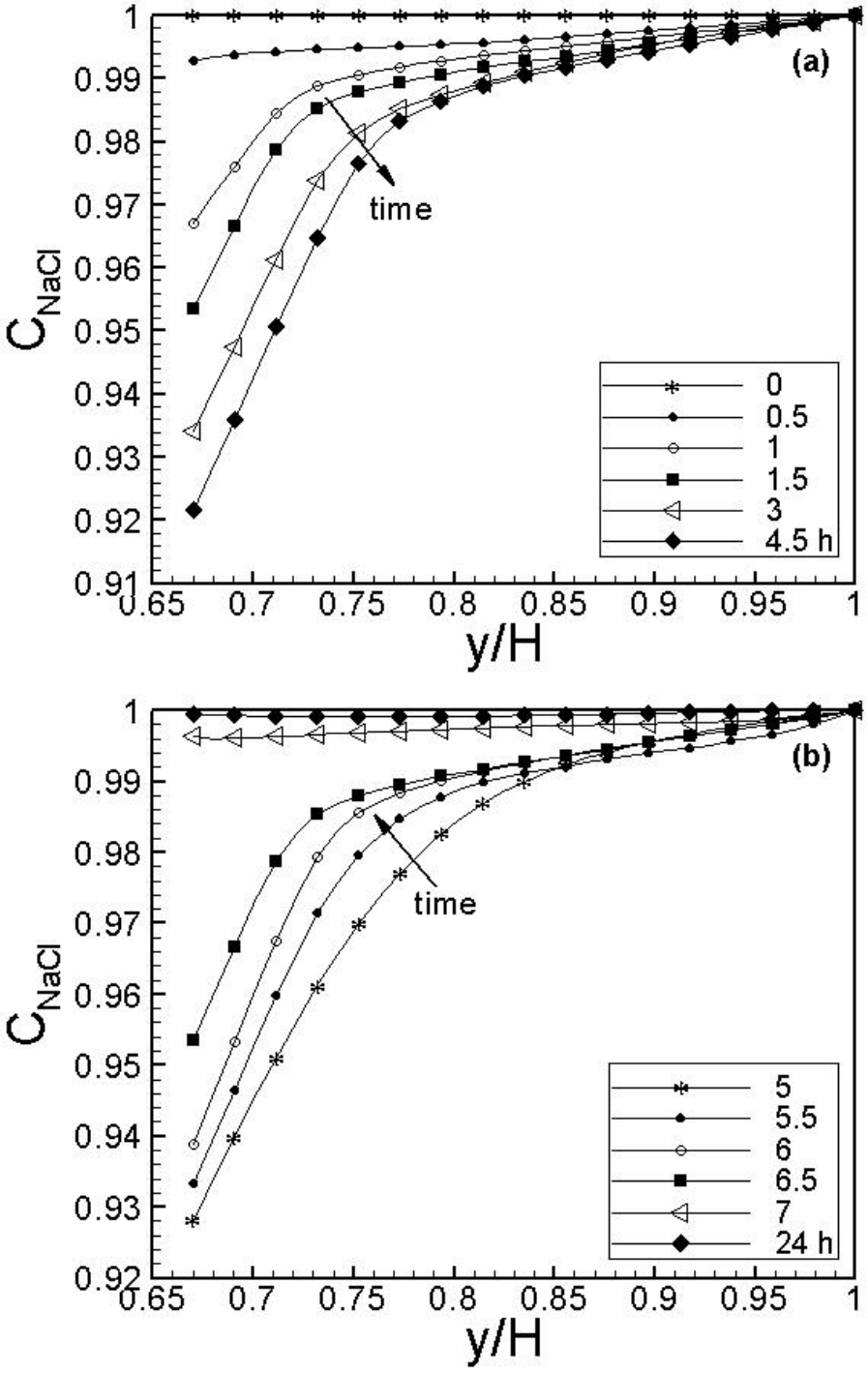

Figure 8.5: Transient evolution of NaCl concentration in the reservoir solution for 7:3 drop concentration. 7 drops of 10 μl volume each with 50 ml reservoir solution is considered. (a) Decresing concentration of NaCl in reservoir solution. (b) Increasing concentration of NaCl in reservoir solution.

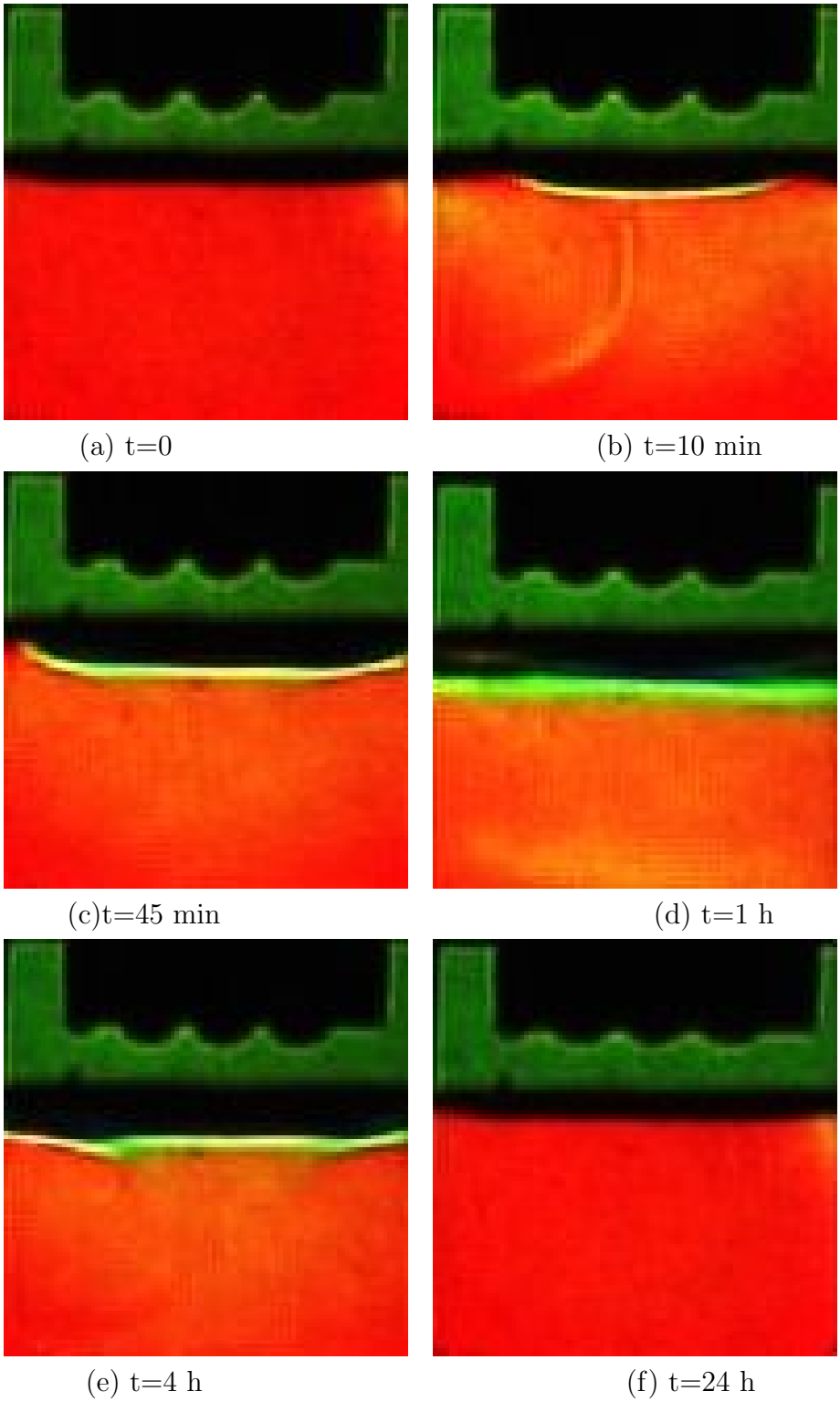

(a) t=0 (b) t=10 min

(c)t=45 min (d) t=1 h

(e) t=4 h (f) t=24 h

Figure 8.6: Colour schlieren images of transient evolution of the diffusive field in the reservoir solution during lysozyme protein crystallization. Drop concentration = 7:3 and size = 10 μl, 7 drops, 75 ml reservoir solution.

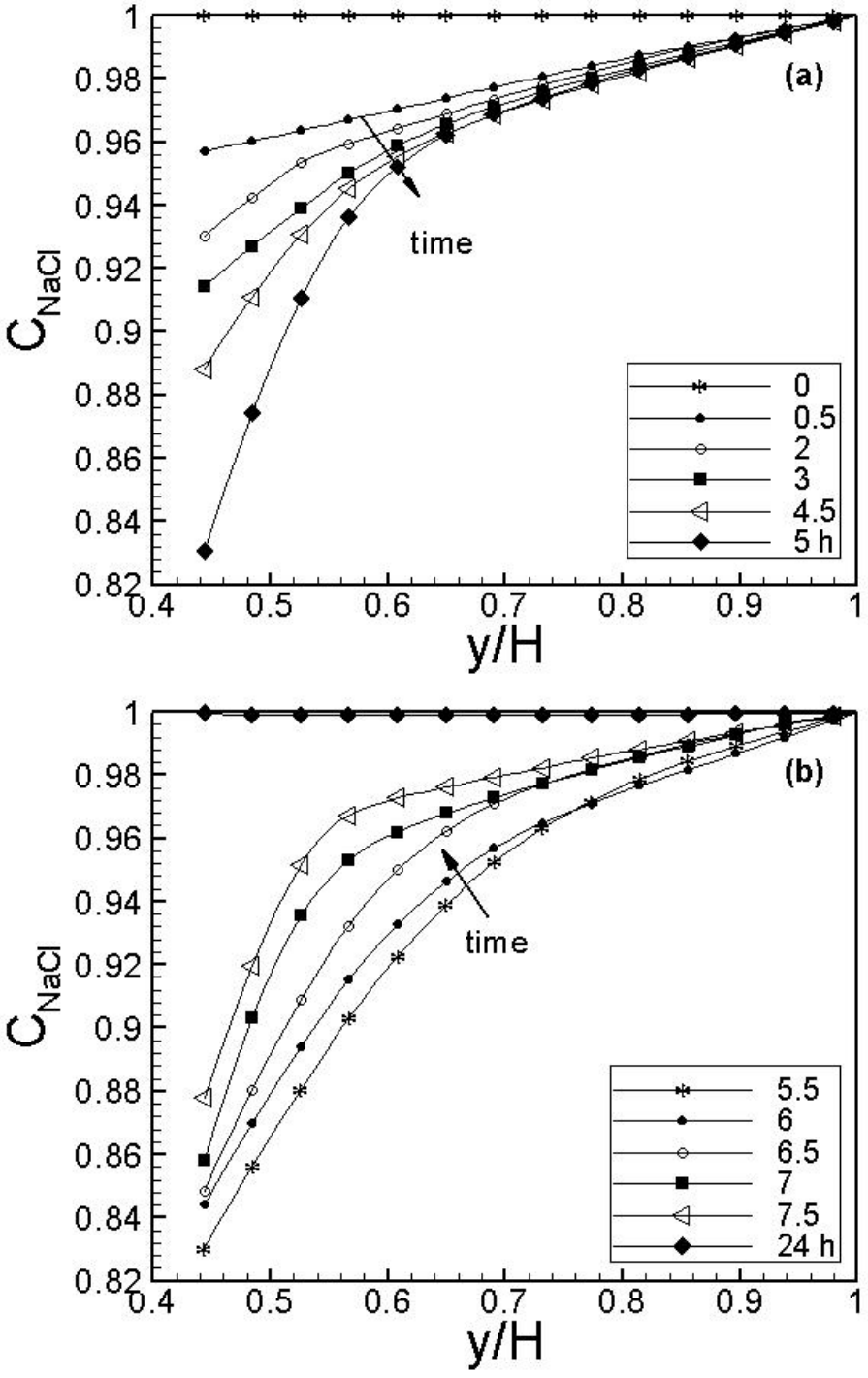

Figure 8.7: Transient evolution of NaCl concentration in the reservoir solution for 7:3 drop concentration. 7 drops of 10 μl volume each with 75 ml reservoir solution is considered. (a) Decreasing concentration of NaCl in reservoir solution. (b) Increasing concentration of NaCl in reservoir solution.

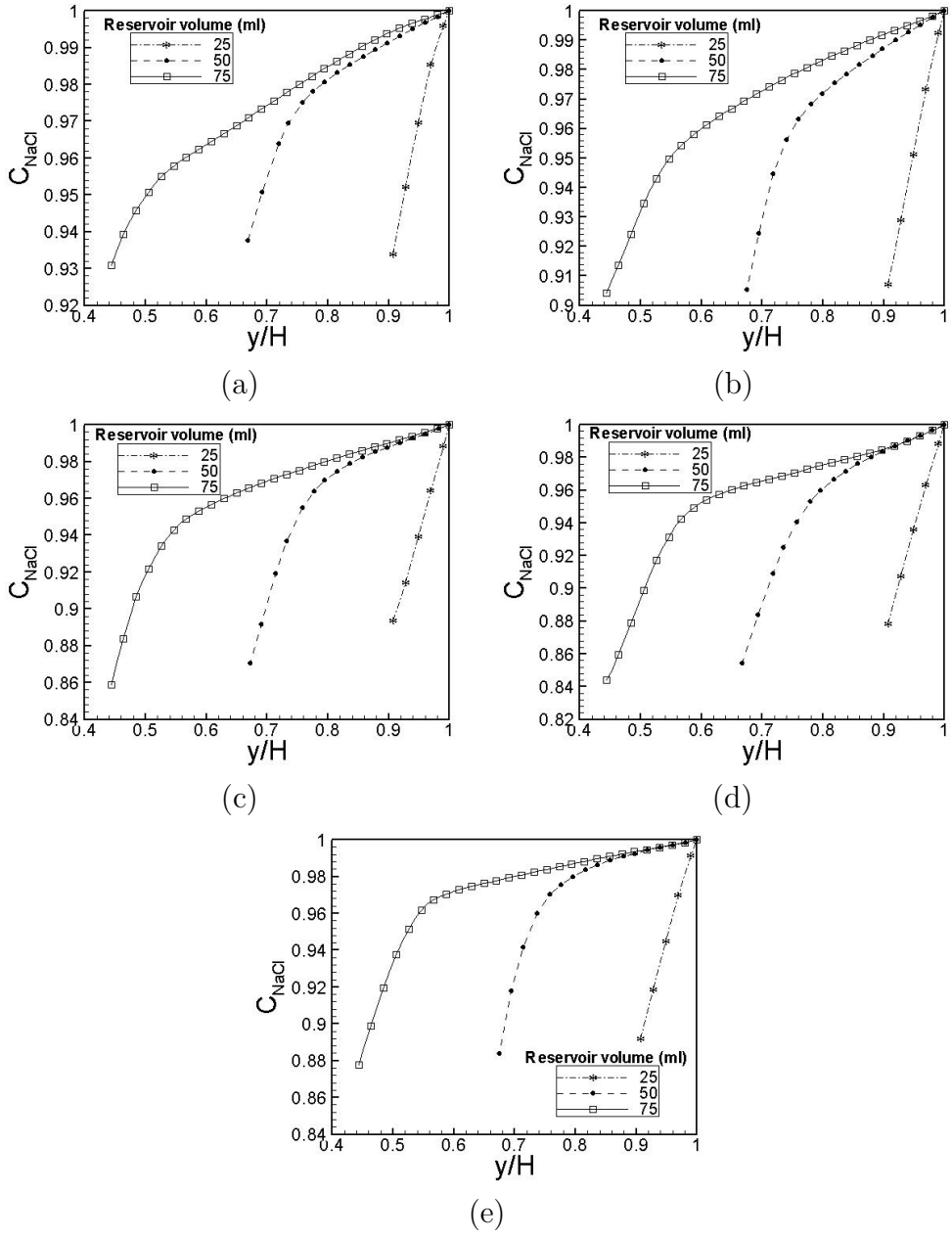

Figure 8.8: Comparison of the concentration profiles of NaCl in reservoir solution when the reservoir volume is varied. Drop volume = 10 μl, p:r = 7:3, and 7 drops at time instants of (a) 0.5 h, (b) 1 h, (c) 2 h, (d) 4 h and (e) 5 h have been used.

concentration change rapidly near interface region. For 50 ml sollution, upto a y/H=7.4 it decreases rapidly and then further slowly decreases. In 75 ml reservoir solution volume, the concentration of NaCl is rapidly changing upto y/H=0.55 and then slowly drops. It is observed that the NaCl concentration is approximately same till 1 hr.

The following section describes the radius profile of the drop as it decreases in

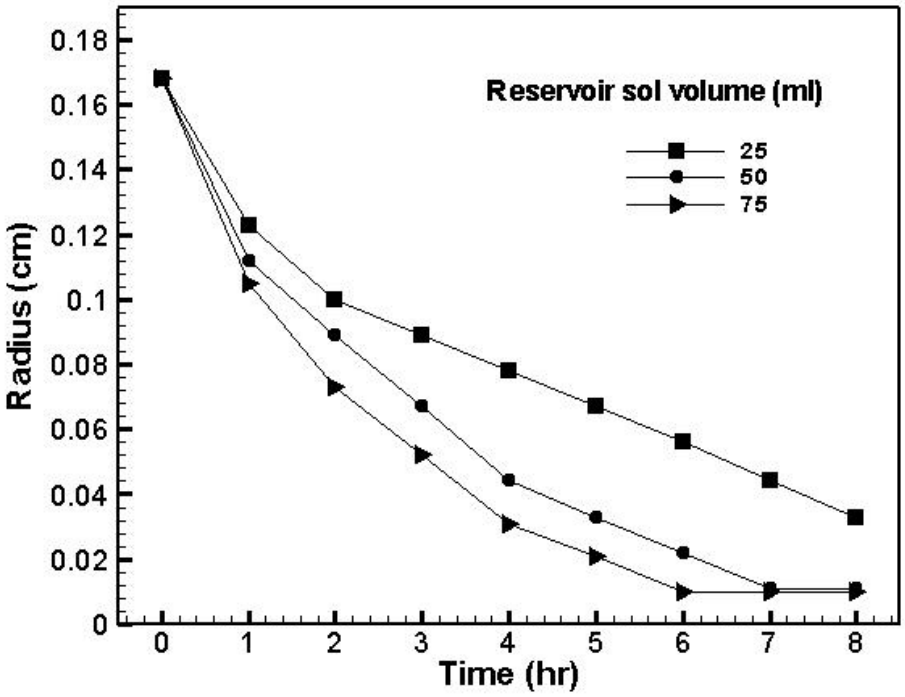

Figure 8.9: Evolution of drop radius at various reservoir volumes. Drop volume = 10 μl, p:r = 7:3, and 7 drops have been considered.

size with evaporation of water. The initial drop radius is determined using the known

Table 8.2: Reduction in drop radius (mm) at various reservoir volumes (v) (ml)

v/time	0	1	2	3	4	5	6	7	8 h
25	0.0168	0.0123	0.0100	0.0089	0.0078	0.0067	0.0056	0.0044	0.0044
50	0.0168	0.0112	0.0089	0.0067	0.0044	0.0033	0.0022	0.0011	0.0011
75	0.0168	0.0105	0.0073	0.0052	0.0031	0.0021	0.0010	0.0010	0.0010

volume of the drop. The final radius is obtained by counting the number of pixels of the image recorded. It is seen that the radius decreases rapidly at the start and finally slows off once the crystals start forming. Since evaporation starts off rapidly, the radius of the drop decreases rapidly. When reservoir height is varied, the rate of decrease of radius is the highest for the highest reservoir height. Figure 8.9 shows the effect of reservoir

volume on drop radius with respect to time. Table 8.2 shows the corresponding variation of drop radius.

8.3 EXPERIMENTS WITH VARYING DROP CONCENTRATIONS

To study the effect of drop concentration on the equilibration process and hence crystal growth, experiments have been conducted with various drop concentrations. Drop concentration is defined as the protein solution:reservoir solution volume (p:r). Here, 7:3, 8:2 and 9:1 concentration ratios have been considered. Figures 8.10, 8.12 and 8.14 show the transient colour schlieren images recorded during the protein crystal growth process. The reservoir cavity is filled with 50 ml reservoir solution with a drop size of 10 μl. Figures 8.10, 8.12 and 8.14 have 7:3, 8:2 and 9:1 concentrations respectively. The drop radius is calculated as 0.168 mm by assuming hemispherical shape of the drop.

Figures 8.11 8.13 8.15 show the transient evolution of NaCl concentration in the reservoir solution for 7:3, 8:2 and 9:1 drop concentration for (a) decreasing normalized concentration of NaCl and (b) increasing normalized concentration of NaCl in the reservoir solution respectively. From these transient curves, it is seen that upto a certain time the NaCl concentration in the reservoir decreases. Later, concentration of NaCl increases with time. After 24 hours the concentration of reservoir solution remains unchanged and reaches a level close to that of the initial concentration. The phenomenon of decreasing and increasing concentration of NaCl in reservoir occurs because of the following reason: As the evaporated water vapour condenses on the reservoir solution, diffusion of water molecules into the reservoir solution starts. Due to the diffusion of water into the reservoir, concentration changes locally in the solution. After a certain time interval, all the condensed water diffuses into the solution. Now the water molecules spread into the entire reservoir leading to an increase in the concentration of NaCl at the interface. The drop size and hence the amount of water evaporated from the drop are very small when compared to the reservoir solution. Hence there is no any significant change in reservoir volume as well as net concentration of NaCl in solution. Therefore, the last colour schlieren image is similar to the first.

Figure 8.16 shows comparison of the concentration of NaCl in reservoir solution for the drop concentrations of 7:3, 8:2 and 9:1 at time instants (a) 0.5 h, (b) 1 h, (c) 2 h, (d) 4 h and (e) 5 h. From these curves it is observed that the NaCl concentration variation is the smallest in higher protein content drop that is 9:1. In 7:3, the variation is the largest. It is because water content in 9:1 drop concentration is less than that of the 7:3 drop. Hence, on evaporation, small amount of water is released from the drop.

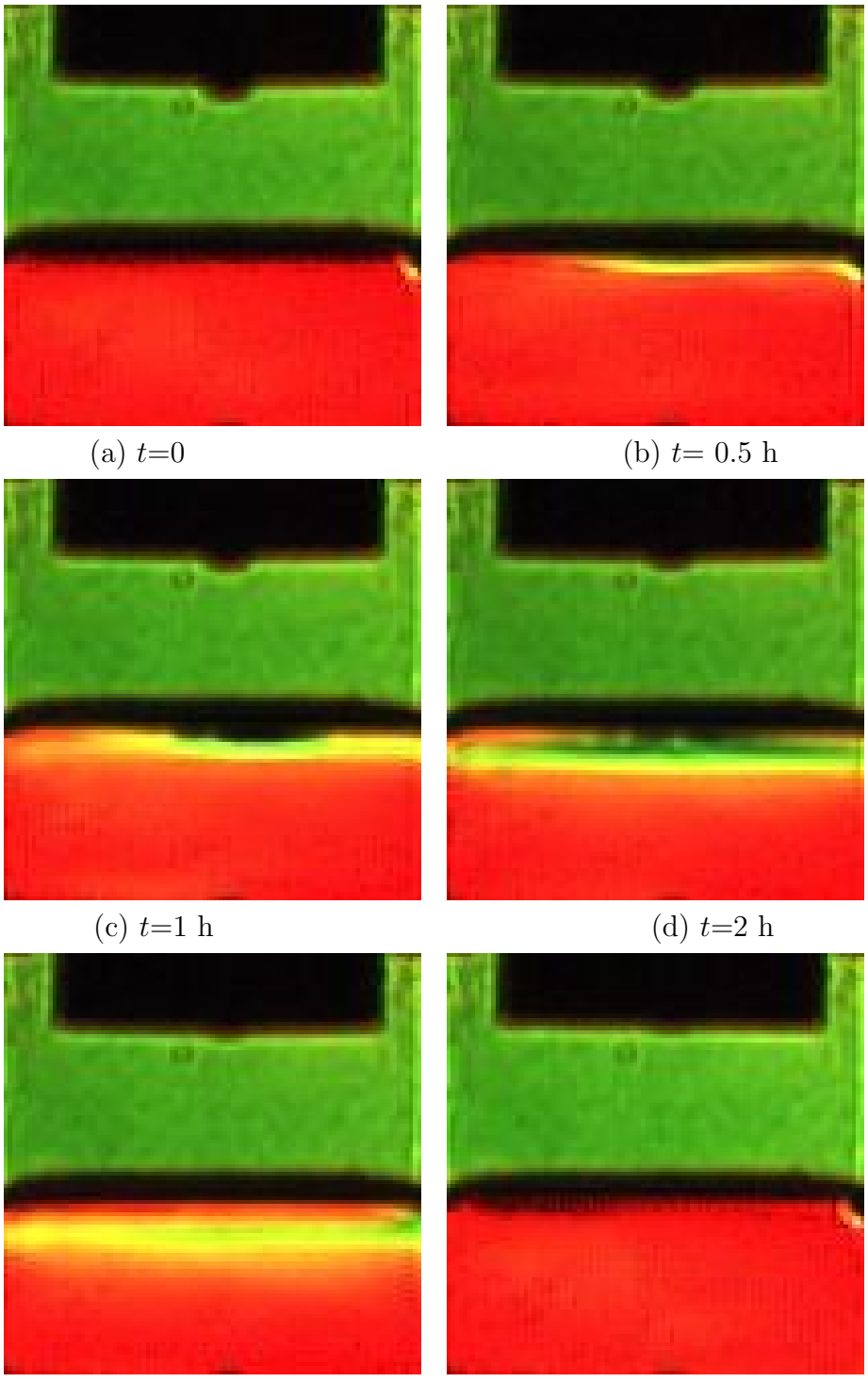

(a) t=0 (b) t= 0.5 h

(c) t=1 h (d) t=2 h

(e) t=4 h (f) t=24 h

Figure 8.10: Colour schlieren images of transient evolution of the diffusive field in the reservoir solution during lysozyme protein crystallization. Drop concentration = 7:3 and size = 10 μl, single drop, 50 ml reservoir solution.

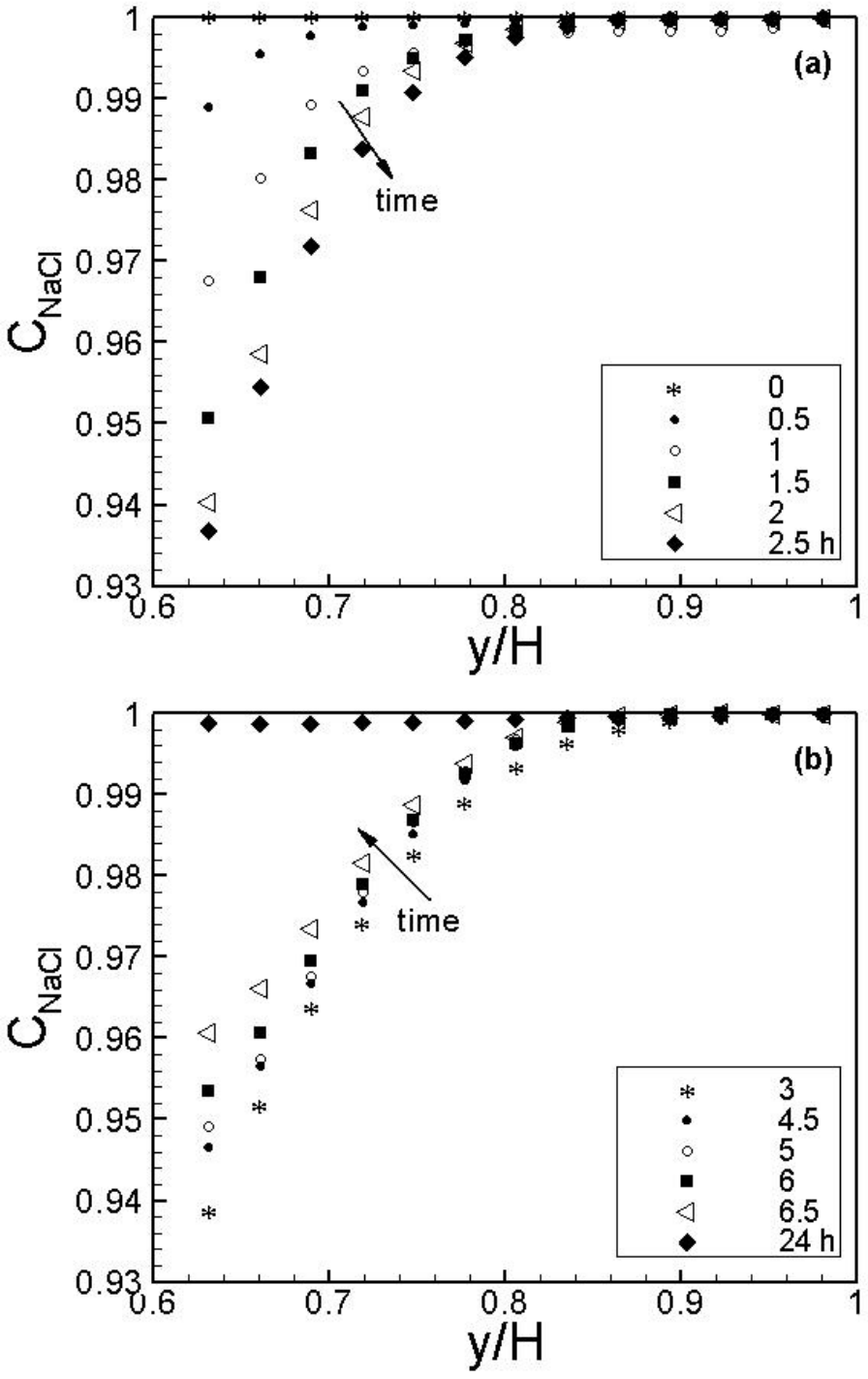

Figure 8.11: Transient evolution of NaCl concentration in the reservoir solution for 7:3 drop concentration. Single drop of 10 μl volume with 50 ml reservoir solution is considered. (a) Decreasing concentration of NaCl in reservoir solution. (b) Increasing concentration of NaCl in reservoir solution.

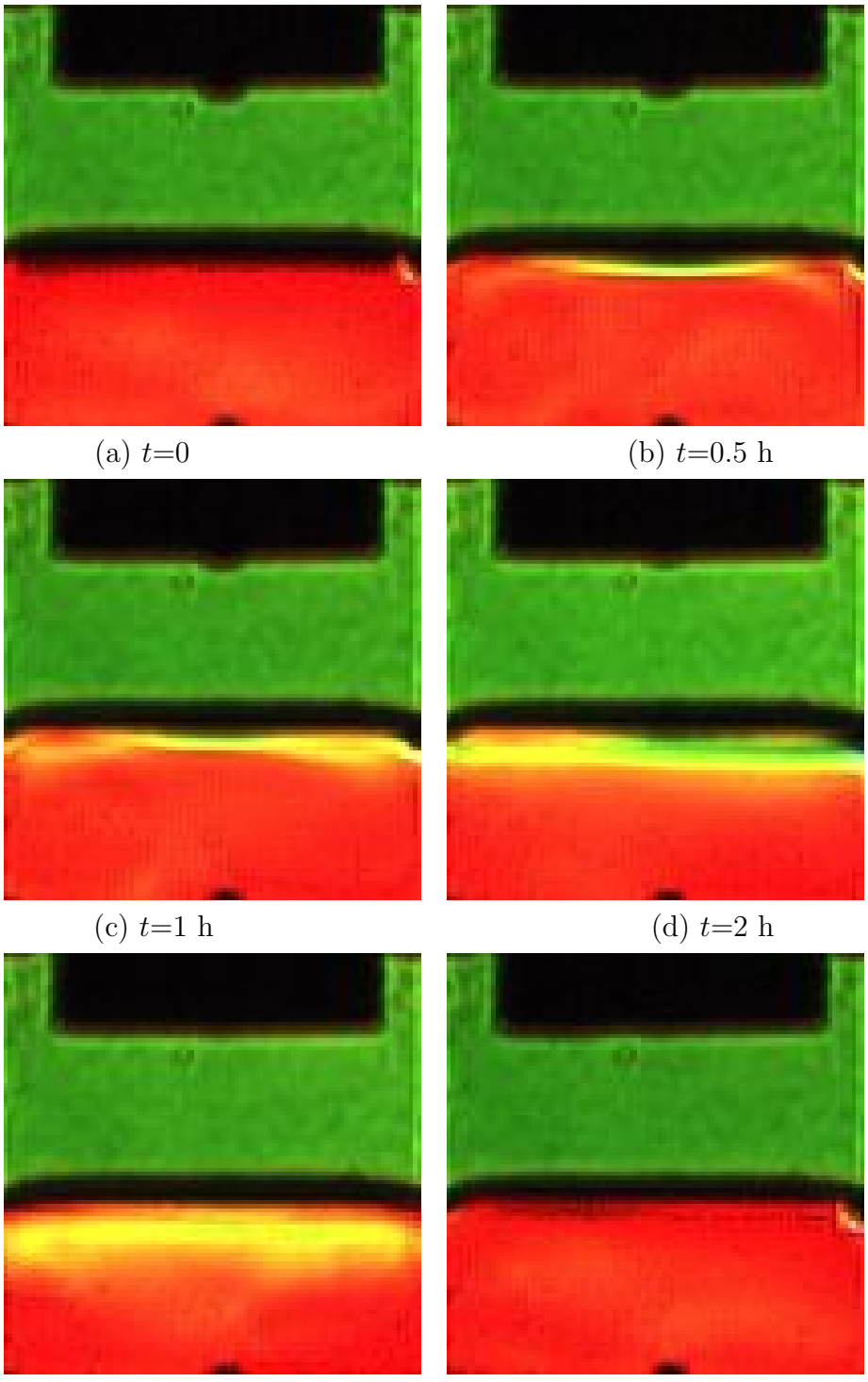

(a) t=0 (b) t=0.5 h

(c) t=1 h (d) t=2 h

(e) t=4 h (f) t=24 h

Figure 8.12: Colour schlieren images of transient evolution of the diffusive field in the reservoir solution during lysozyme protein crystallization. Drop concentration = 8:2 and size = 10 μl, single drop, 50 ml reservoir solution.

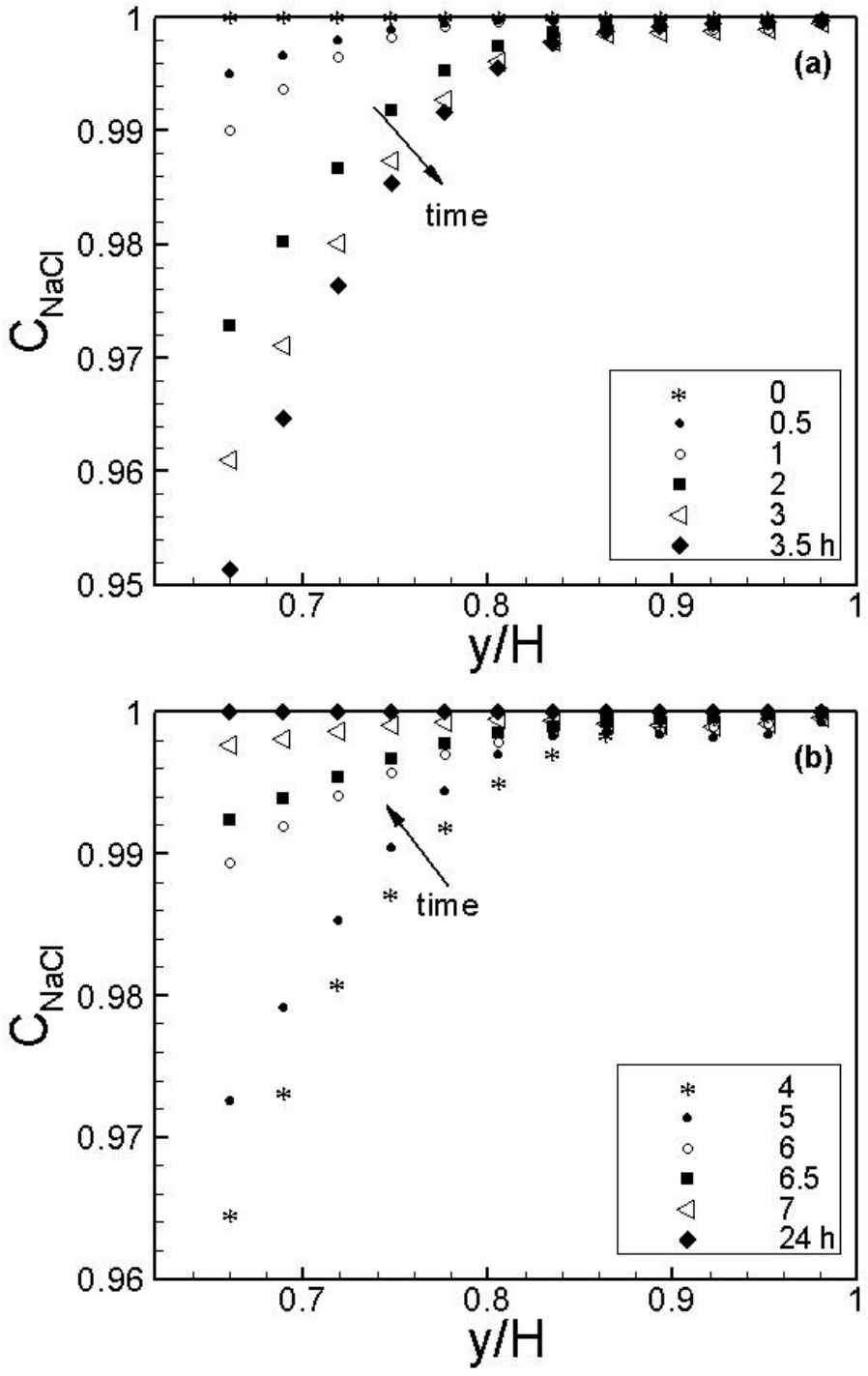

Figure 8.13: Transient evolution of NaCl concentration in the reservoir solution for 8:2 drop concentration. Single drop of 10 μl volume with 50 ml reservoir solution is considered. (a) Decreasing concentration of NaCl in reservoir solution. (b) Increasing concentration of NaCl in reservoir solution.

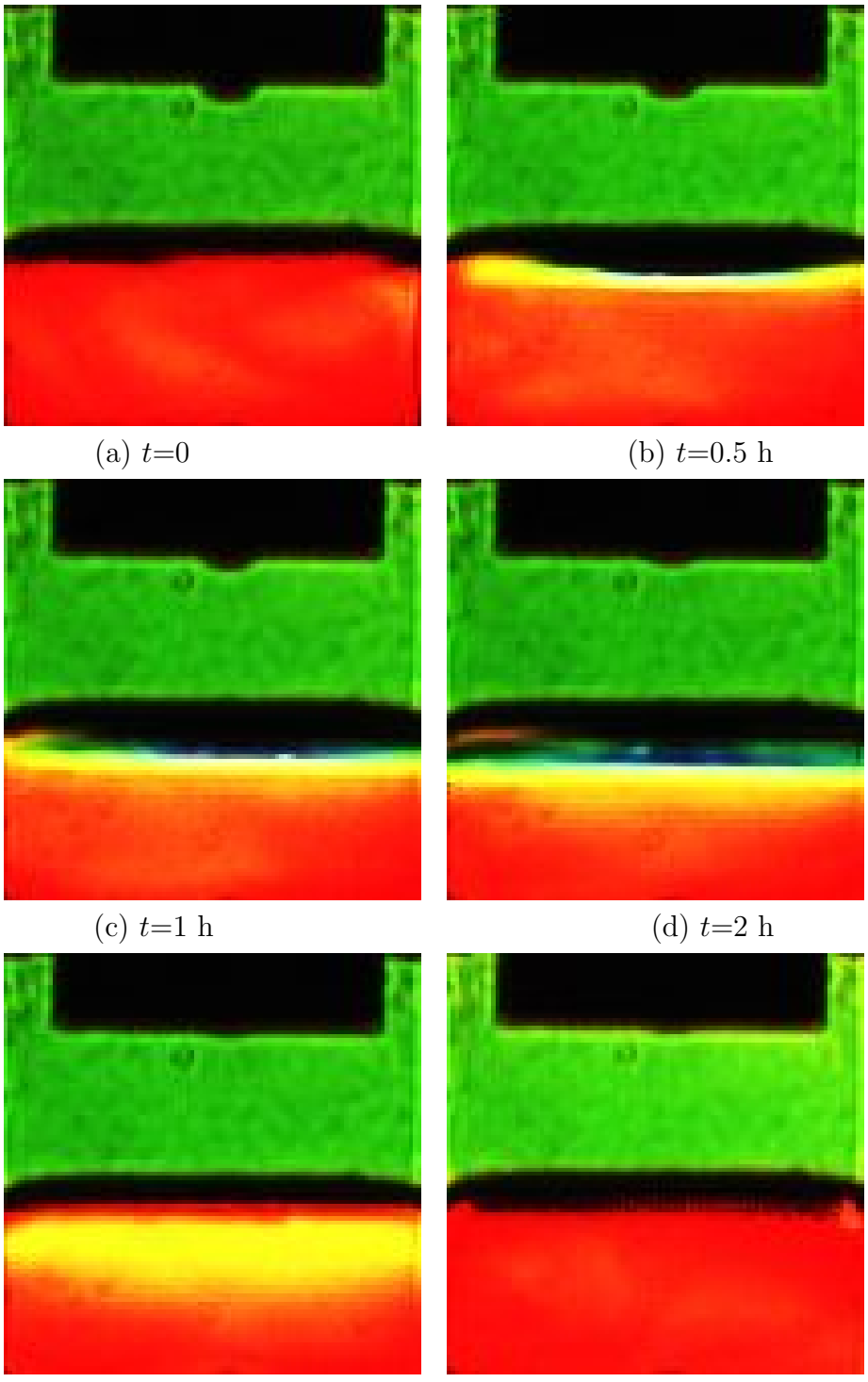

(a) t=0 (b) t=0.5 h

(c) t=1 h (d) t=2 h

(e) t=4 h (f) t=24 h

Figure 8.14: Colour schlieren images of transient evolution of the diffusive field in the reservoir solution during lysozyme protein crystallization. Drop concentration = 9:1 and size = 10 μl, single drop, 50 ml reservoir solution.

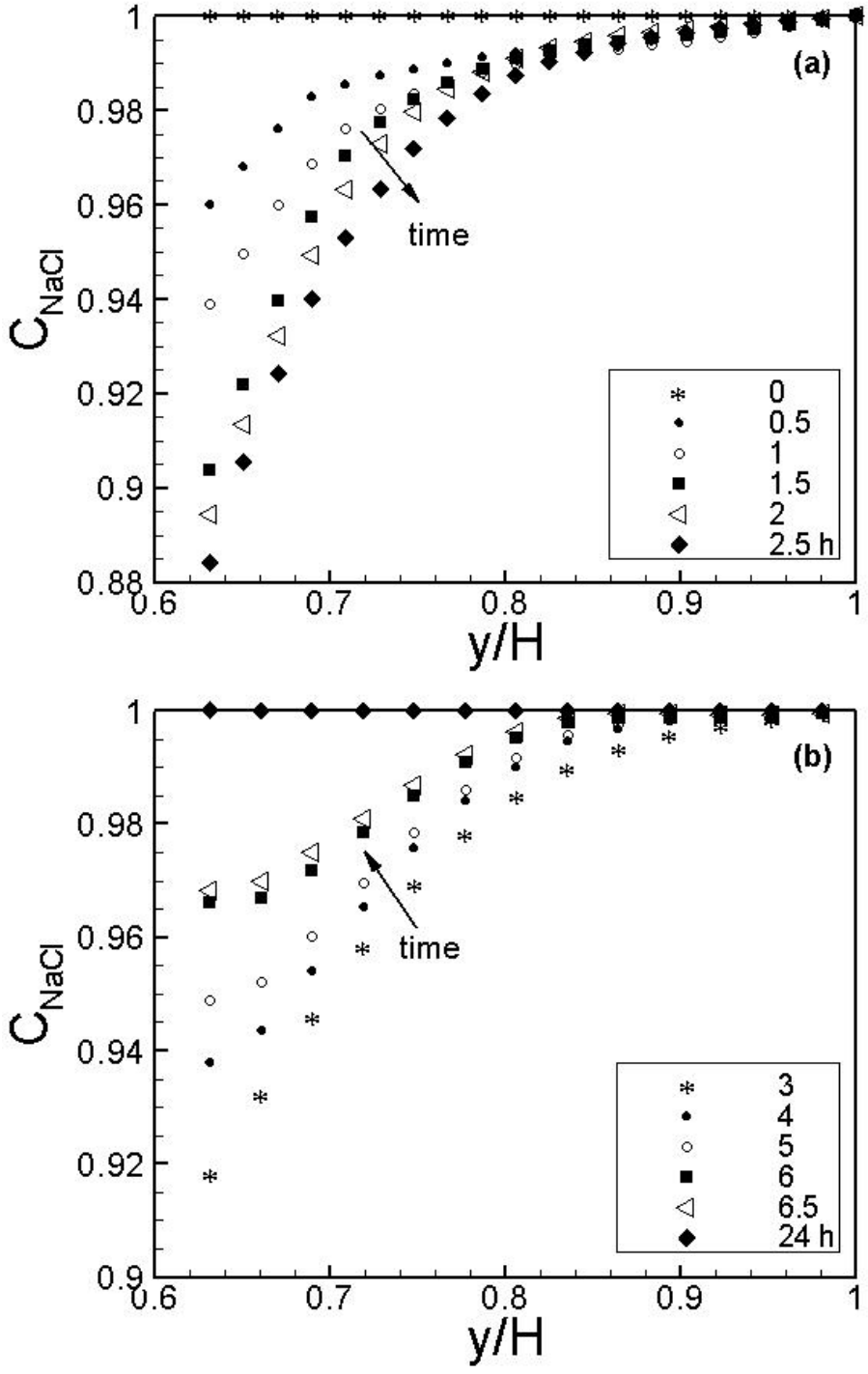

Figure 8.15: The transient evolution of NaCl concentration in the reservoir solution for 9:1 drop concentration. Single drop of 10 μl volume with 50 ml reservoir solution is considered. (a) Decreasing concentration of NaCl in reservoir solution. (b) Increasing concentration of NaCl in reservoir solution.

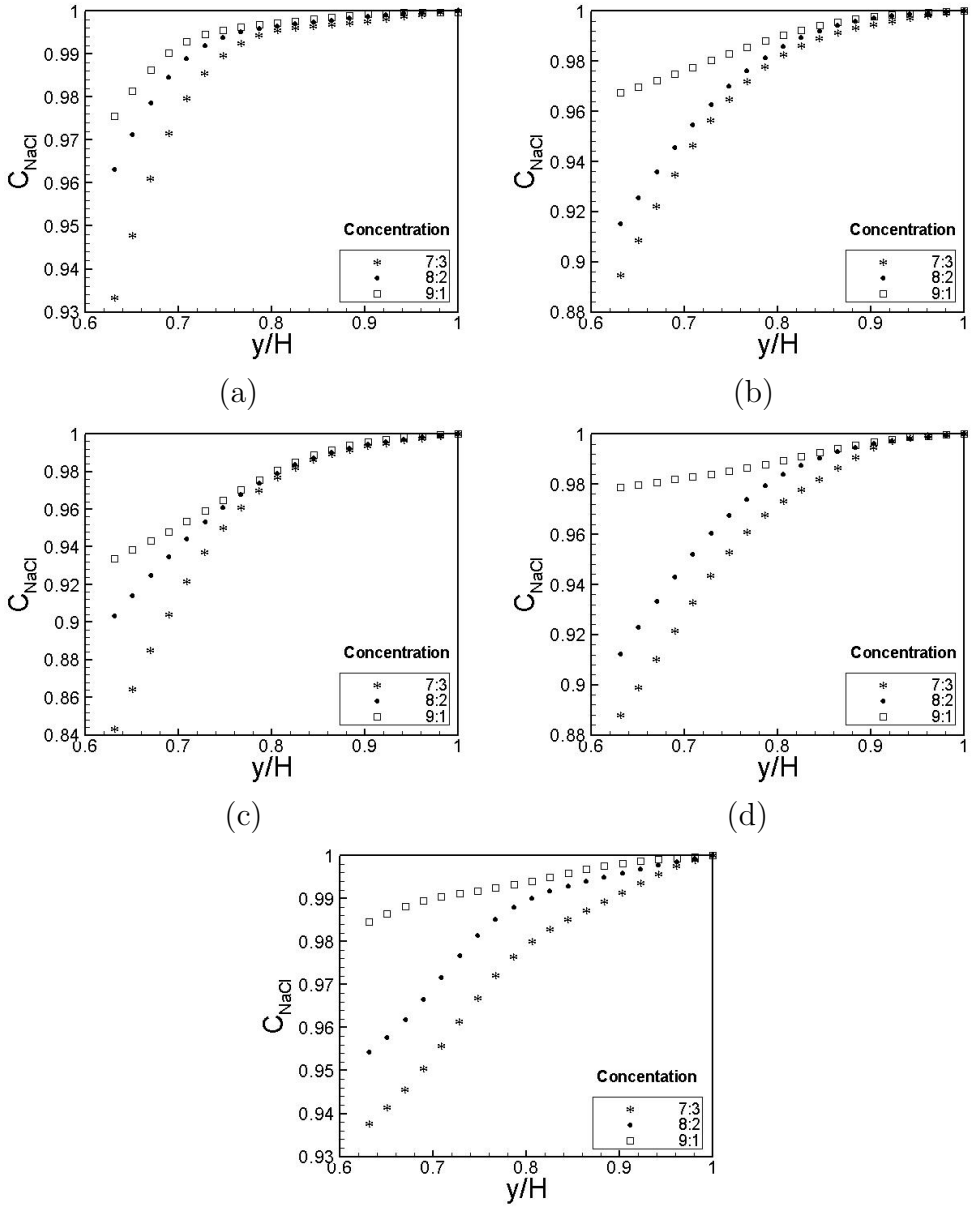

Figure 8.16: Comparison of the concentration profiles of NaCl in reservoir solution when the drop concentration (p:r) is varied. Drop volume = 10 μl, reservoir volume = 50 ml at time instants of (a) 0.5 h, (b) 1 h, (c) 2 h, (d) 4 h and (e) 5 h have been used.

From a drop of 7:3 concentration, a large amount of water is evaporated causing a large reduction in NaCl concentration in the solution.

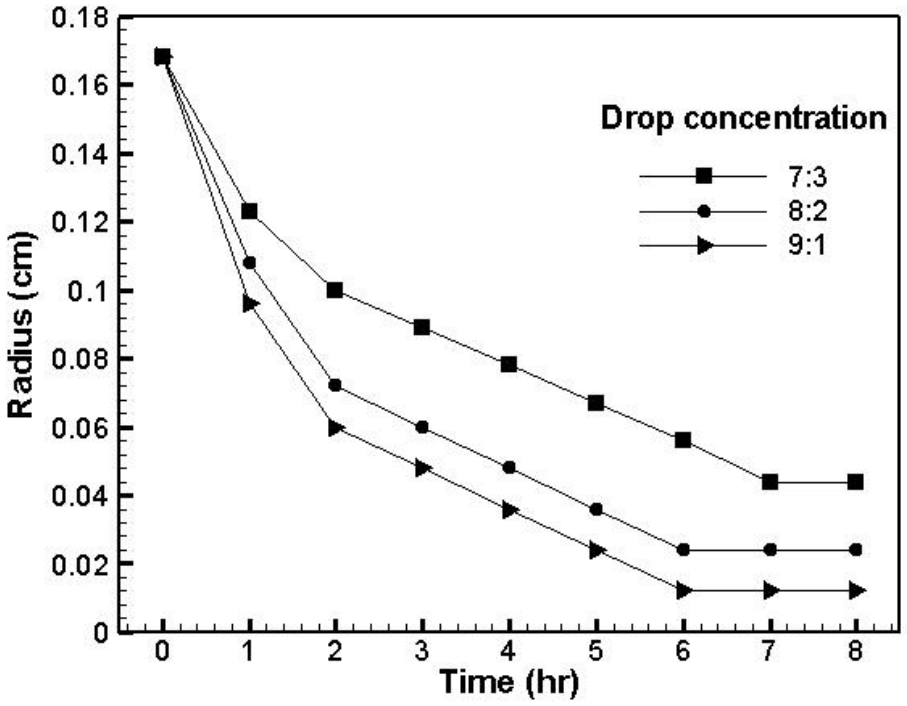

Figure 8.17: Evolution of drop radius at various drop concentrations. Drop volume = 10 μl, single drop, reservoir volume = 50 ml

Table 8.3: Reduction in drop radius (mm) at various drop concentrations (p:r)

p:r/time	0	1	2	3	4	5	6	7	8 h
7:3	0.0168	0.0123	0.0100	0.0089	0.0078	0.0067	0.0056	0.0044	0.0044
8:2	0.0168	0.0108	0.0072	0.0060	0.0048	0.0036	0.0024	0.0024	0.0024
9:1	0.0168	0.0096	0.0060	0.0048	0.0036	0.0024	0.0012	0.0012	0.0012

The drop radius decreases in size with evaporation of water. The initial drop radius is determined by using the known volume of the drop. The final radius is obtained by counting the number of pixels of the image recorded. It is seen that the radius decreases rapidly at the start and finally slows off once the crystals start to form. Since evaporation starts off rapidly, the radius of the drop decreases rapidly.

When the concentration (p:r) is varied, it is seen that the crystals form early in the case of the highest concentration. The number of crystals formed is also the largest in this case. The drop with the highest concentration contains the largest protein content.

This results in a large number of crystals being formed. Since the concentration is high, the water content in the drop is less. As the water evaporates, it takes less time for the protein drop to reach supersaturation. Hence, crystals are readily formed. Equilibrium is also attained soon. The reduction in drop radius with time is shown in Table 8.3. Figure 8.17 shows the variation of drop radius with time on varying the concentration of the drop medium. The rate of decrease is the largest with the highest concentration. This shows that evaporation is the most rapid in this experiment.

8.4 EXPERIMENTS WITH VARYING DROP SIZE

Experiments have been performed to study the effect of drop size on the protein crystal growth process. Figures 8.18, 8.20 and 8.22 show the colour schlieren images for the crystal growth process having drop sizes of 10, 15 and 20 μl. The drop concentration in this case is taken as 8:2 with 50 ml volume of reservoir solution. Since the drop sizes vary, so does the water evaporated from the drops. The smallest drop will produce the least amount of water and the largest drop produces the largest amount of water. The colour schlieren images show this trend in terms of colours and depth near the interface. Figure 8.18(c) for 10 μl drop shows fewer number of colours near the interface as compared to those obtained in Figure 8.20(c) for 15 μl and Figure 8.22(c) for 20 μl. Number of colours increases with increase of drop size.

To extract data from the colour schlieren images, the relationship between refractive index and NaCl concentration in reservoir solution is required. This relationship is used to determine the evolution of the concentration distribution within the reservoir solution and is shown in Figures 8.19, 8.21 and 8.23. The concentration of NaCl is normalized with its maximum value at saturation. The transient evolution of salt concentration in the reservoir arises from the diffusion of the condensed water at the air-solution interface. These data correspond to the vertical mid-plane covering the distance from the interface to the base of the cavity. The plot shows a constant initial concentration of NaCl in the reservoir solution (Figures 8.19(a), 8.21(a) and 8.23(a)). With condensation of water at the interface, the concentration of NaCl reduces with time till t=3.5 h. The reduction in NaCl concentration is higher in the interface region compared to that away from it. After 3.5 h, the average NaCl concentration increases (Figures 8.19(b), 8.21(b) and 8.23(b)). This trend is attributed to both the reduction in the evaporation rate of the drop and also the diffusion of the fresh water into the reservoir solution. At t=24 h, the drop has completely evaporated and NaCl concentration attains a distribution similar to the initial. Negligible difference between the initial and final NaCl concentration is because of a very small water content in the evaporating drops. For the 10 μl drop the

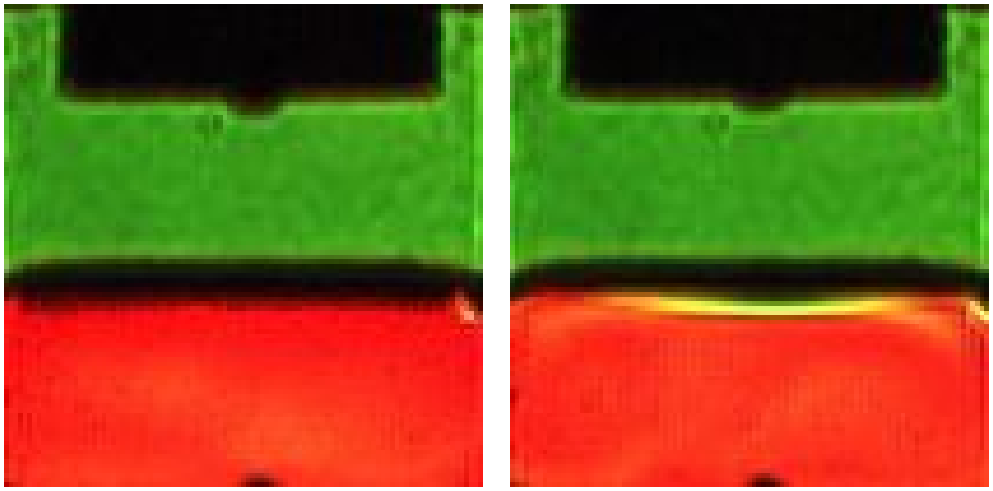

(a) t=0

(b) t=30min

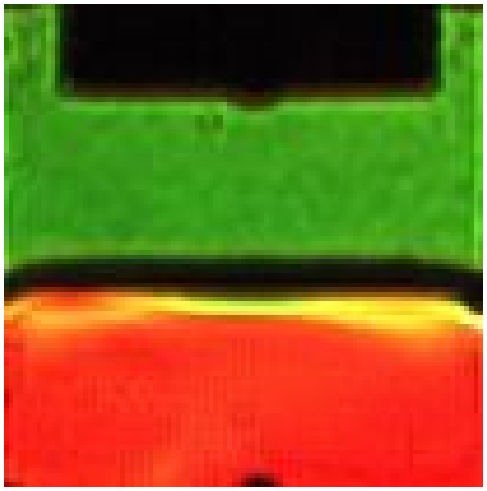

(c) t=1hr

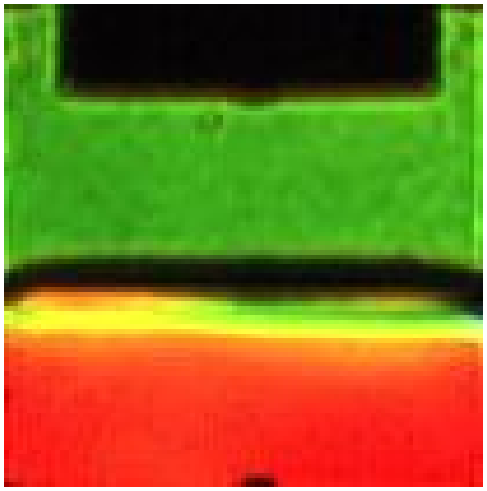

(d) t=2hr

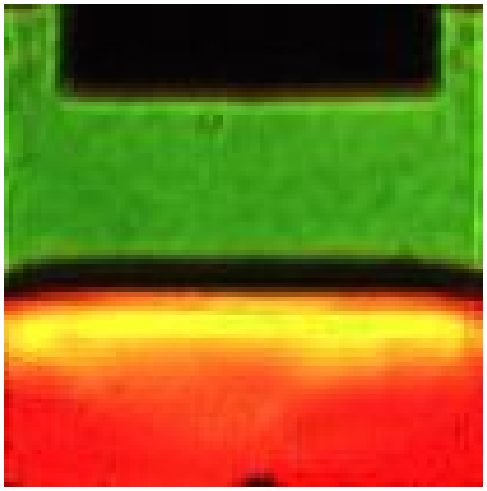

(e) t=4hr

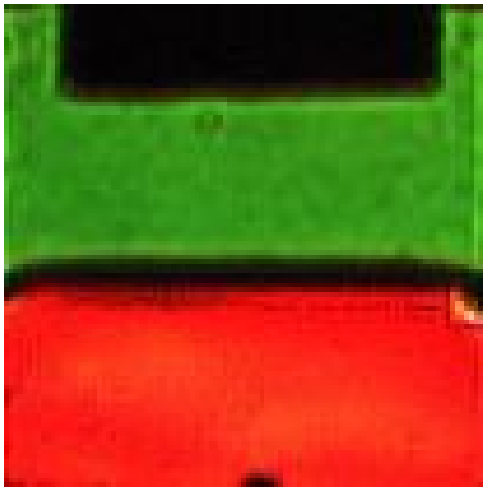

(f) t=24hr

Figure 8.18: Colour schlieren images of transient evolution of the diffusive field in the reservoir solution during lysozyme protein crystallization. Drop concentration = 8:2 and size = 10 μl, single drop, 50 ml reservoir solution.

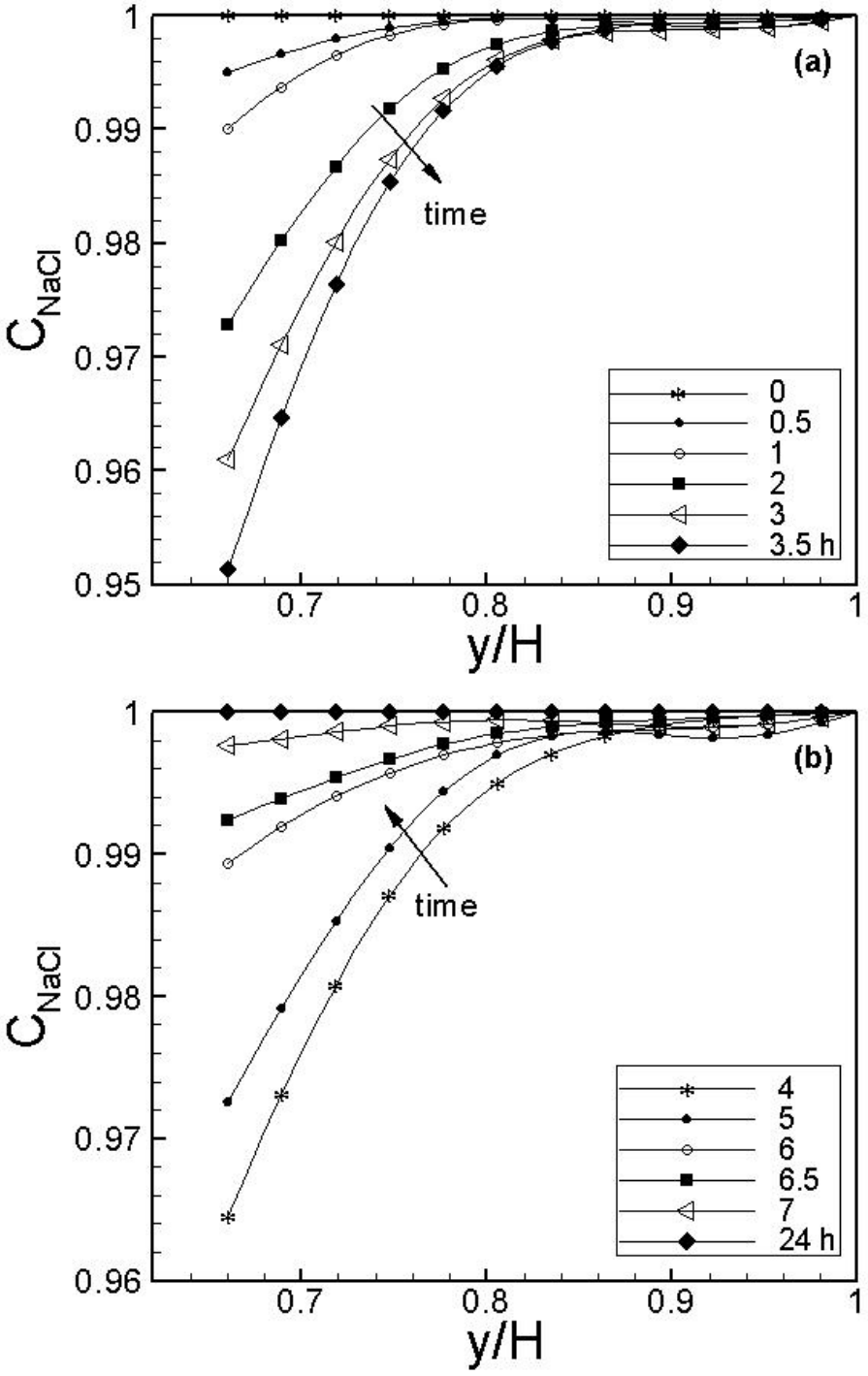

Figure 8.19: Transient evolution of NaCl concentration in the reservoir solution for 8:2 drop concentration. Single drop of 10 μl volume with 50 ml reservoir solution is considered. (a) Decreasing concentration of NaCl in reservoir solution. (b) Increasing concentration of NaCl in reservoir solution.

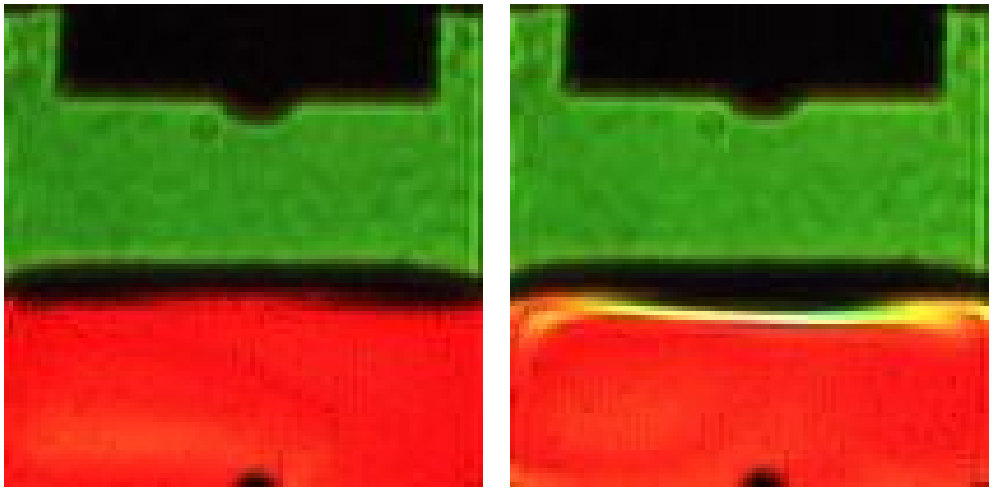

(a) t=0

(b) t=0.5 h

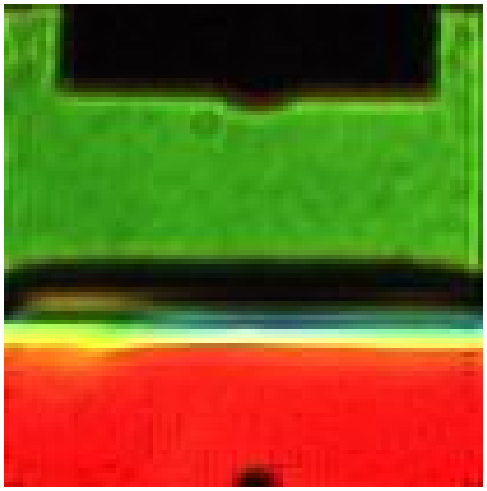

(c) t=1 h

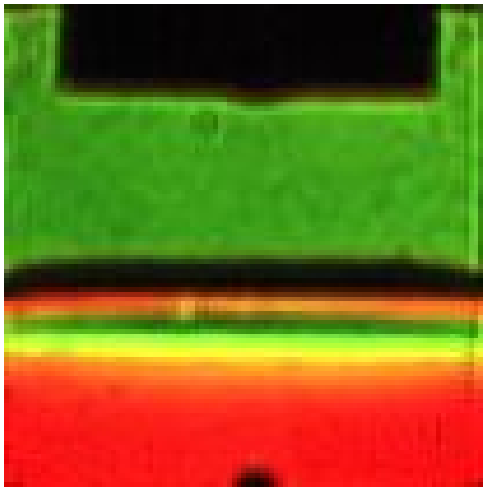

(d) t=2 h

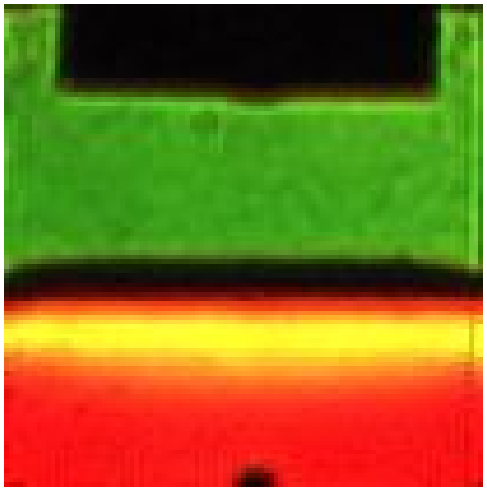

(e) t=4 h

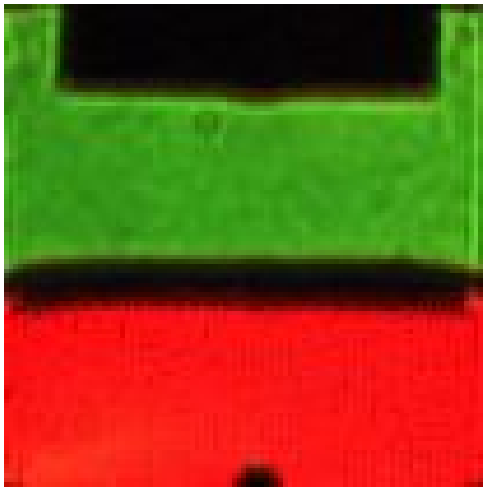

(f) t=24 h

Figure 8.20: Colour schlieren images of transient evolution of the diffusive field in the reservoir solution during lysozyme protein crystallization. Drop concentration = 8:2 and size = 15 μl, single drop, 50 ml reservoir solution.

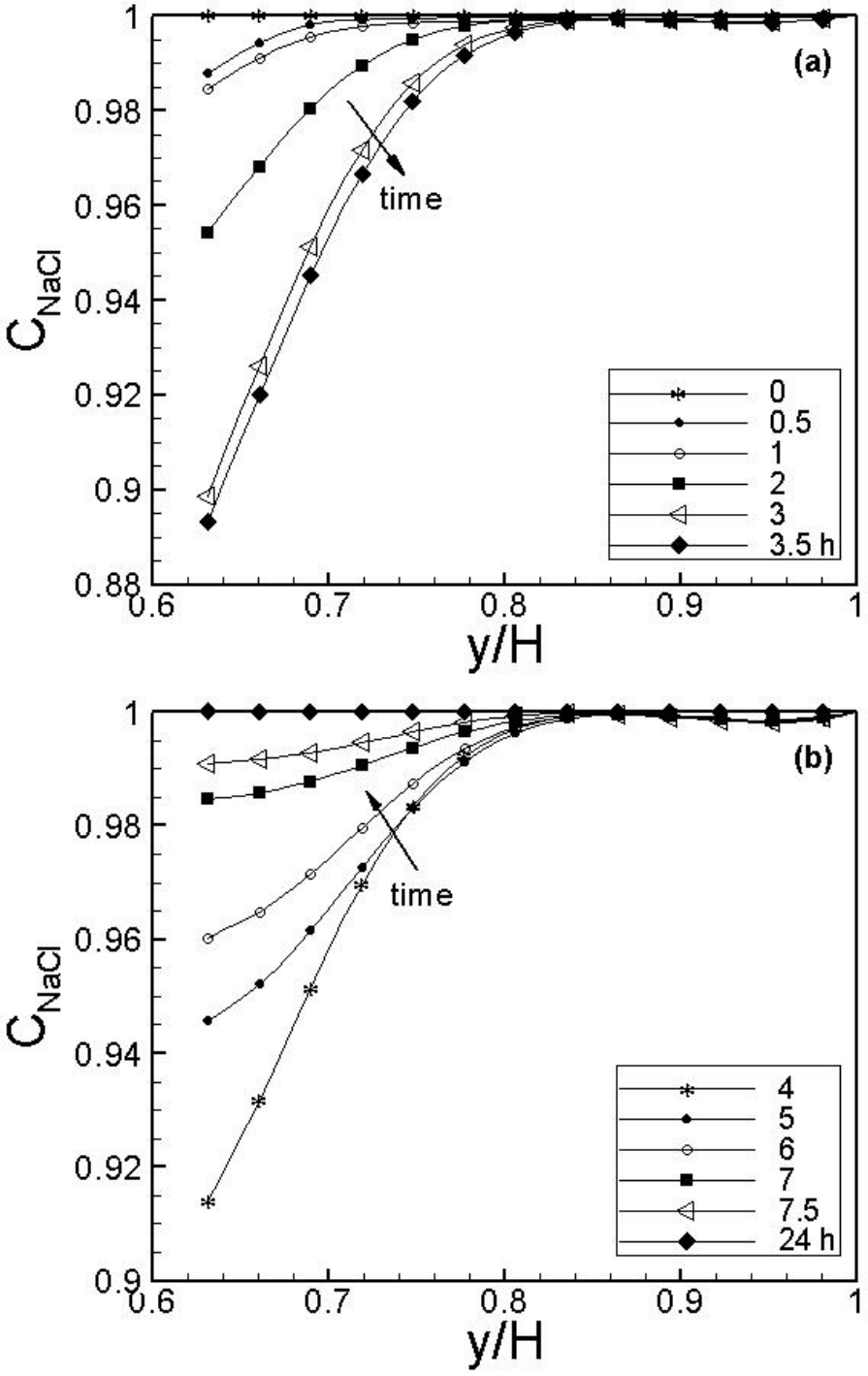

Figure 8.21: Transient evolution of NaCl concentration in the reservoir solution for 8:2 drop concentration. Single drop of 15 μl volume with 50 ml reservoir solution is considered. (a) Decreasing concentration of NaCl in reservoir solution. (b) Increasing concentration of NaCl in reservoir solution.

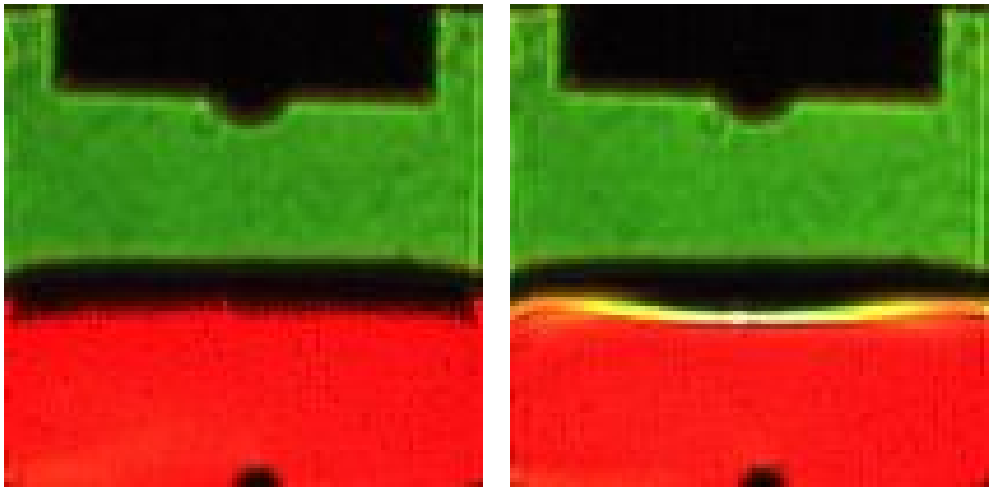

(a) t=0 (b) t=0.5 h

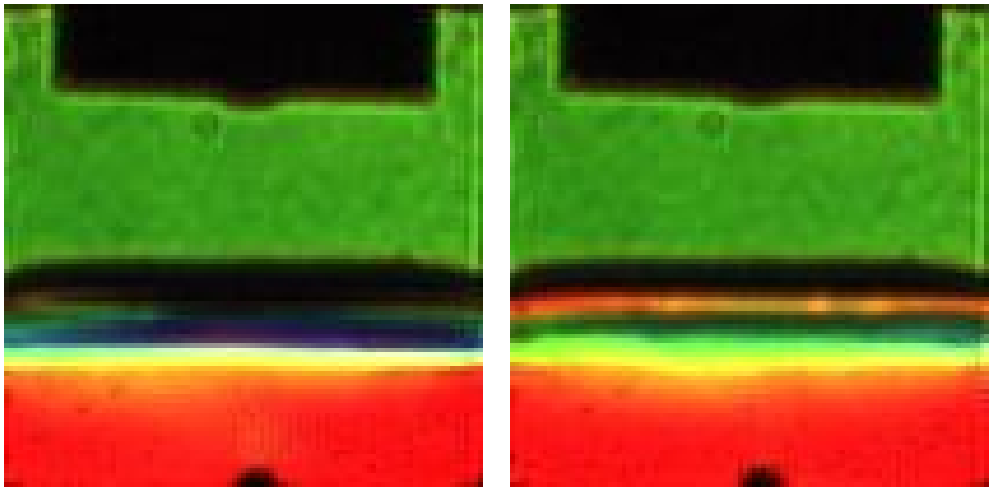

(c) t=1 h (d) t=2 h

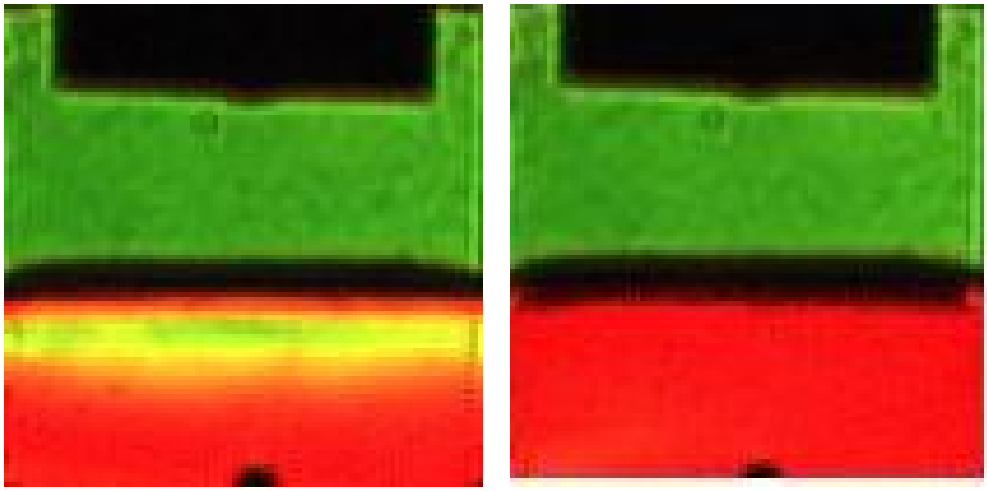

(e) t=4 h (f) t=24 h

Figure 8.22: Colour schlieren images of transient evolution of thhe diffusive field in the reservoir solution during lysozyme protein crystallization. Drop concentration = 8:2 and size = 20 μl, single drop, 50 ml reservoir solution.

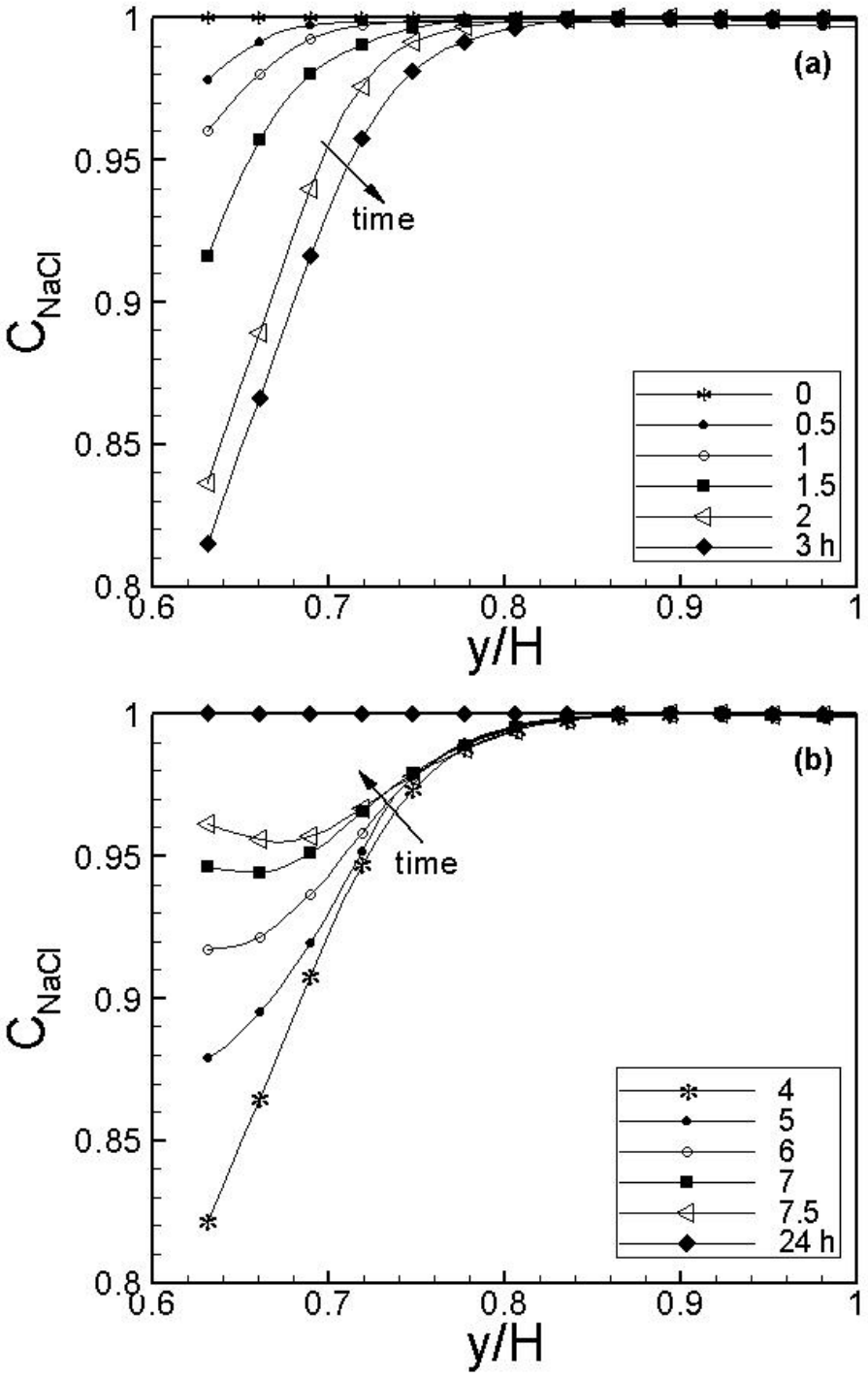

Figure 8.23: Transient evolution of NaCl concentration in the reservoir solution for 8:2 drop concentration. Single drop of 20 μl volume with 50 ml reservoir solution is considered. (a) Decreasing concentration of NaCl in reservoir solution. (b) Increasing concentration of NaCl in reservoir solution.

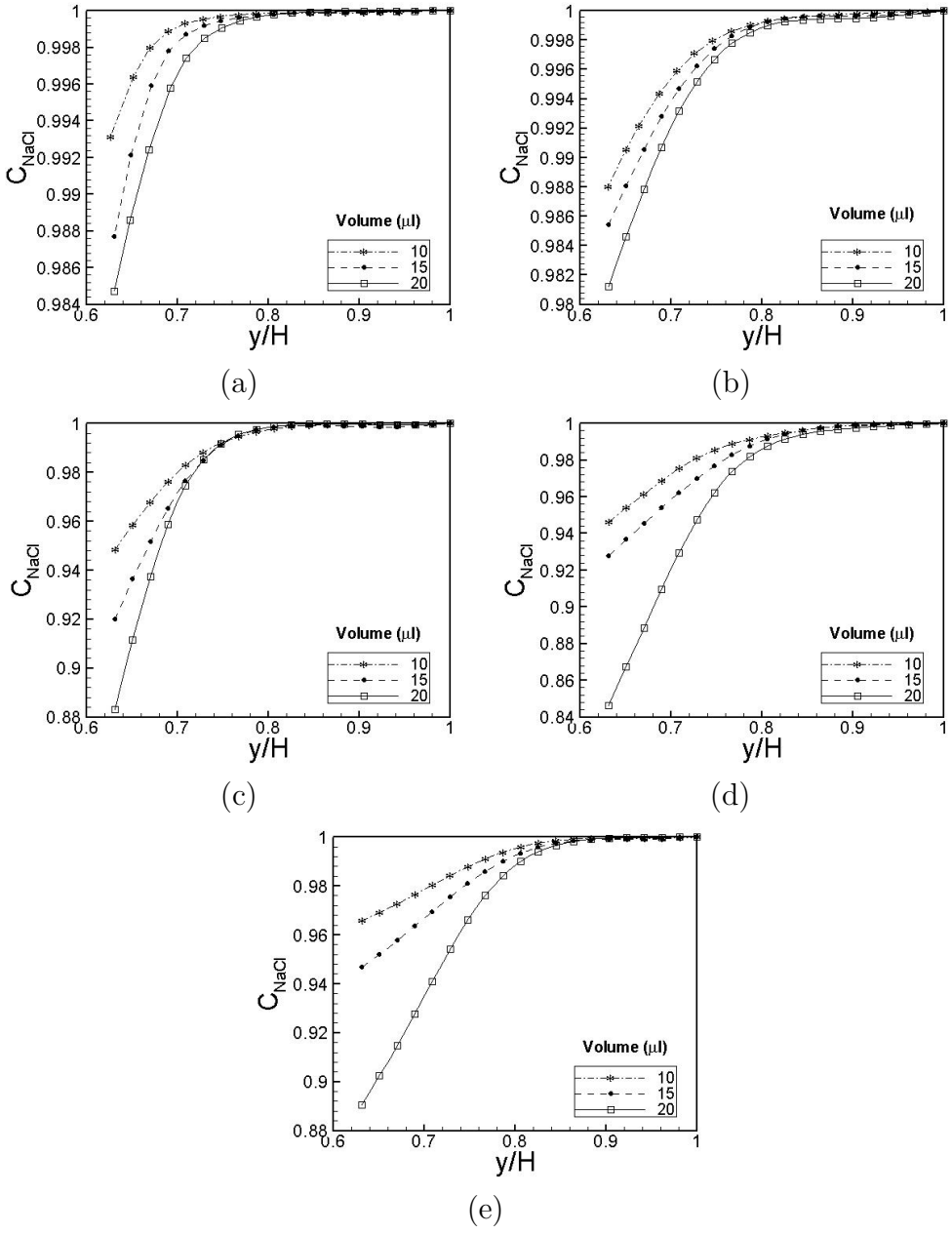

Figure 8.24: Comparison of the concentration profiles of NaCl in reservoir solution when the drop volumes are varied. p:r = 8:2, reservoir volume = 50 ml at time instants of (a) 0.5 h, (b) 1 h, (c) 2 h, (d) 4 h and (e) 5 h have been used.

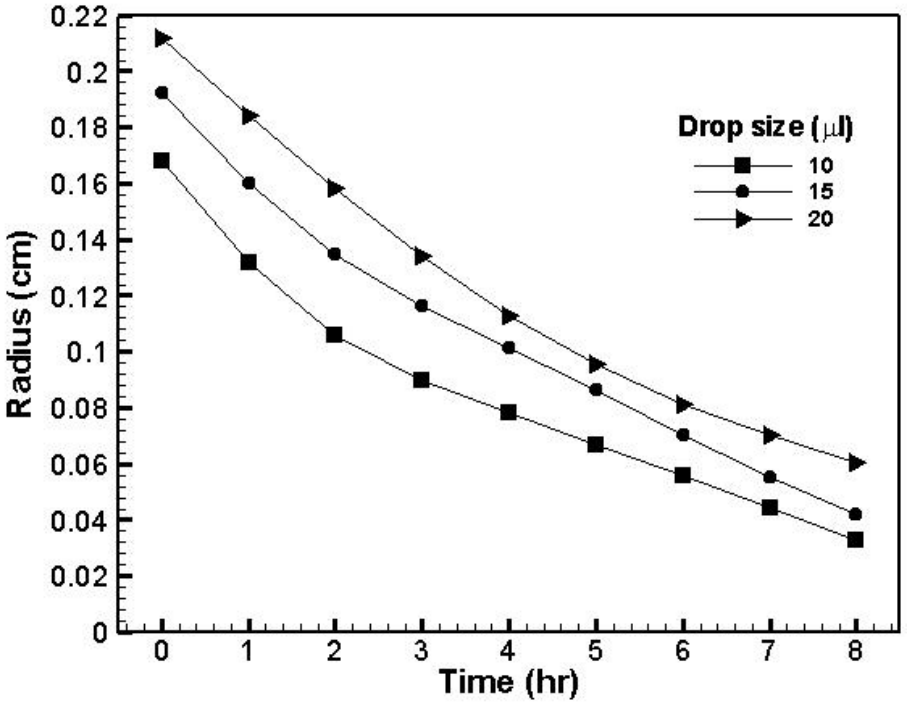

Figure 8.25: Evolution of drop radius at various drop volumes. Single drop, p:r = 8:2, reservoir volume = 50 ml.

concentration of NaCl changes till 0.95 and then starts increasing. For the 15 μl drop, the concentration of NaCl drops to 0.89 and then starts increasing. For 20 μl drop the concentration of NaCl reduces to 0.82 and then starts to increase.

Figure 8.24 shows the comparison of the concentration of NaCl in the reservoir when the drop concentration is 8:2 for 10, 15 and 20 μl drops. The reservoir solution is 50 ml and time instants considered are (a) 0.5 h, (b) 1 h, (c) 2 h, (d) 4 h and (e) 5 h. These plots show that the smallest drop (10 μl) produces the least effect on the concentration of NaCl of reservoir. The largest drop (20 μl) has the highest effect on NaCl concentration and penetrates a greater depth of the reservoir. After 4 hours, the concentration of NaCl increases in 10 μl and 15 μl drop experiments whereas in 20 μl drop it continues to decrease (Figure 8.24(d)). In Figure 8.24(e) NaCl concentrations increase in all experiments.

The radius of the drop as it decreases in size with evaporation of water is described here. The initial drop radius is determined using the known volume of the drop. The final radius is obtained by counting the number of pixels of the image. It is seen that the radius decreases rapidly at the start and finally slows off once the crystals start to form. Since evaporation starts off rapidly, the radius of the drop decreases rapidly.

When the drop size is varied, the rate of reduction of radius is the highest for the

Table 8.4: Reduction in drop radius (mm) with time for various drop volumes (d)

d/time	0	1	2	3	4	5	6	7	8 h
10	0.0168	0.0123	0.0100	0.0089	0.0078	0.0067	0.0056	0.0044	0.0033
15	0.0192	0.0149	0.0128	0.0117	0.0096	0.0074	0.0064	0.0053	0.0042
20	0.0212	0.01817	0.01514	0.01211	0.00909	0.00909	0.00606	0.00606	0.0606

smallest drop. Figure 8.25 shows the effect of drop size on the variation of drop radius with respect to time. Table 8.4 shows this variation of drop radius in numerical form.

8.5 EXPERIMENTS WITH VARYING NUMBER OF DROPS

The experiments have been conducted to study the effect of the number of drops on equilibrium and diffusion process. Figures 8.26, 8.28 and 8.30 show the colour schlieren images for the evolution patterns of single, three and seven protein drops of 10 μl each having 7:3 drop concentration hanging over a 50 ml reservoir solution. Since the number of drops are different, the amount of water evaporated and condensed over the interface would vary. Therefore, the diffusion of water into the reservoir solution will be longer for a large number of drops.

The relationship between the refractive index and the concentration of NaCl obtained from refractometer data is used to determine the evolution of the concentration distribution within the reservoir solution and is shown in Figure 8.27, 8.29 and 8.31. The concentration of NaCl is normalized with its maximum value at saturation. The transient evolution of salt concentration in the reservoir arises from the diffusion of the condensed water at the air-solution interface. Figure 8.27, 8.29 and 8.31 correspond to the vertical mid-plane covering the distance from the interface to the base of the cavity. The plots show a constant initial concentration of NaCl in the reservoir solution (Figure 8.27(a), 8.29(a) and 8.31(a)). With condensation of the water at the interface, the concentration of NaCl reduces with time till t=2.5 h with single drop, t=3.5 h with 3 drops and t=4.5 h with 7 drops. The reduction in NaCl concentration is higher in the interface region compared to that away from it. Later, the average NaCl concentration increases (Figure 8.27(b), 8.29(b) and 8.31(b)). This trend is attributed to both the reduction in the evaporation rate of the drop and also the diffusion of the fresh water into the reservoir solution. At t=24 h, the drop has completely evaporated and NaCl concentration attains a distribution similar to the initial (t=0) value.

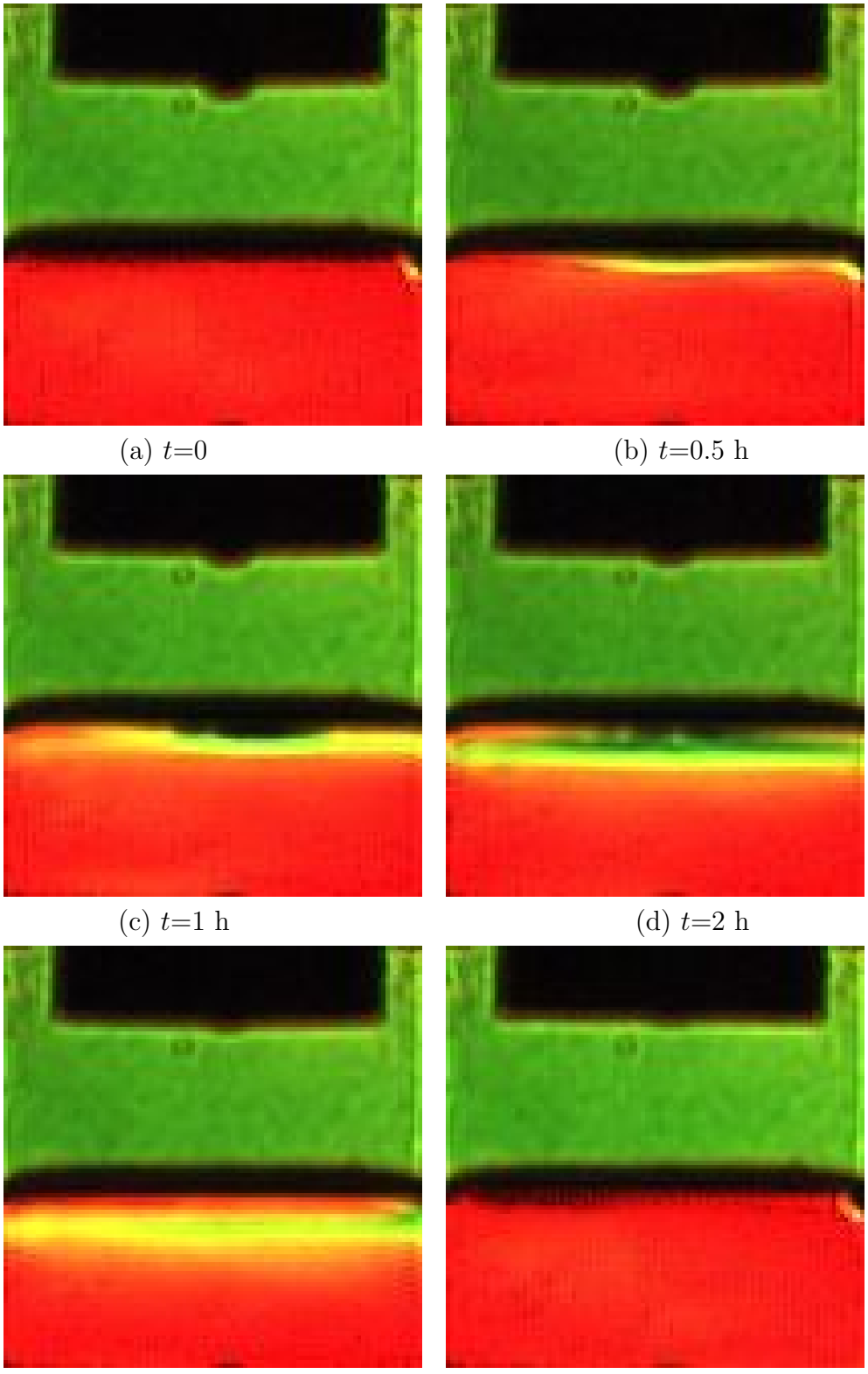

(a) t=0 (b) t=0.5 h

(c) t=1 h (d) t=2 h

(e) t=4 h (f) t=24 h

Figure 8.26: Colour schlieren images of transient evolution of the diffusive field in the reservoir solution during lysozyme protein crystallization. Drop concentration = 7:3 and size = 10 μl, single drop, 50 ml reservoir solution.

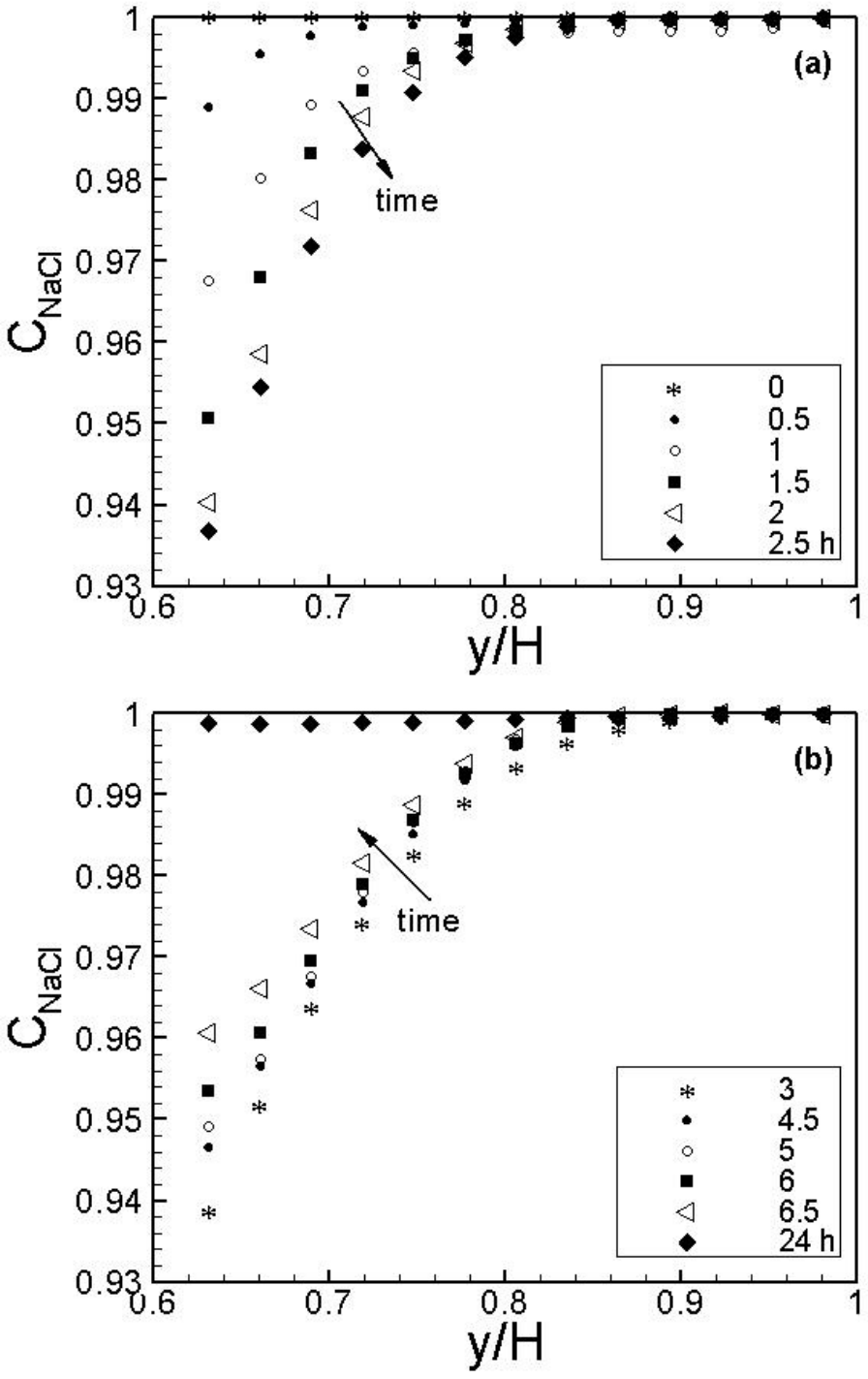

Figure 8.27: Transient evolution of NaCl concentration in the reservoir solution for 7:3 drop concentration. Single drop of 10 μl volume with 50 ml reservoir solution is considered. (a) Decreasing concentration of NaCl in reservoir solution. (b) Increasing concentration of NaCl in reservoir solution.

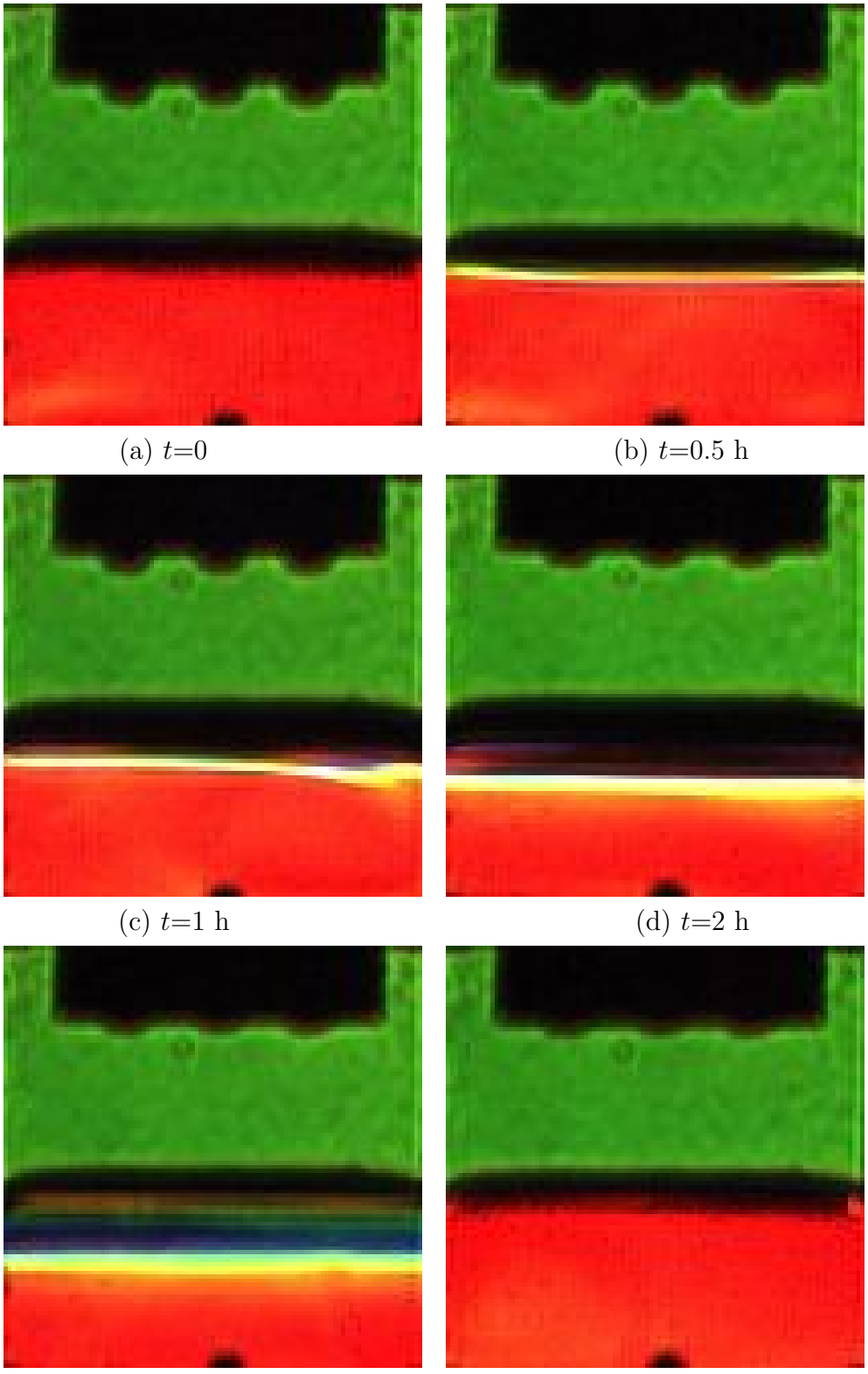

(a) t=0 (b) t=0.5 h

(c) t=1 h (d) t=2 h

(e) t=4 h (f) t=24 h

Figure 8.28: Colour schlieren images of transient evolution of the diffusive field in the reservoir solution during lysozyme protein crystallization. Drop concentration = 7:3 and size = 10 μl, 3 drops, 50 ml reservoir solution.

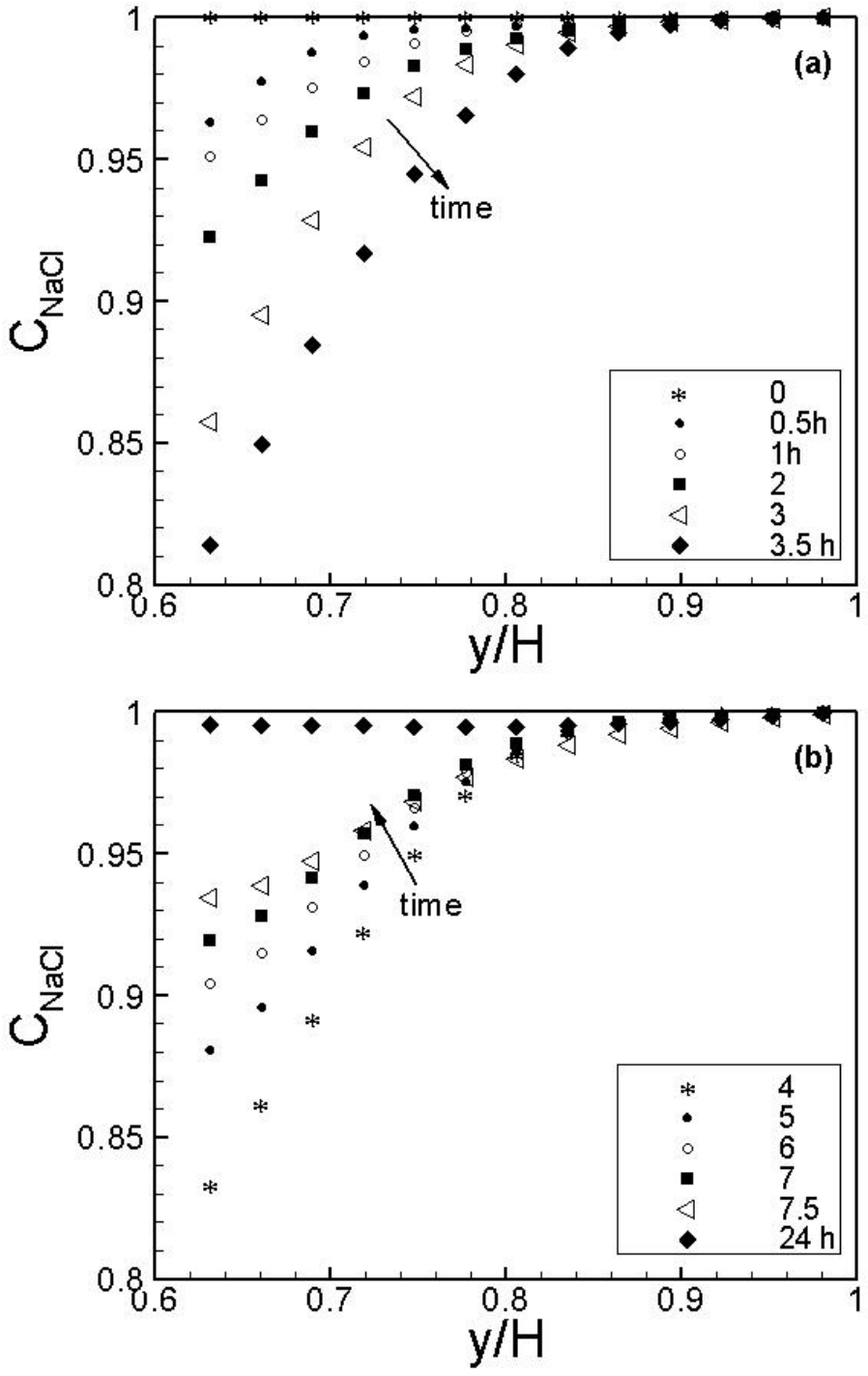

Figure 8.29: Transient evolution of NaCl concentration in the reservoir solution for 7:3 drop concentration. Three drops of 10 μl volume each with 50 ml reservoir solution is considered. (a) Decreasing concentration of NaCl in reservoir solution. (b) Increasing concentration of NaCl in reservoir solution.

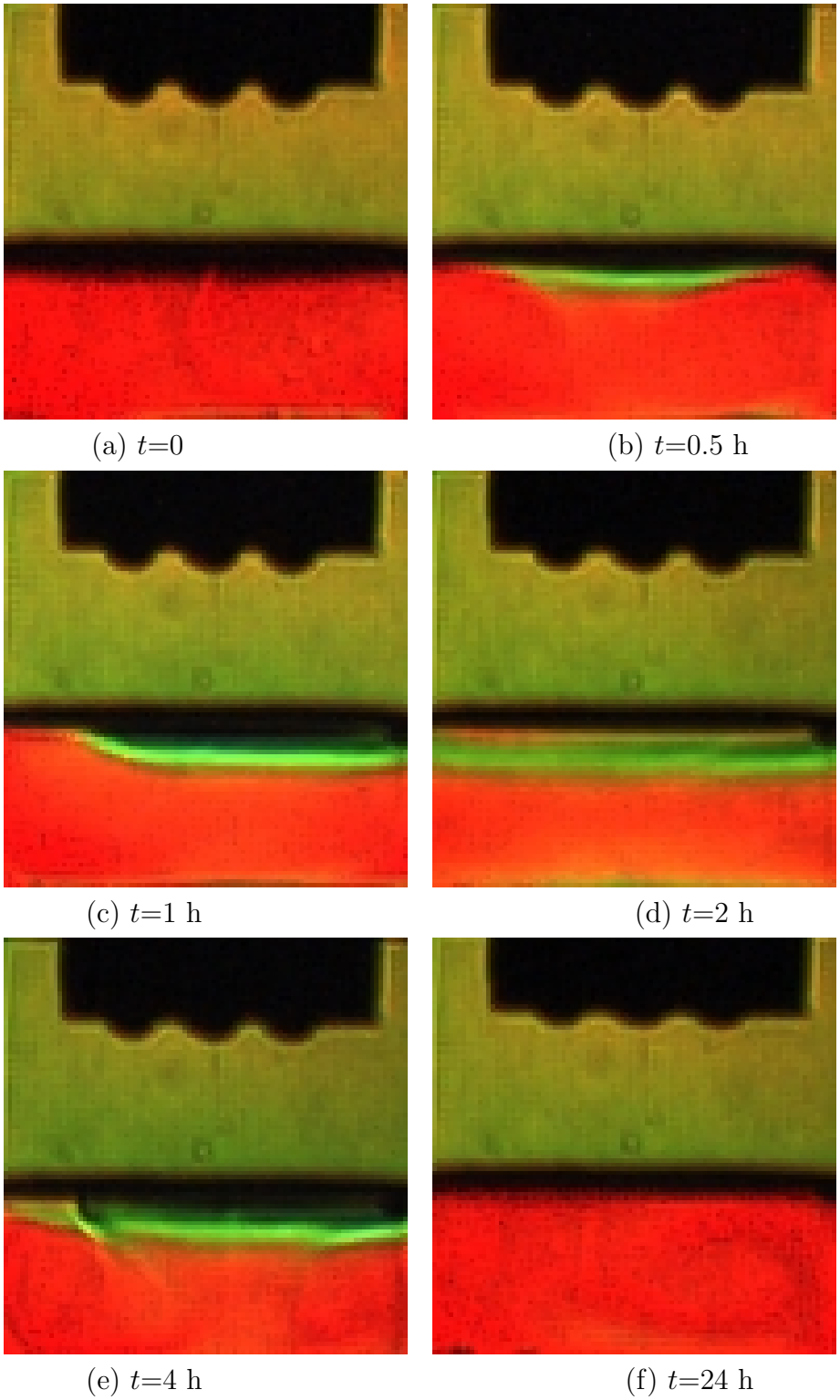

(a) t=0 (b) t=0.5 h

(c) t=1 h (d) t=2 h

(e) t=4 h (f) t=24 h

Figure 8.30: Colour schlieren images of transient evolution of the diffusive field in the reservoir during lysozyme protein crystallization. Drop concentration = 7:3 and size = 10 μl, 7 drops, 50 ml reservoir solution.

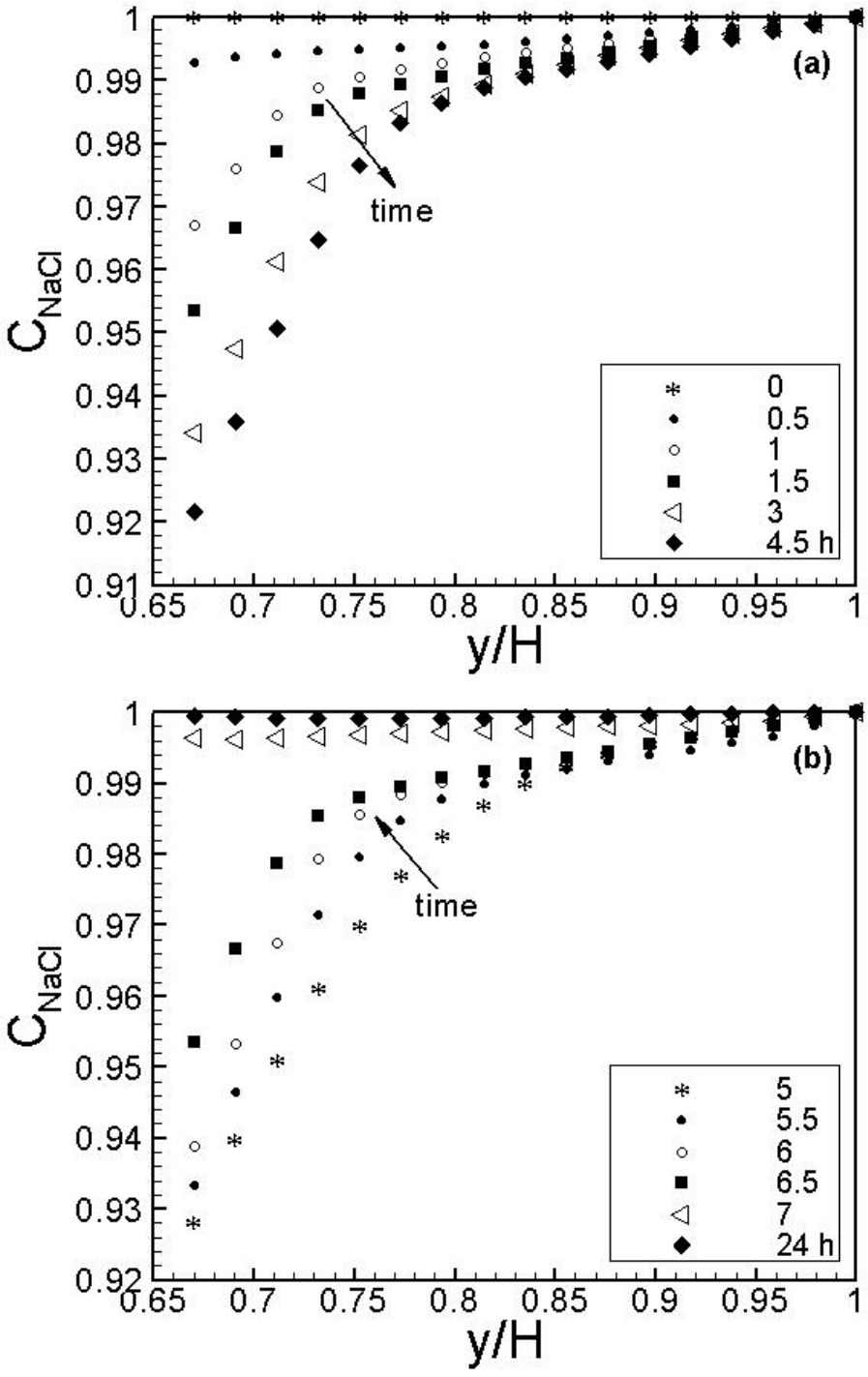

Figure 8.31: Transient evolution of NaCl concentration in the reservoir solution for 7:3 drop concentration. Seven drops of 10 μl volume each with 50 ml reservoir solution is considered. (a) Decreasing concentration of NaCl in reservoir solution. (b) Increasing concentration of NaCl in reservoir solution.

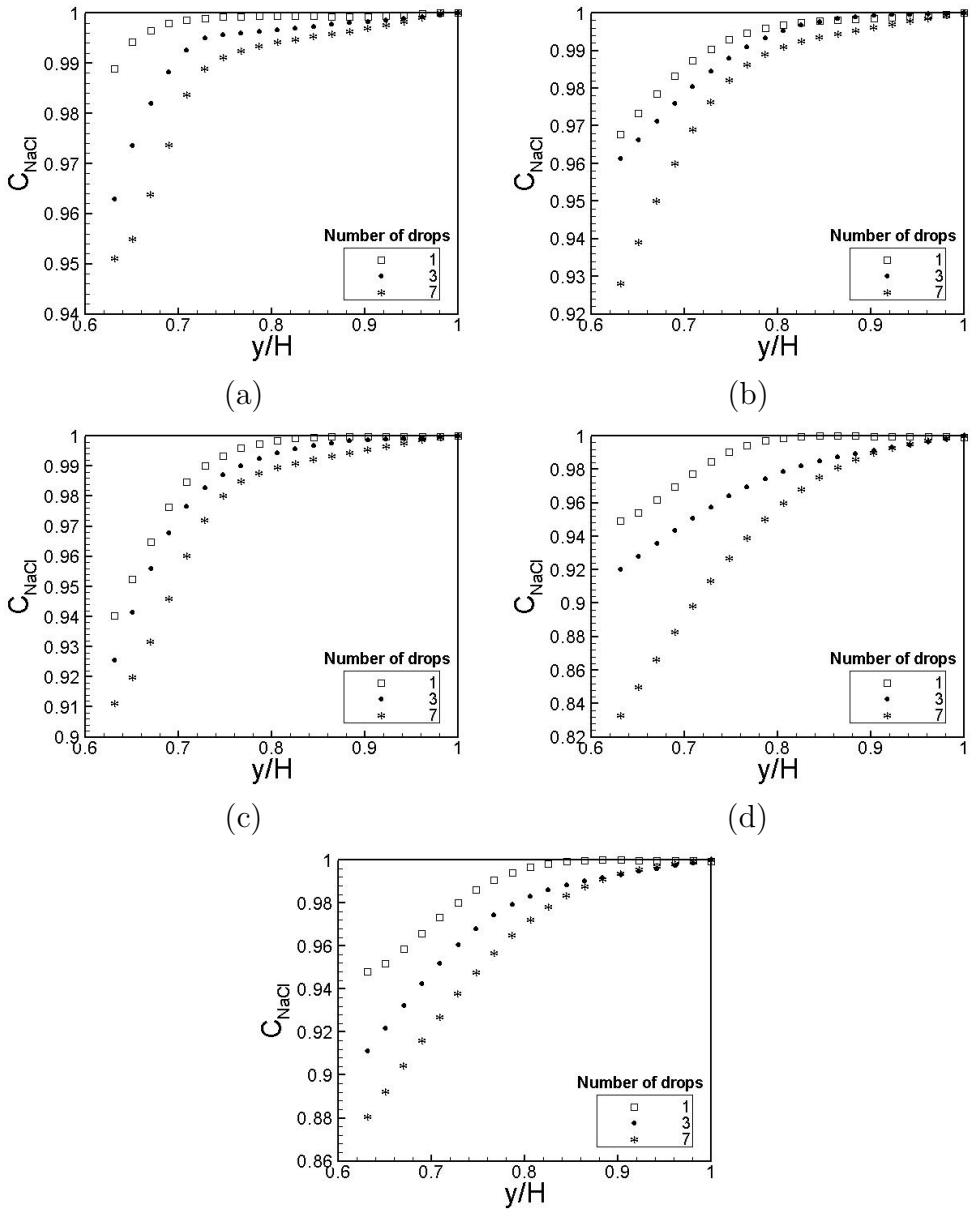

Figure 8.32: Comparison of the concentration profiles of NaCl in reservoir solution when the number of drops are varied. Drop volume = 10 μl, p:r = 7:3 and reservoir volume = 50 ml at time instants of (a) 0.5, (b) 1 h, (c) 2 h, (d) 4 h and (e) 5 h have been used.

Figure 8.32 shows the comparison of the concentration of normalized NaCl in reservoir solution when the drop concentration is 7:3 with 1, 3 and 7 drops of 10 μl. The reservoir solution has a volume of 50 ml at time instants (a) 0.5 h, (b) 1 h, (c) 2 h, (d) 4 h and (e) 5 h. From these plots it is seen that the normalized NaCl concentration for single drop is higher than that of 3 and 7 drops in the reservoir. From 7 drops, the amount of evaporated water is the highest as compared to other experiments. The concentration of NaCl in reservoir solution is strongly affected here when compared to a single drop. Since the drops are of the same size, the reduction in drop radius are equal in all the three experiments.

8.6 VISUALIZATION OF DIFFERENT ANGLES

The effect of drop orientation with respect to the line joining the source and the camera is discussed here. These experiments have been conducted for the reservoir filled with 50 ml solution, drop concentration of 7:3 and 10 μl drop volume. Here 3 drops have been arranged in-line and perpendicular to the light beam so that single drop and three drops are respectively seen (Figure 8.1(b)). Figure 8.33 shows the in-line position of the drops. In Figure 8.35 the three drops are clearly visualized. Figures 8.33 and 8.35 show the colour schlieren images of transients seen in these experiments.

Since the conditions are similar except that visualization is from two different angles. Hence there is no change in the physical mechanisms in progress as well as the time required to reach equilibrium. The changes can be seen only in the pattern of condensation and diffusion of water into the reservoir solution. In Figure 8.33, the three drops are visualized cummulativly as a single drop. First image of the experiment is the base image. After placing the drops and sealing the cavity, evaporation has started and condensation taken place. Figure 8.33(b) shows a boat like structure at the interface and Figure 8.35(b) shows nearly a straight patch at the interface. In Figure 8.33(b), water has condensed over the interface with a maximum under the central drop. In Figure 8.35(b), water spreads over the interface because three drops are parallel to the smaller side of the cavity. Hence a uniform spreading is to be seen. Later, the images shown are comparable to each other. Various colour distributions are seen in Figures 8.33(e) and 8.35(e) recorded after 5 h.

Figures 8.34 and 8.36 show the transient evolution of normalized NaCl concentration in the reservoir solution for the three hanging drops in the in-line position and at right angles respectively. Both phases, (a) increasing concentration of NaCl and (b) decreasing concentration of NaCl in the reservoir are presented. In Figures 8.34(a) and 8.36(a) the plots are quite similar but the concentration of NaCl in former decreases

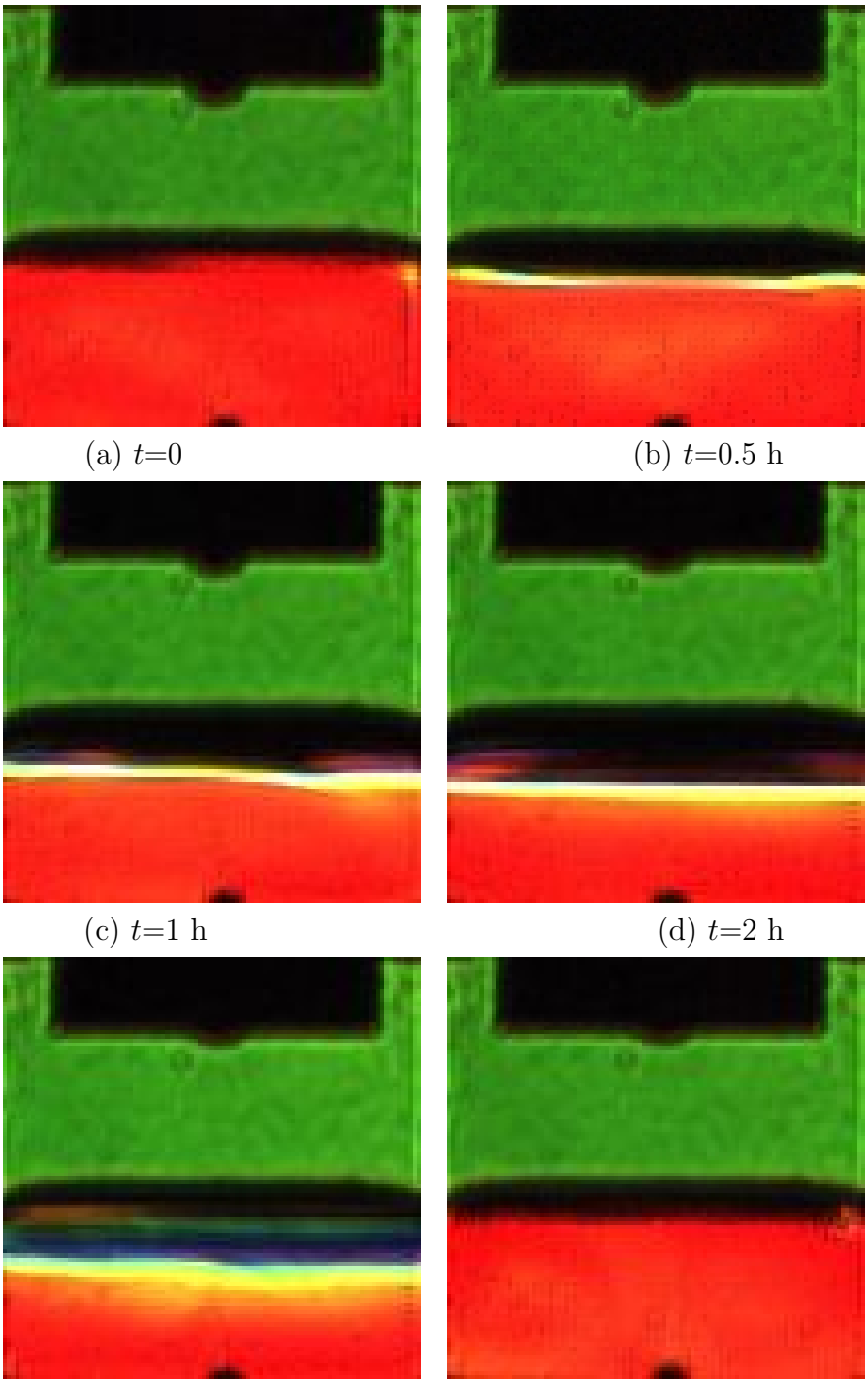

(a) t=0 (b) t=0.5 h

(c) t=1 h (d) t=2 h

(e) t=4 h (f) t=24 h

Figure 8.33: Colour schlieren images of transient evolution of the diffusive field in the reservoir solution during lysozyme protein crystallization with three protein drops (in-line position). Drop concentration = 7:3 and size = 10 μl, 50 ml reservoir solution.

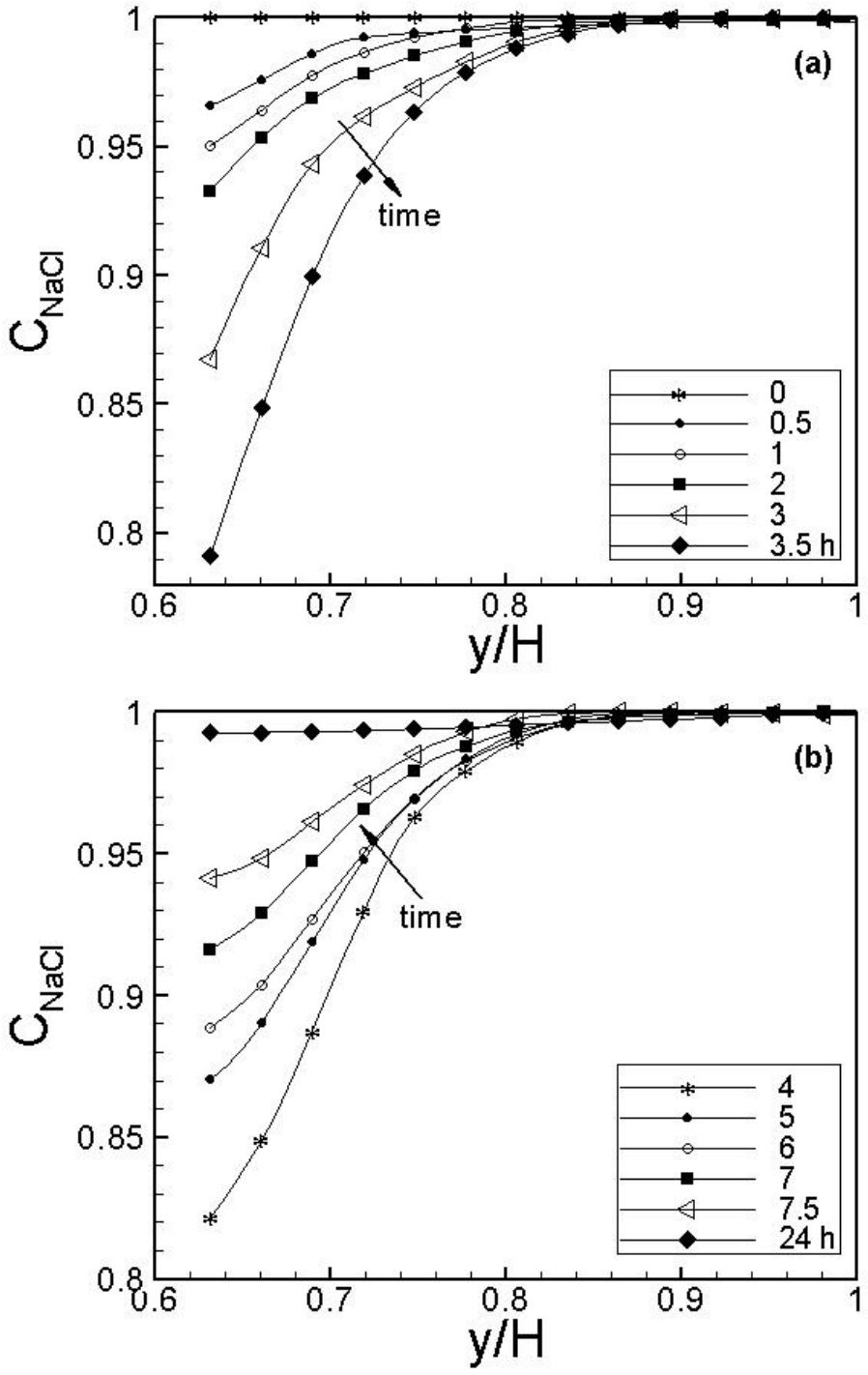

Figure 8.34: Transient evolution of NaCl concentration in the reservoir solution for 7:3 drop concentration. Three drops (in-line position) of 10 μl volume with 50 ml reservoir solution is considered. (a) Decreasing concentration of NaCl in reservoir solution. (b) Increasing concentration of NaCl in reservoir solution.

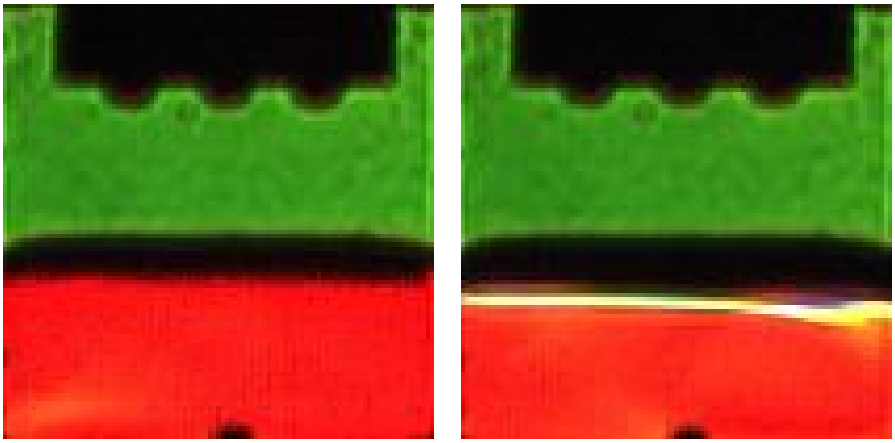

(a) t=0 (b) t=0.5 h

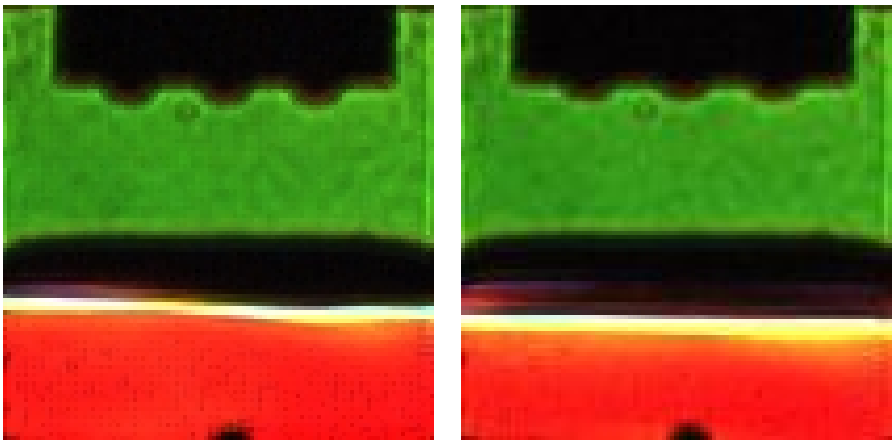

(c) t=1 h (d) t=2 h

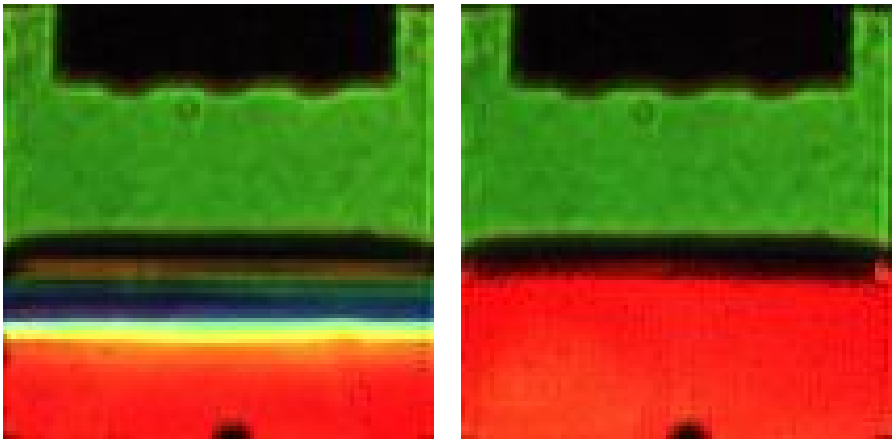

(e) t=4 h (f) t=24 h

Figure 8.35: Colour schlieren images of transient evolution of the diffusive field in the reservoir solution during lysozyme protein crystallization with three protein drops. Drop concentration = 7:3 and size = 10 μl, 50 ml reservoir solution.

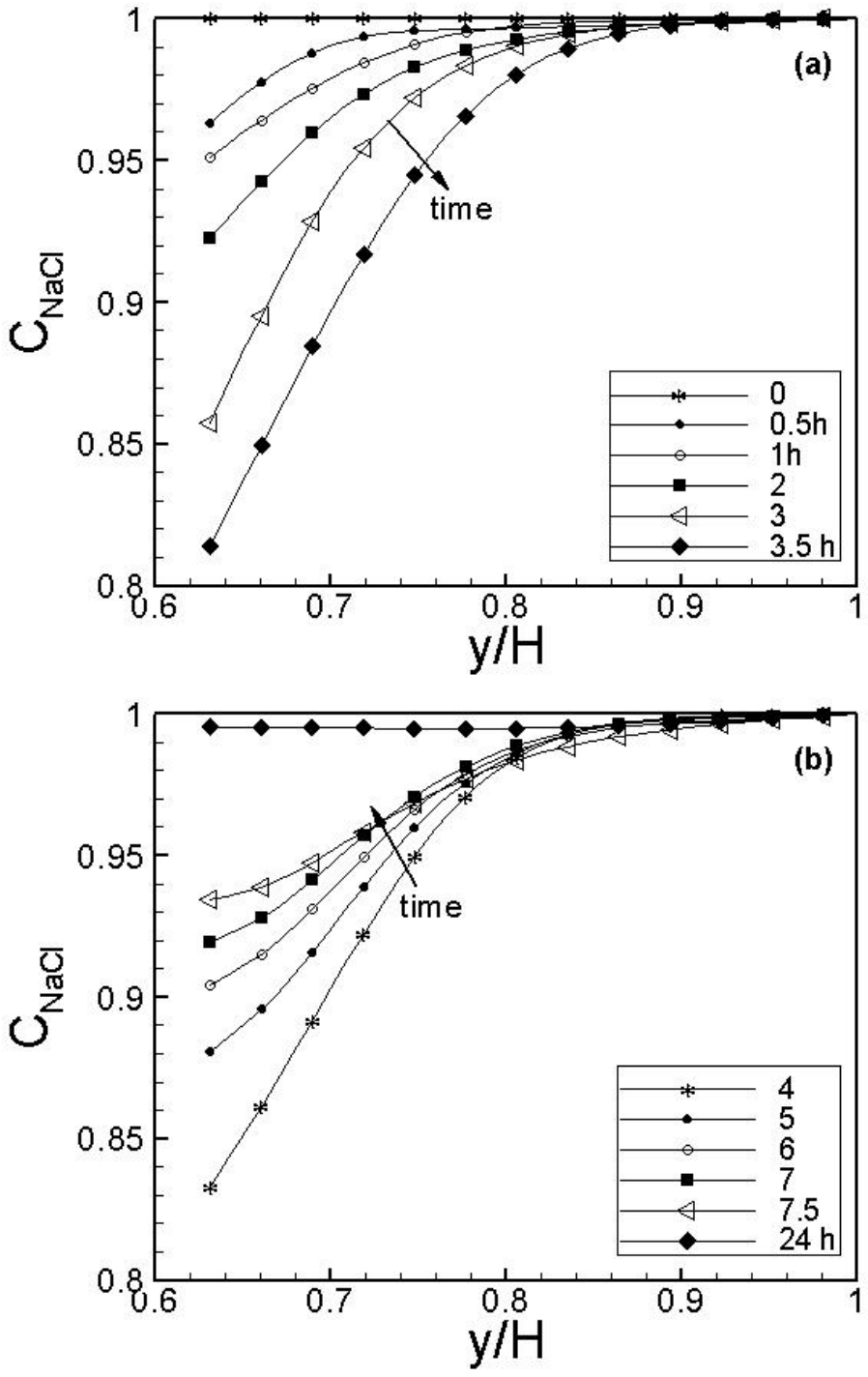

Figure 8.36: Transient evolution of NaCl concentration in the reservoir solution for 7:3 drop concentration. Three drops of 10 μl volume with 50 ml reservoir solution is considered. (a) Decreasing concentration of NaCl in reservoir solution. (b) Increasing concentration of NaCl in reservoir solution.

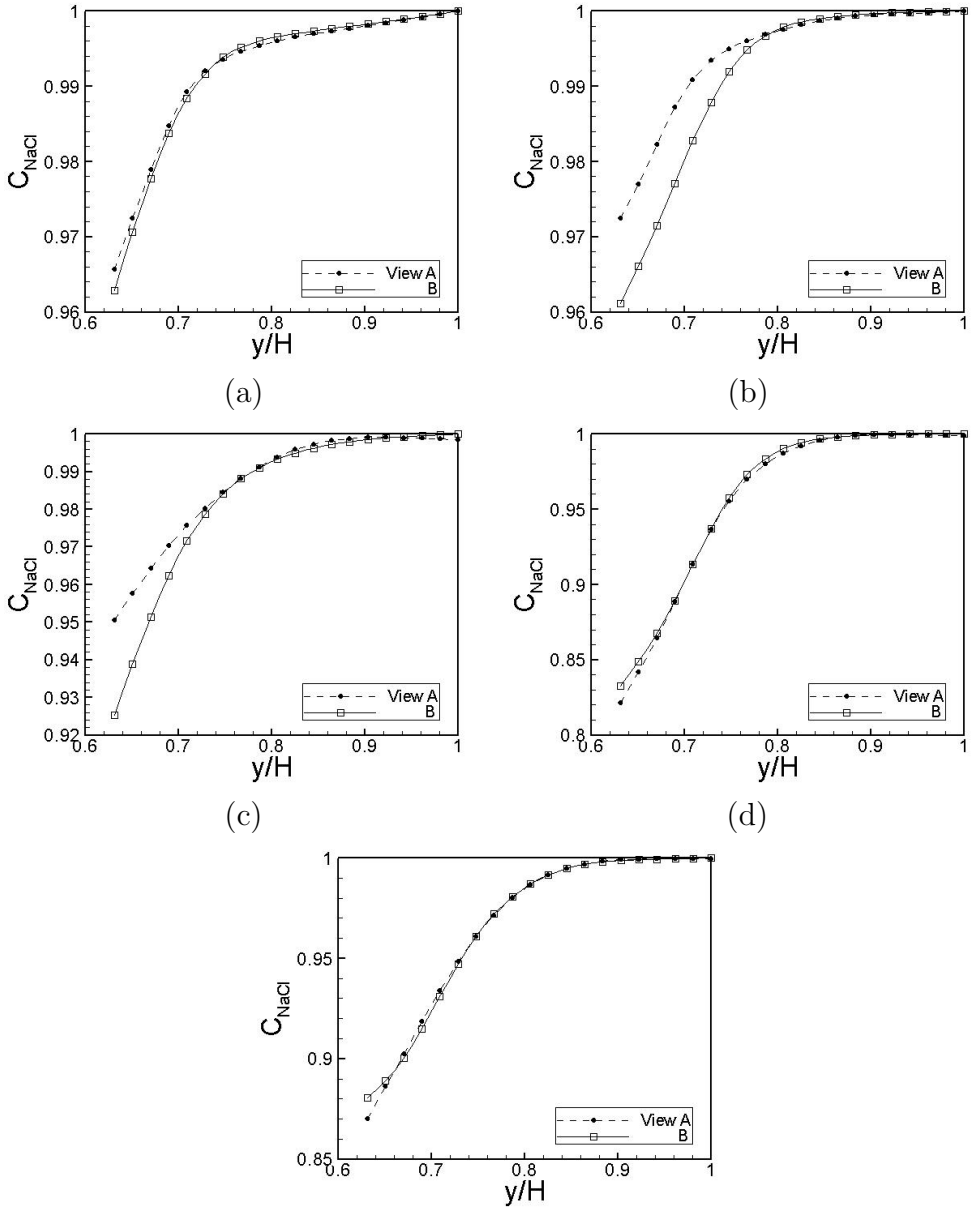

Figure 8.37: Nondimensional NaCl concentration profiles in the reservoir obtained from views A and B. Three drops with volume = 10 μl, p:r = 7:3, and reservoir volume = 50 ml at time instants of (a) 0.5, (b) 1 h, (c) 2 h, (d) 4 h and (e) 5 h have been used.

rapidly as compared to the later. Till 3.5 hrs the concentration of NaCl decreases in both view angles. After 4 hrs the concentration of NaCl in the reservoir solution increases and finally reaches to same level for both projections. The penetration depth is higher when the three drops are individually seen. From the Figure 8.34(a) the NaCl concentration changes upto a depth of $y/H = 0.86$ whereas in Figure 8.36(a) it is upto $y/H = 0.09$.

Comparative information of NaCl concentration in the reservoir for the two view angles is shown in Figure 8.37 for time instants of (a) 0.5 h, (b) 1 h, (c) 2 h, (d) 4 h and (e) 5 h. At t=0.5 h, the concentration of NaCl near the interface is smaller in the view carrying three drops (view B) and in the single drop view angle (view A), it is higher. It is because the volume of condensed water in view B has to spread over the visualized width (31 mm) of the cavity. In view A it has to spread over the length (127 mm) of the cavity. The concentration of NaCl is lower in initial stages of the view B experiment. After 1 and 2 hrs, this trend is seen further but the concentration difference is high. At time instants of 4 and 5 hrs, Figures 8.37(d - f), the concentrations are almost identical, a slightly opposite trend near the interface is seen. These images show phase reversal in that the increasing phase of NaCl concentration has started. The minimum normalized concentration of NaCl reached is around 0.79 for view A (Figure 8.34(a)) and 0.81 for view B (Figure 8.36(a)). These observations are summarized in Table 8.5.

Table 8.5: Comparison of minimum concentration, maximum depth for two views

View	minimum concentration	maximum depth	time of phase reversal (h)
A	0.79	0.86	4
B	0.81	0.90	4

8.7 X-RAY DIFFRACTION PATTERNS OF GROWN CRYSTALS

A digital camera attached to the WILD M3Z stereomicroscope Figure 4.20 provides the images of the growing lysozyme crystals at various time instants. X-ray diffraction has been carried out for some of these grown crystals. The maximum size of the grown crystal is about 350 × 250 μm^2. X-ray diffraction (wavelength=1.541790 Å, detector MAR345) showed the crystals to be of good quality with tetragonal shape. The X-ray diffraction data were autoindexed and integrated using the program XDS software. The unit cell constants were determined as a=b=78.98 Å and c=36.92 Å with α=β=γ=90^o. Figure 8.38 shows some diffraction patterns obtained from the grown lysozyme protein crystal at different angles. These parameters confirm that the growth process generated

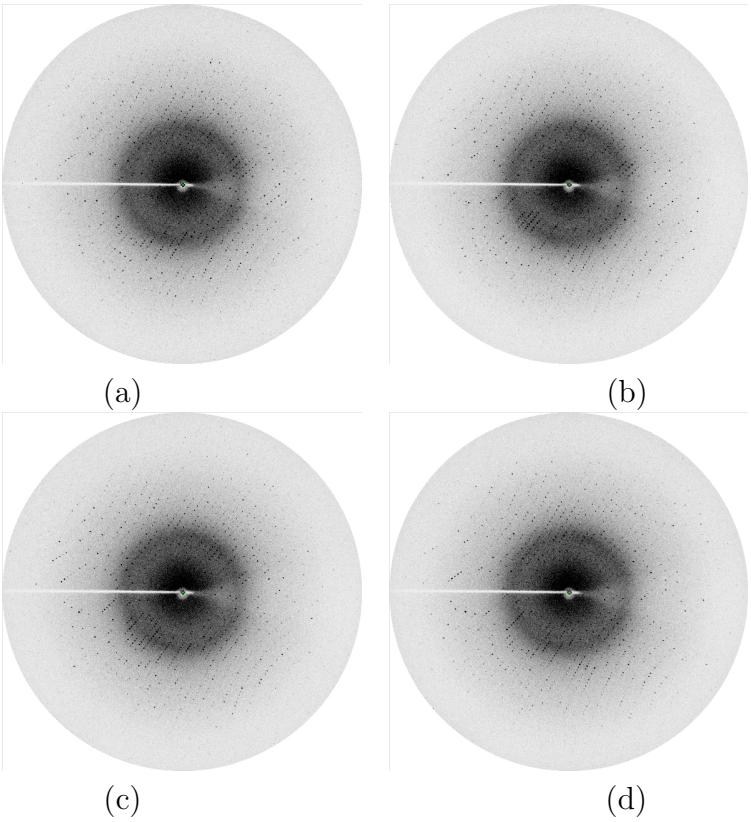

Figure 8.38: X-ray diffraction patterns of the protein crystal at two different angles.

Table 8.6: Comparison of lattice constants (Å) for grown lysozyme crystals with literature

Lattice constants	Hodgson, *et al.*, 1999	Yoshizaki, *et al.*, 2002	Experimental result
a=b	78	79.1	78.98
c	39	38.0	36.92

meaningful crystals for the range of process parameters studied. The unit constants are compared with literature and given in Table 8.6.

8.8 CLOSURE

Parametric study of protein crystal growth process using colour schlieren technique is reported. Reservoir height, drop concentration, drop size, number of drops and viewing angle are used as parameters with a focus on diffusion phenomenon in the reservoir solution. Water evaporates from the drop and condenses on the air-reservoir interface. Subsequently, water starts diffusing into the reservoir, resulting in lowering of concen-

tration of NaCl in the reservoir. After some time, phase reversal takes place and the concentration of NaCl increases. This phase reversal takes place when all the condensed water diffuses into the reservoir. It is observed that after phase reversal, crystals appear in the drop and grow with time.

On varying the reservoir volume, it is observed that the drop radius reduces the fastest in the largest reservoir volume when the air gap is the least. This result is related to a reduction in mass transfer resistance for small air gaps. The changes in drop radius with time depend on concentration of the drop medium. The rate of reduction of drop radius is the largest for the highest drop concentration. This shows that water evaporates rapidily in the experiment having largest drop concentration. In addition, the rate of reduction of radius is the highest for the smallest drop. Water evaporating from drops depends on the number of drops in the experiment phase reversal occurs early for the smallest number of drops and is delayed when more drops are used. Drops are visualized through two orthogonal directions. The concentration of NaCl in the reservoir for in-line viewing decreases rapidly in one projection as compared to the other at right angles. The X-ray diffraction studies show crystals grown to be good quality. A good match is obtained for the lattice constants with the literature.